Electronic Supplementary Information (ESI)

Metal-Induced Supramolecular Chirality Inversion of Small Self-Assembled Molecules in Solution

Zoran Kokan,[a,*] Berislav Perić,[a] Mario Vazdar,[a] Željko Marinić,[a] Dražen Vikić-Topić,[a] Ernest Meštrović,[b] and Srećko I. Kirin[a,*]

[a] *Ruđer Bošković Institute, Bijenička c. 54, 10000 Zagreb, Croatia*
[b] *PLIVA Croatia d.o.o., Prilaz baruna Filipovića 25, 10000 Zagreb, Croatia*
* E-mail: zoran.kokan@irb.hr, srecko.kirin@irb.hr

Contents

General Methods

Reactions were carried out in ordinary glassware and chemicals were used as purchased from commercial suppliers without further purification. Reactions were monitored by TLC on Silica Gel 60 F254 plates and detected with UV lamp (254 nm); organic compounds were purified using automated flash chromatography equipped with a UV detector (254 nm) and prepacked silica columns. NMR spectra were obtained on spectrometers operating at 300.13 or 600.13 MHz for ^{1}H, and 150.92 MHz for ^{13}C nuclei. The CD spectra were recorded on a JASCO J-810 spectropolarimeter equipped with Peltier thermostat, using 10, 1, and 0.1 mm Suprasil quartz cells depending on the sample concentration. The CD data was corrected for a path length of 10 mm. The UV spectra were recorded on Varian Cary 50 Spectrophotometer using 10, 1, and 0.1 mm Suprasil quartz cells depending on the sample concentration. FT-IR spectra were recorded on a Bruker Alpha-T FT-IR spectrometer using a Specac cell for liquid samples with 0.050 mm path length and CaF_2 windows.

X-Ray Crystallographic Details

Single-crystal analysis was performed on an Oxford Xcalibur Gemini diffractometer equipped with a Sapphire CCD detector and graphite-monochromated Cu *K*α radiation (λ = 1.5418 Å). The diffraction data were collected at 293(3) K. The CrysAlis CCD and CrysAlis RED (Version 1.171.36.32) programs were employed for data collection, cell refinement and data reduction. The structure has been solved by direct methods using program SIR2011[S1] and refined by full-matrix least square method on F^2 using program SHELXL.[S2] The structure contained four voids (solvent accessible areas) where residual electron density was treated by SQUEEZE procedure[S3] in the program PLATON.[S4]

MD Simulation Details

We performed 500 ns molecular dynamics simulations (after 1 ns of equilibration) of **1a** described with the OPLS/AA force field[S5]in acetonitrile and chloroform. Atomic charges of ligand **1a** were calculated by the Merz-Singh-Kollman scheme[S6] with B3LYP/6-31G(d) optimized geometry and a single point ESP charge calculation using B3LYP/cc-pVTZ method. A final charge refinement was performed with the RESP method.[S7] The unit cell size was approximately 0.4 × 0.4 × 0.4 nm containing 10 molecules of**1a** solvated in ≈ 1000 molecules of acetonitrile or ≈ 400 molecules of chloroform. Both solvents were also described with the OPLS/AA force field.[S8] 3D periodic boundary conditions were used with long range electrostatic interactions beyond the non-bonded cut-off of 1 nm, accounted for using the particle-mesh Ewald procedure[S9] with Fourier spacing of 0.12 nm. The Nose-Hoover thermostat[S10] and Parrinello-Rahman[S11] barostat with temperature of 298 K (independently controlled for **1a** and solvent phase) and pressure of 1 atm was used. The LINCS algorithm[S12] was employed to constrain all bonds containing hydrogen atoms. Time step used in all simulation was set to 2 fs. Molecular dynamics simulations were performed with GROMACS 4.6.3.[S13]

Quantum-Chemical Calculations

Density functional theory (DFT) was used for geometry optimizations of **1a** and **2a**, together with their corresponding ½ helix turn structures, at the M06-2X/6-31G(d) level of theory.[S14,S15] During geometry optimization of **1a** and **2a** solvation effects were taken into account by the SMD solvation model[S16] with acetonitrile as a solvent at 298 K and 1 bar. Due to convergence issues, geometry optimizations of ½ helix turn structures of **1a** and **2a** were executed in the gas phase. Time dependent density functional theory (TD-DFT)[S17] calculations for **1a** and **2a** were calculated for the lowest 40 excited states in acetonitrile using long range corrected wB97XD functional[S18] and 6-31G(d) basis set on top of M06-2X optimized geometries. Corresponding UV spectra were generated by convolution of Gaussian functions using calculated excitation wavelengths and oscillatory strengths. All quantum chemical calculations were performed with Gaussian09 suite of codes.[S19]

General Procedure for Variable Concentration NMR Measurements

The compounds were dissolved in 0.6 mL of deuterated solvent and the spectra obtained for the corresponding concentration ranges by successive dilution, keeping the total volume constant.

General Procedure for CD Measurements

For v*ariable concentration measurements* (25 °C), a stock solution of the compounds was prepared in 1 mL of solvent and the aliquots were diluted to obtain the desired concentration range. For v*ariable temperature measurements*, the samples were left to equilibrate for 2 min before recording the CD spectra.

General Procedure for Boc-Protecting Group Removal

The corresponding Boc-protected amino acid or peptide was disolved in DCM–trifluoroacetic acid (1:1, 5 mL) and stirred for 2 h at room temperature. The volatiles were evaporated under reduced pressure and the viscous residue dissolved in 10 mL of DCM. The residual trifluoroacetic acid was neutralized with excess of DIPEA (0.5 mL). This solution was used as is, for further coupling reaction.

Synthetic Procedures

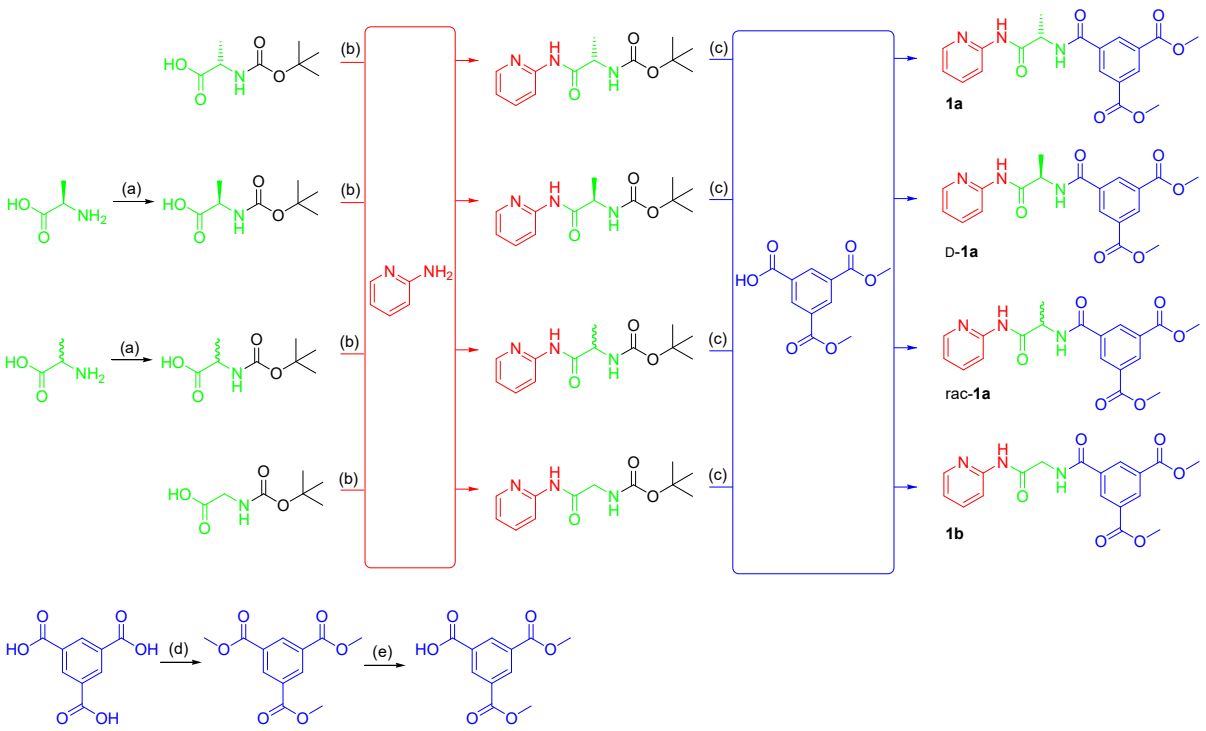

Scheme S1. Ligand preparation: (a) Boc_2O, dioxane/ NaOH(aq), 5 °C to RT, 3 d; (b) DCC/ DCM, RT, 20 h; (c) 1. TFA/DCM (1:1), RT, 2 h, 2. TBTU/ HOBt/ DIPEA/ DCM, RT, 20 h; (d) $MeOH/H_2SO_4$ (conc.), MW/ reflux; (e) NaOH(aq)/MeOH, MW, 50 °C, 15 min.

Preparation of Me_3BTC

1,3,5-benzene tricarboxylic acid (2.61 g, 12.4 mmol) was added in 50 mL of methanol with 0.5 mL of conc. sulphuric acid and heated in a CEM Microwave Reactor for 1 h (150 W, 58 °C). The solution was then refluxed on a conventional oil bath for 15 h. The solvent was evaporated and 100 mL of dichloromethane was added, washed twice with 100 mL $NaHCO_3$ (aq. sat.) and water, dried on Na_2SO_4 (anhydr.), and the solvent evaporated under reduced pressure. Yield: 2.86 g (91 %), white powder. ^{1}H NMR (300.13 MHz, $CDCl_3$) δ/ppm: 3.98 (s, 9H, OMe), 8.86 (s, 3H, Ph).

Preparation of Me_2BTC-OH

Me_3BTC (530.9 mg, 2.11 mmol) was put in methanol/water mixture (50mL : 25 mL) and heated until dissolution. NaOH (83.9 mg in 610 µL, 2.10 mmol, aq.) was added and the solution heated in a CEM Microwave Reactor for 15 min (150 W, 50 °C). Methanol was evaporated under reduced pressure and the aqueous residue was washed with 30 mL of dichloromethane. HCl (178 µL conc. in 10 mL, 2.10 mmol, aq.) was added and the white precipitate was extracted with EtOAc(3×30 mL), dried on Na_2SO_4 (anhydr.), and the solvent evaporated under reduced pressure . Yield: 417.4 mg (83 %), white powder.^{1}H NMR (300.13

MHz, DMSO-d_6) δ/ppm: 3.93 (s, 6H, OMe), 8.64 (t, 1H, J = 2 Hz, *p*-Ph), 8.66 (d, 2H, J = 2 Hz, *o*-Ph), 13.69 (s, 1H, COOH).

Preparation of Boc-D-Ala-OH

D-Alanine (820 mg, 9.20 mmol) was dissolved in 44 mL of a 1:1 dioxane/NaOH (451 mg, 11.28 mmol, aq.) mixture and cooled in an ice bath. Boc_2O (2.5 mL, 10.88 mmol, ρ = 0.950 g cm^{-3}) was added dropwise and continued stirring for 3 days at room temperature. Dioxane was evaporated under reduced pressure and 30 mL of Citric Acid (10 %, aq) and extracted with EtOAc (3×40 mL). The organic layers were washed with 100 mL of NaCl (aq. sat.) and water, dried on Na_2SO_4 (anhydr.), and the solvent evaporated under reduced pressure. Yield: 1.51 g (87 %), white powder.^{1}H NMR (600.14 MHz, DMSO-d_6) δ/ppm: 1.22 (d, 3H, J = 7.5 Hz, β), 1.38 (s, 9H, Boc), 3.89–3.94 (m, 1H, α), 7.09 (d, 1H, J = 7.5 Hz, NH), 12.37 (s, 1H, COOH).

Preparation of Boc-L,D-Ala-OH

L,D-Alanine (406.1 mg, 4.56 mmol) was dissolved in 22 mL of a 1:1:1 dioxane/water/1M NaOH (5.5 mmol, aq.) mixture and cooled in an ice bath. Boc_2O (1.15 mL, 5.01 mmol, ρ = 0.950 g cm^{-3}) was added dropwise and continued stirring for 4 days at room temperature. Dioxane was evaporated under reduced pressure and 30 mL of Citric Acid (10 %, aq) and extracted with EtOAc (3×30 mL). The organic layers were washed with 100 mL of NaCl (aq, sat.) and water, dried on Na_2SO_4 (anhydr.), and the solvent evaporated under reduced pressure . Yield: 675.6 mg (78 %), white powder. ^{1}H NMR (600.14 MHz, DMSO-d_6) δ/ppm: 1.22 (d, 3H, J = 7.5 Hz, β), 1.38 (s, 9H, Boc), 3.87–3.97 (m, 1H, α), 7.06 (d, 1H, J = 7.5 Hz, NH), 12.36 (s, 1H, COOH).

Preparation of Boc-Gly-2ampy

Boc-Gly-OH (744.7 mg, 4.25 mmol) was dissolved in 50 mL of dichloromethane and DCC (876.6 mg, 4.25 mmol) was added and stirred for 0.5 h. To a chalky solution, 2-aminopyridine (399.4 mg, 4.24 mmol) was added and the mixture continued stirring at room temperature overnight. The white precipitate was filtered off (white ribbon), the solvent evaporated and the crude product purified by automated flash chromatography on a pre-packed silica gel column (24 g) using EtOAc/hexane gradient (R_f = 0.36, EtOAc:hexane = 1:1). Yield: 392.3 mg (37 %), white powder.^{1}H NMR (300.13 MHz, $CDCl_3$) δ/ppm: 1.48 (s, 9H, Boc), 4.00 (d, 2H, J = 5.5 Hz, α), 5.22 (ws, 1H, NH-Gly), 7.04–7.08 (m, 1H, 5-py), 7.69–7.74 (m, 1H, 4-py), 8.20 (d, 1H, J = 8.5 Hz, 3-py), 8.28–8.30 (m, 1H, 6-py), 8.59 (s, 1H, NH-py).

Preparation of Boc-L-Ala-2ampy

Boc-L-Ala-OH (765.1 mg, 4.04 mmol) was dissolved in 50 mL of dichloromethane and DCC (835.2 mg, 4.05 mmol) was added and stirred for 0.5 h. To a chalky solution, 2-aminopyridine (392.5 mg, 4.17 mmol) was added and the mixture continued stirring at room temperature overnight. The white precipitate was filtered off (white ribbon), the solvent evaporated and the crude product purified by automated flash chromatography on a pre-packed silica gel column (24 g) using EtOAc/hexane gradient (R_f = 0.46, EtOAc:hexane = 1:1). Yield: 586.2 mg (55 %), white powder. ^{1}H NMR (300.13 MHz, $CDCl_3$) δ/ppm: 1.46 (s, 9H, Boc), 1.49 (d,

3H, *J* = 7 Hz, β), 4.37 (ws, 1H, α), 5.09 (ws, 1H, NH-Ala), 7.04–7.06 (m, 1H, 5-py), 7.70–7.73 (m, 1H, 4-py), 8.22 (d, 1H, *J* = 8.5 Hz, 3-py), 8.28–8.29 (m, 1H, 6-py), 8.78 (s, 1H, NH-py).

Preparation of Boc-D-Ala-2ampy

Boc-D-Ala-OH (393.6 mg, 2.08 mmol) was dissolved in 50 mL of dichloromethane and DCC (440.2 mg, 2.14 mmol) was added and stirred for 0.5 h. To a chalky solution, 2-aminopyridine (210.6 mg, 2.24 mmol) was added and the mixture continued stirring at room temperature overnight. The white precipitate was filtered off (white ribbon), the solvent evaporated and the crude product purified by automated flash chromatography on a pre-packed silica gel column (12 g) using EtOAc/hexane gradient (R_f = 0.46, EtOAc:hexane = 1:1). Yield: 206.9 mg (38 %), white powder. ^{1}H NMR (300.13 MHz, CD_3CN) δ/ppm: 1.35 (d, 3H, *J* = 7 Hz, β), 1.41 (s, 9H, Boc), 4.16–4.25 (m, 1H, α), 5.74 (ws, 1H, NH-Ala), 7.06–7.10 (m, 1H, 5-py), 7.72–7.77 (m, 1H, 4-py), 8.10 (d, 1H, *J* = 8.5 Hz, 3-py), 8.26–8.29 (m, 1H, 6-py), 8.82 (s, 1H, NH-py).

Preparation of Boc-L,D-Ala-2ampy

Boc-L,D-Ala-OH (1025.5 mg, 5.38 mmol) was dissolved in 50 mL of dichloromethane and DCC (1084.9 mg, 5.27 mmol) was added and stirred for 0.5 h. To a chalky solution, 2-aminopyridine (511.1 mg, 5.44 mmol) was added and the mixture continued stirring at room temperature overnight. The white precipitate was filtered off (white ribbon), the solvent evaporated and the crude product purified by automated flash chromatography on a pre-packed silica gel column (40 g) using EtOAc/hexane gradient (R_f = 0.46, EtOAc:hexane = 1:1). Yield: 776.7 mg (56 %), white powder. ^{1}H NMR (600.14 MHz, $CDCl_3$) δ/ppm: 1.46 (d, 3H, *J* = 7 Hz, β), 1.46 (s, 9H, Boc), 4.38 (ws, 1H, α), 5.10 (ws, 1H, NH-Ala), 7.04–7.06 (m, 1H, 5-py), 7.70–7.72 (m, 1H, 4-py), 8.21 (d, 1H, *J* = 8.5 Hz, 3-py), 8.29–8.30 (m, 1H, 6-py), 8.74 (s, 1H, NH-py).

Preparation of **1a**, Me_2BTC-L-Ala-2ampy

Me_2BTC-OH (209.2, 0.88 mmol), TBTU (282.8 mg, 0.88 mmol), HOBt (117.2 mg, 0.87 mmol), and DIPEA (580 µL, 3.51 mmol) were added in 50 mL of dichloromethane and stirred for 1 h at room temperature. Dichloromethane solution of deprotected amine H-Ala-2ampy (0.94 mmol) was added and continued stirring overnight. The reaction mixture was washed with 50 mL $NaHCO_3$ (aq, sat.), Citric Acid (aq, 10 %), and water, dried on Na_2SO_4 (anhydr.) and and the product purified by automated flash chromatography on a pre-packed silica gel column (12 g) using EtOAc/hexane gradient (R_f = 0.16, EtOAc:hexane = 1:1). Yield: 189.1 mg (56 %), white powder. ^{1}H NMR (300.13 MHz, $CDCl_3$) δ/ppm: 1.64 (d, 3H, *J* = 7 Hz, β), 3.97 (s, 6H, OMe), 4.94–5.03 (m, 1H, α), 7.05–7.09 (m, 1H, 5-py), 7.28 (d, 1H, NH-Ala, solvent peak overlap), 7.70–7.76 (m, 1H, 4-py), 8.20 (d, 1H, *J* = 8 Hz, 3-py), 8.30–8.32 (m, 1H, 6-py),8.68 (d, 2H, *J* = 1.5 Hz, *o*-Ph), 8.80 (t, 1H, *J* = 1.5 Hz, *p*-Ph), 8.98 (s, 1H, NH-py).^{13}C NMR (150.92 MHz, $CDCl_3$) δ/ppm: 18.7 (Cβ), 50.6 (Cα), 52.8 (OMe), 114.5 (C3-py), 120.4 (C5-py), 131.3 (C3-Ph), 132.5 (C2-Ph), 133.7 (C4-Ph), 134.6 (C1-Ph), 138.7 (C4-py), 148.1 (C6-py), 151.2 (C2-py), 165.6 (COO), 171.3 (CONH, Ph). MALDI-HRMS (*m*/*z*): calcd 386.1352 ($[C_{19}H_{20}N_3O_6 + H]^+$), found 386.1337.

Preparation of D-**1a**, Me_2BTC-D-Ala-2ampy

Me_2BTC-OH (141.6, 0.59 mmol), TBTU (189.6 mg, 0.59 mmol), and DIPEA (165 μL, 1.00 mmol) were added in 50 mL of dichloromethane and stirred for 1 h at room temperature. Dichloromethane solution of deprotected amine H-D-Ala-2ampy (0.63 mmol) was added and continued stirring overnight. The reaction mixture was washed with 50 mL $NaHCO_3$ (aq, sat.), Citric Acid (aq, 10 %), and water, dried on Na_2SO_4 (anhydr.) and and the product purified by automated flash chromatography on a pre-packed silica gel column (12 g) using EtOAc/hexane gradient (R_f = 0.16, EtOAc:hexane = 1:1). Yield: 123.3 mg (54 %), white powder. ^{1}H NMR (300.13 MHz, CD_3CN) δ/ppm: 1.53 (d, 3H, J = 7 Hz, β), 3.93 (s, 6H, OMe), 4.68–4.77 (m, 1H, α), 7.06–7.10 (m, 1H, 5-py), 7.72–7.77 (m, 1H, 4-py), 7.76 (d, 1H, NH-Ala, 4-py peak overlap), 8.20 (dt, 1H, J_1 = 8.5 Hz, J_2 = 1 Hz, 3-py), 8.26–8.29 (m, 1H, 6-py), 8.65–8.67 (m, 3H, *o,p*-Ph), 9.07 (s, 1H, NH-py).

Preparation of rac-**1a**, Me_2BTC-L,D-Ala-2ampy

Me_2BTC-OH (209.4, 0.88 mmol), TBTU (281.2 mg, 0.88 mmol), HOBt (123.1 mg, 0.91 mmol), and DIPEA (580 μL, 3.51 mmol) were added in 50 mL of dichloromethane and stirred for 1 h at room temperature. Dichloromethane solution of deprotected racemic amine H-Ala-2ampy (0.93 mmol) was added and continued stirring overnight. The reaction mixture was washed with 50 mL $NaHCO_3$ (aq, sat.), Citric Acid (aq, 10 %), and water, dried on Na_2SO_4 (anhydr.) and and the product purified by automated flash chromatography on a pre-packed silica gel column (12 g) using EtOAc/hexane gradient (R_f = 0.16, EtOAc:hexane = 1:1). Yield: 141.6 mg (42 %), white powder. ^{1}H NMR (300.13 MHz, $CDCl_3$) δ/ppm: 1.64 (d, 3H, J = 7 Hz, β), 3.97 (s, 6H, OMe), 4.94–5.04 (m, 1H, α), 7.05–7.09 (m, 1H, 5-py), 7.29 (d, 1H, J= 7.5 Hz, NH-Ala), 7.70–7.76 (m, 1H, 4-py), 8.20 (d, 1H, J = 8.5 Hz, 3-py), 8.30–8.32 (m, 1H, 6-py), 8.69 (d, 2H, J = 1.5 Hz, *o*-Ph), 8.81 (t, 1H, J = 1.5 Hz, *p*-Ph), 9.00 (s, 1H, NH-py).

Preparation of **1b**, Me_2BTC-Gly-2ampy

Me_2BTC-OH (204.7, 0.86 mmol), TBTU (275.5 mg, 0.86 mmol), HOBt (116.6 mg, 0.86 mmol), and DIPEA (220 μL, 1.33 mmol) were added in 50 mL of dichloromethane and stirred for 1 h at room temperature. Dichloromethane solution of deprotected racemic amine H-Gly-2ampy (0.95 mmol) was added and continued stirring overnight. The reaction mixture was washed with 50 mL $NaHCO_3$ (aq, sat.), Citric Acid (aq, 10 %), and water, dried on Na_2SO_4 (anhydr.) and and the product purified by automated flash chromatography on a pre-packed silica gel column (12 g) using EtOAc/hexane gradient (R_f = 0.16, EtOAc:hexane = 1:1). Yield: 200.8 mg (63 %), white powder. ^{1}H NMR (300.13 MHz, $CDCl_3$) δ/ppm: 3.98 (s, 6H, OMe), 4.41 (d, 1H, J = 5 Hz, α), 7.06–7.11 (m, 1H, 5-py), 7.22 (t, 1H, J = 5 Hz, NH-Gly), 7.71–7.77 (m, 1H, 4-py), 8.17 (d, 1H, J = 7 Hz, 3-py), 8.30–8.32 (m, 1H, 6-py), 8.55 (s, 1H, NH-py), 8.71 (d, 2H, J = 1.5 Hz, *o*-Ph), 8.84 (t, 1H, J = 1.5 Hz, *p*-Ph). Due to the low solubility ^{13}C NMR spectra were not recorded. MALDI-HRMS (*m*/*z*): calcd 372.1196 ($[C_{18}H_{18}N_3O_6 + H]^+$), found 372.1197.

Preparation of **2a**, $[Zn(\mathbf{1a})_2(NO_3)_2]$

To a 4 mL acetonitrile solution of $Zn(NO_3)_2 \times 4H_2O$ (18.38 mg, 0.070 μmol) the ligand, **1a**, (54.14 mg, 0.140 mmol) was added and the mixture was shortly boiled. The solvent was

evaporated and dried under vacuum (5 mbar, 30 min). Yield: quantitative (by NMR). ^{1}H NMR (600.14 MHz, $CDCl_3$) δ/ppm: 1.56 (d, 6H, *J* = 7 Hz, β), 3.93 (s, 12H, OMe), 4.69–4.74 (m, 2H, α), 7.18–7.20 (m, 1H, 5-py), 7.65 (ws, 2H, 3-py), 7.83 (ws, 2H, NH-Ala), 7.87–7.89 (m, 2H,4-py), 8.32 (d, 2H, J = 3.5 Hz, 6-py), 8.61 (s, 4H, *o*-Ph), 8.65 (s, 2H, *p*-Ph), 9.80 (s, 1H, NH-py).^{13}C NMR (150.92 MHz, acetonitrile-d_3) δ/ppm: 17.2 (Cβ), 52.5 (Cα), 53.3 (OMe), 117.0 (C3-py), 122.3 (C5-py), 132.2 (C3-Ph), 133.3 (C2-Ph), 133.7 (C4-Ph), 135.4 (C1-Ph), 142.3 (C4-py), 148.1 (C6-py), 152.3 (C2-py), 166.2 (COO), 167.0 (CONH, Ph), 177.5 (CONH, alanine). MALDI-HRMS (*m*/*z*): calcd 833.1761 ($[C_{38}H_{37}N_6O_{12}Zn - H]^+$), found 833.1789.

Preparation of **3a**, $[Zn(\mathbf{1a})_2(BF_4)_2]$

To a 4 mL acetonitrile solution of $Zn(BF_4)_2 \times nH_2O$ (13.18 mg, 0.052 μmol) the ligand, **1a**, (40.44 mg, 0.105 mmol) was added and the mixture was shortly boiled. The solvent was evaporated and dried under vacuum (5 mbar, 1 h). Yield: quantitative (by NMR). ^{1}H NMR (600.14 MHz, acetonitrile-d_3) δ/ppm:1.53 (d, 6H, *J* = 7 Hz), 3.92 (s, 6H), 4.63–4.68 (m, 2H), 7.18 (t, 2H, *J* = 6 Hz), 7.28 (s, 2H), 7.90 (s, 4H), 8.18 (s, 2H), 8.44 (s, 4H), 8.57 (s, 2H), 10.02 (s, 2H). MALDI-HRMS (*m*/*z*): calcd 833.1761 ($[C_{38}H_{37}N_6O_{12}Zn - H]^+$), found 833.1753.

Assigned NMR Spectra

^{1}H NMR ($CDCl_3$) of Me_3BTC

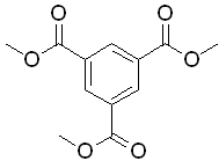

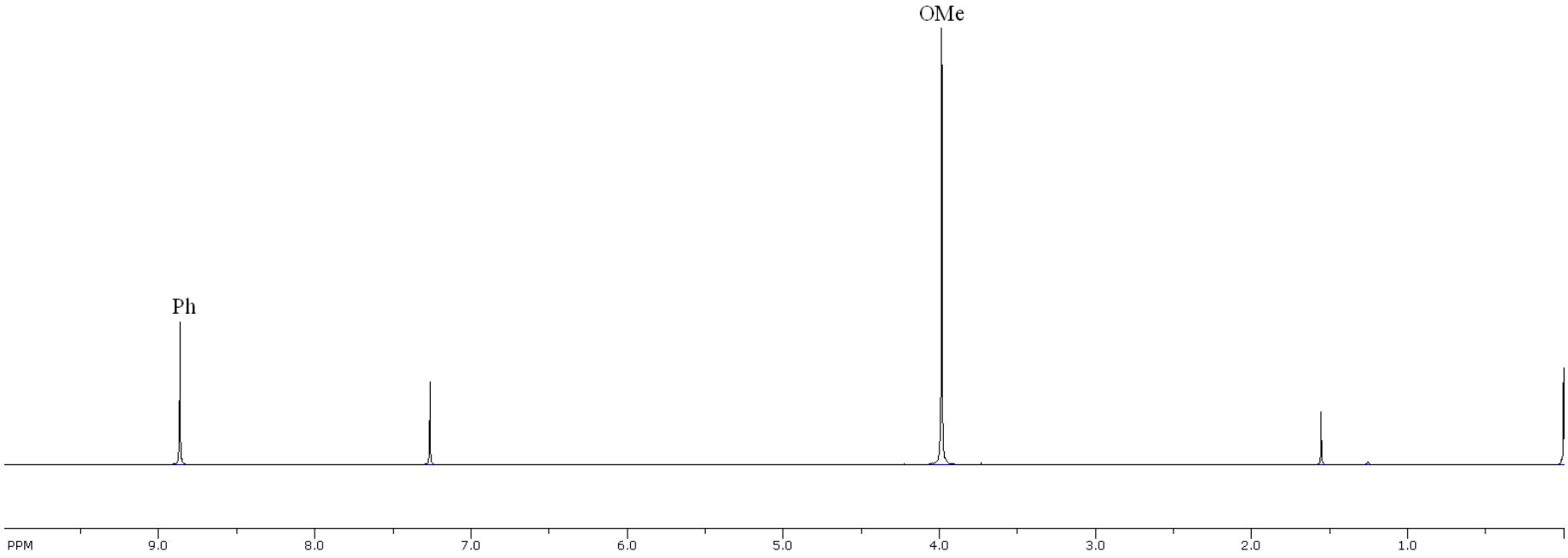

^{1}H NMR (DMSO-d_6) of Me_2BTC-OH

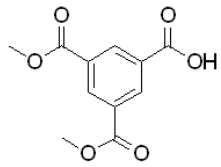

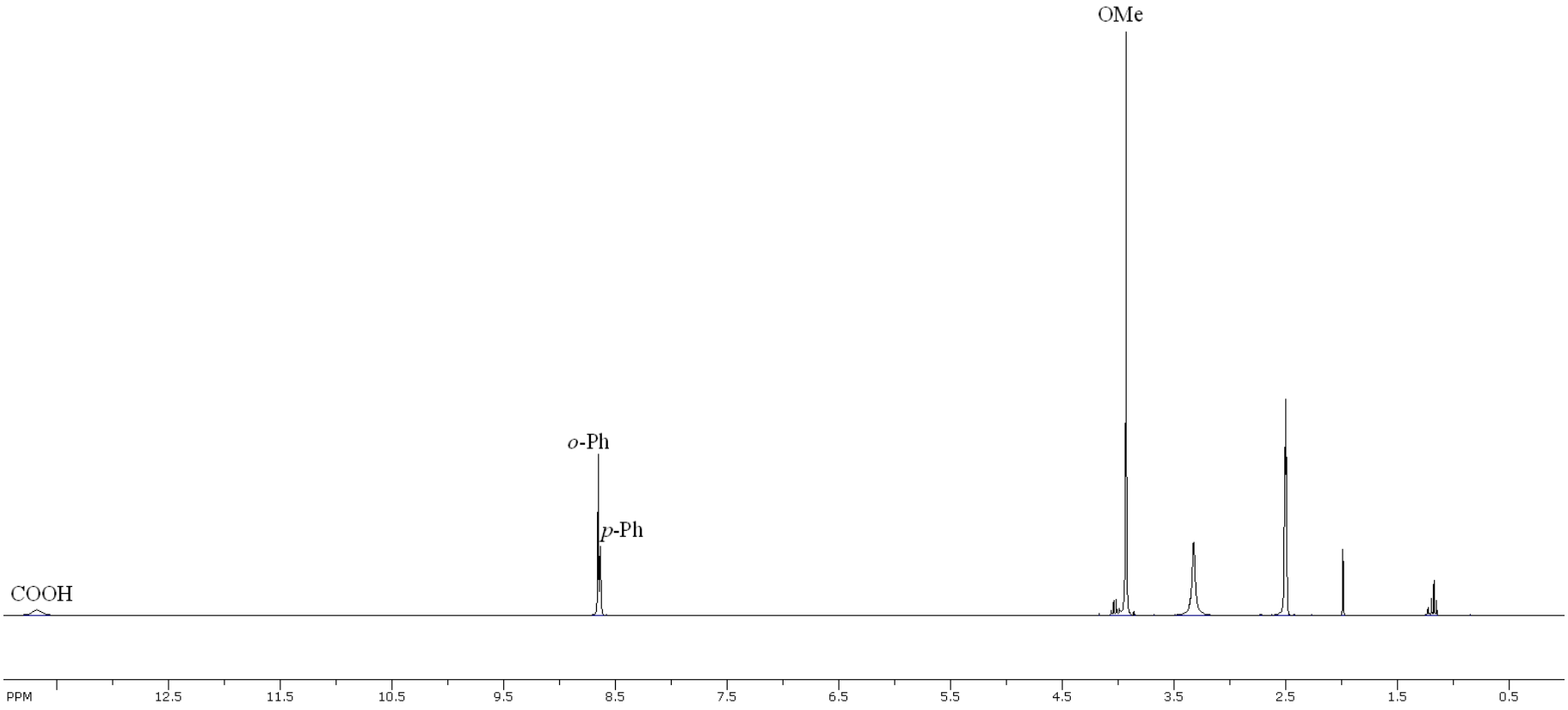

^{1}H NMR (DMSO-d_6) of Boc-D-Ala-OH

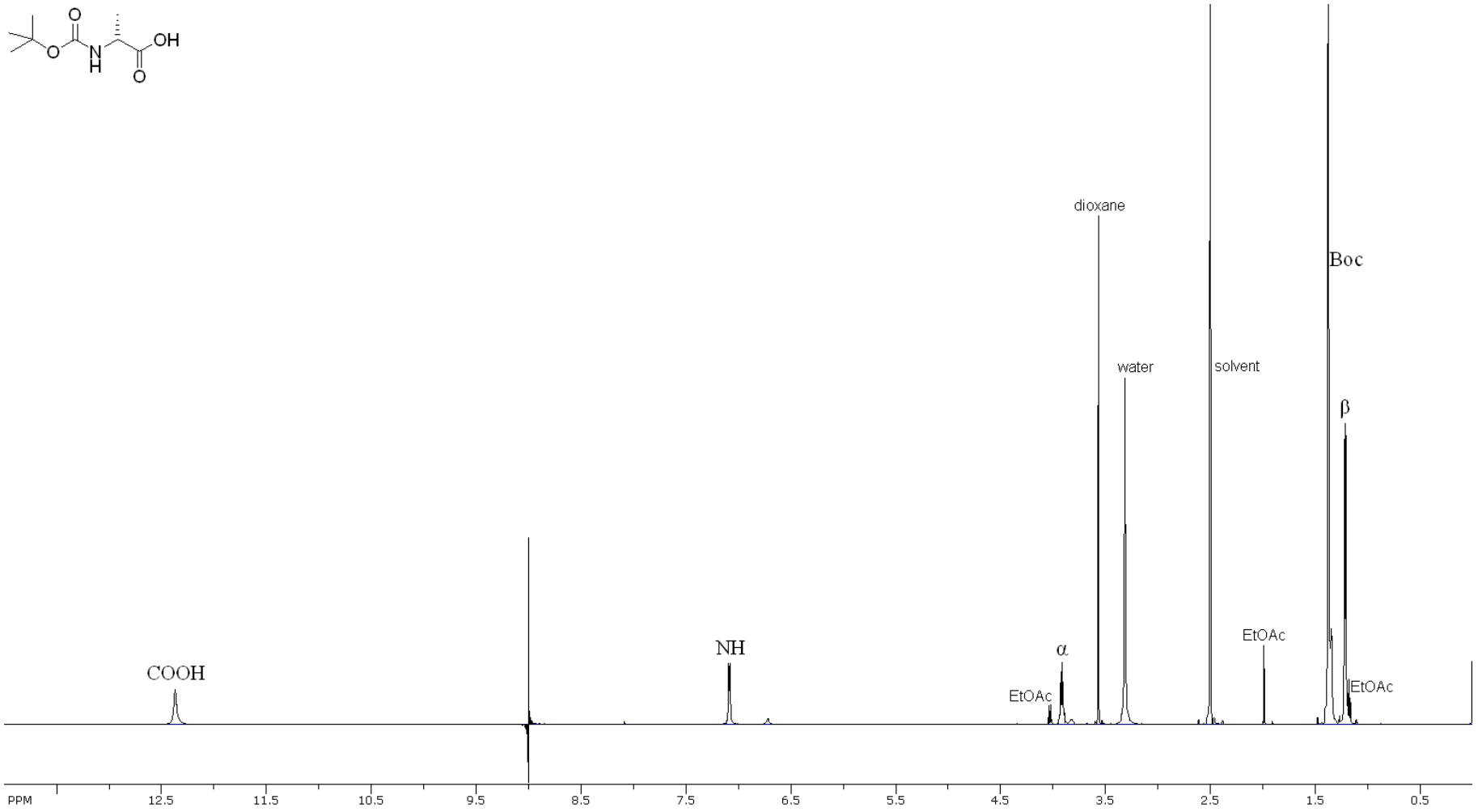

^{1}H NMR (DMSO-d_6) of Boc-D,L-Ala-OH

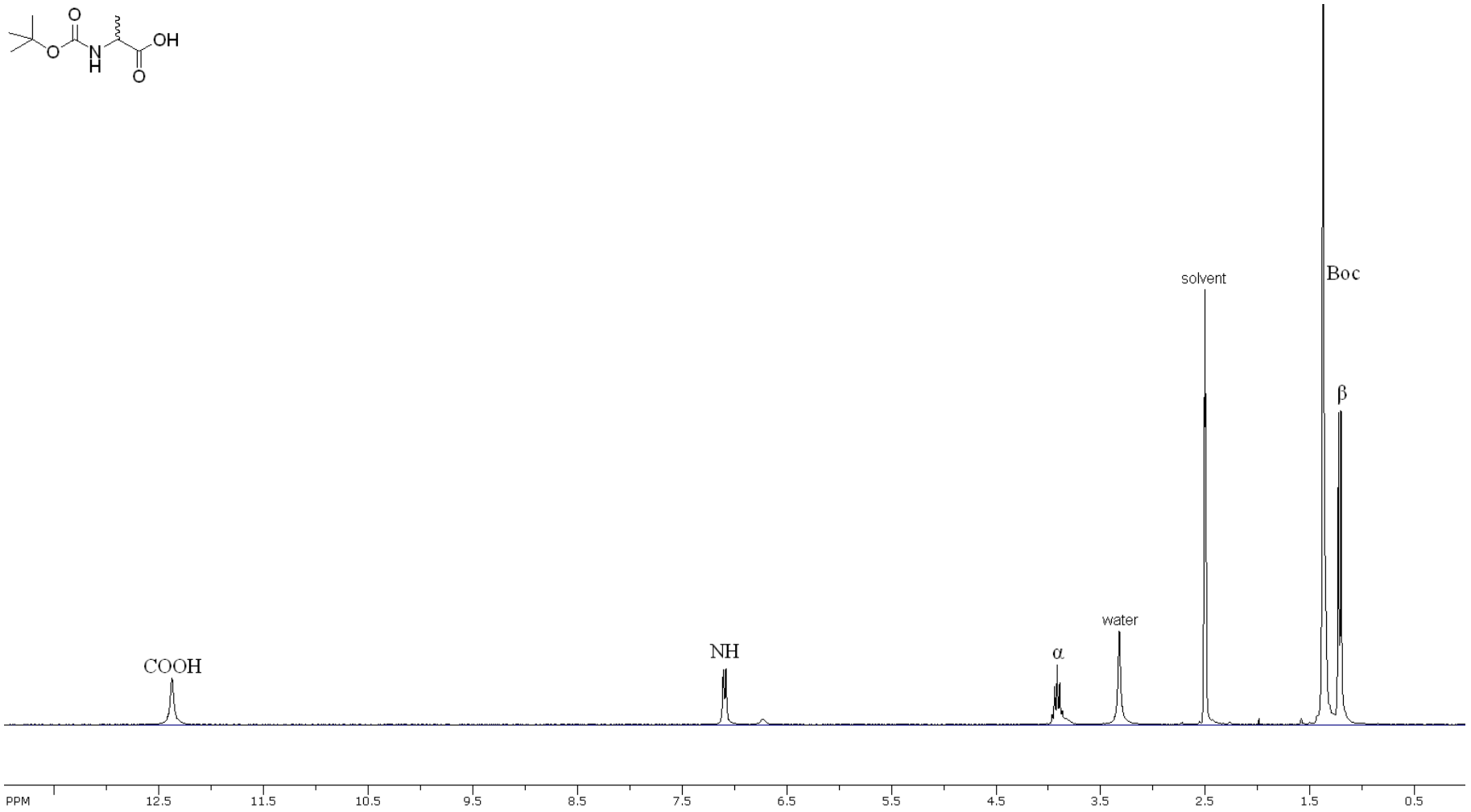

^{1}H NMR ($CDCl_3$) of Boc-Gly-2ampy

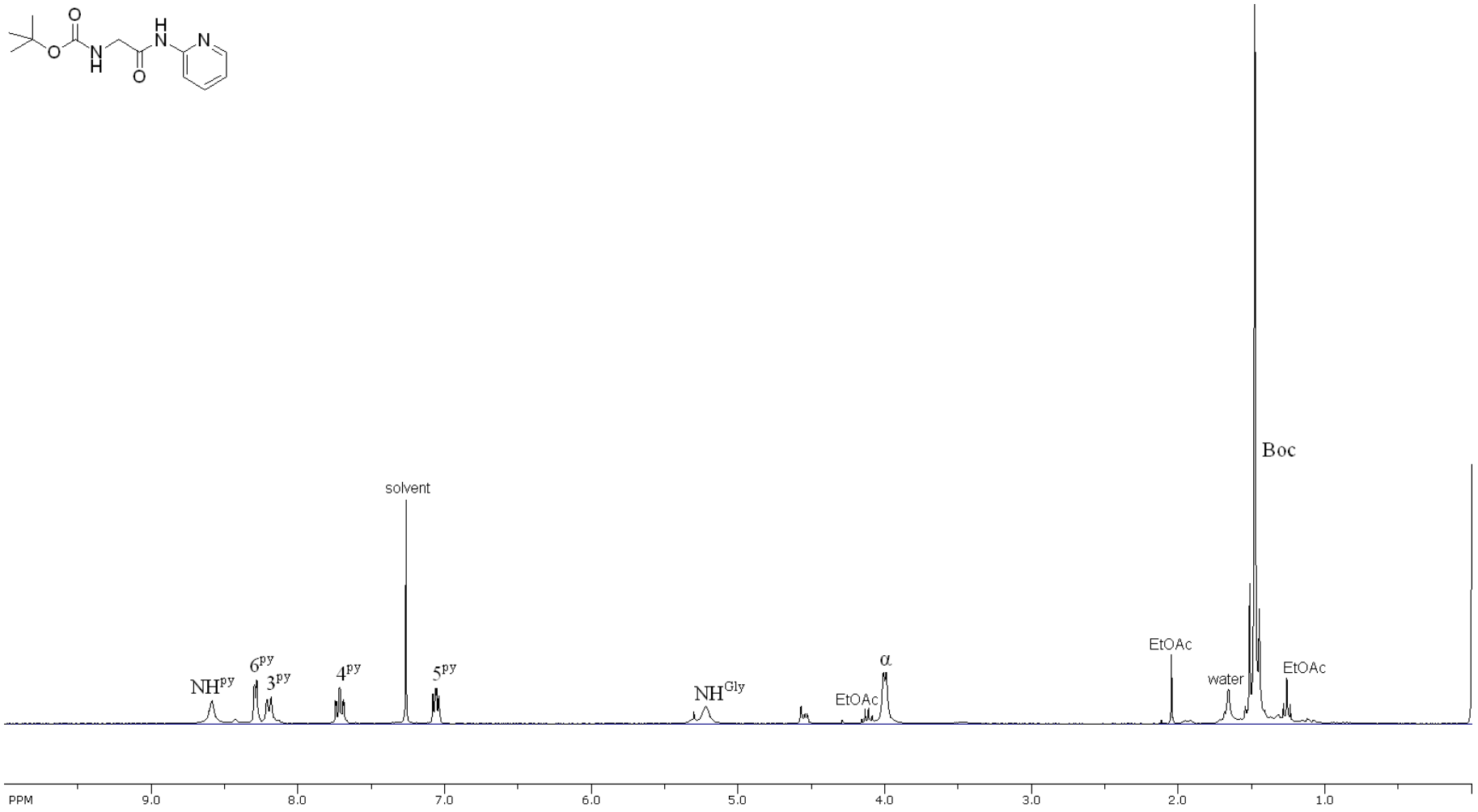

^{1}H NMR ($CDCl_3$) of Boc-L-Ala-2ampy

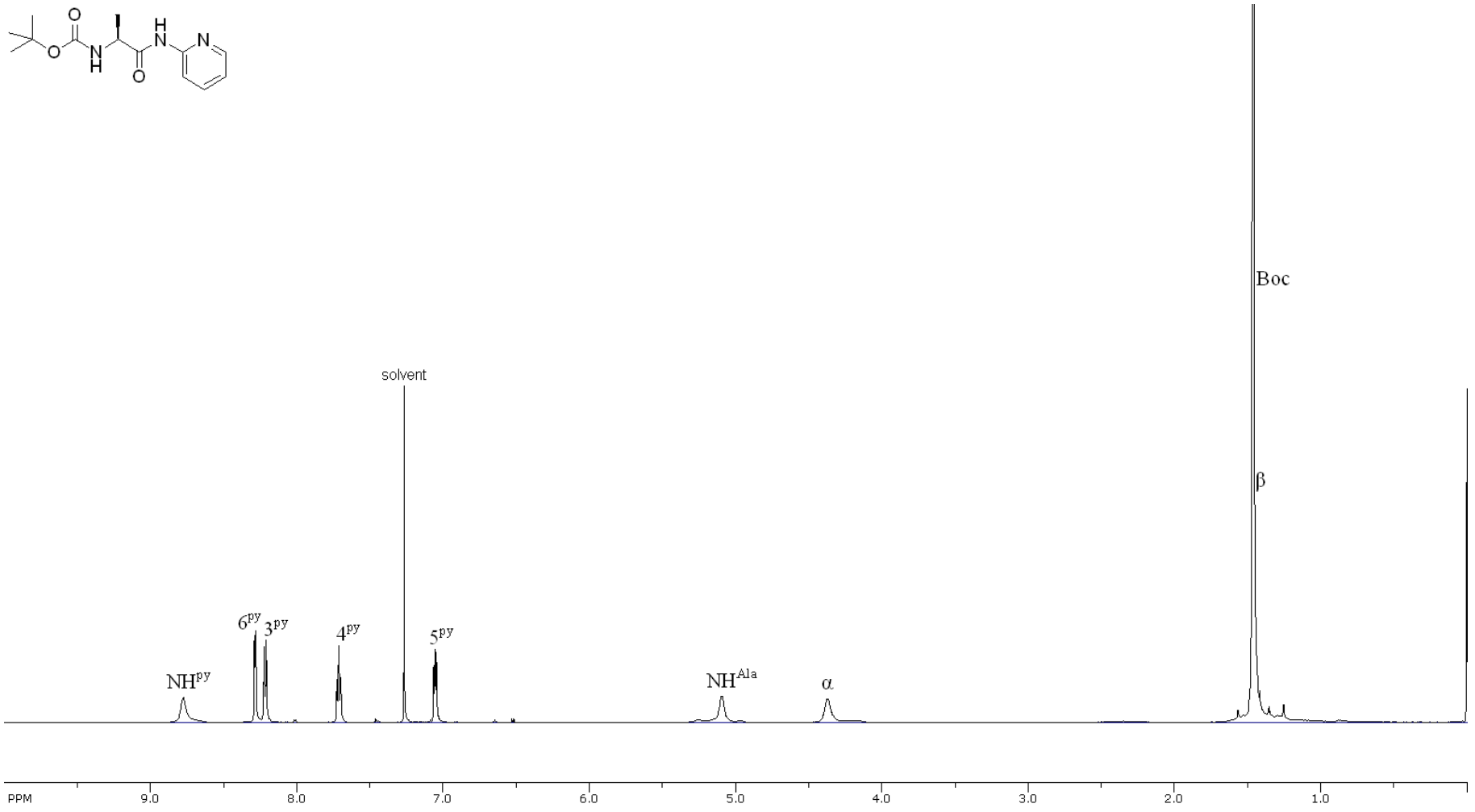

^{1}H NMR (CD_3CN) of Boc-D-Ala-2ampy

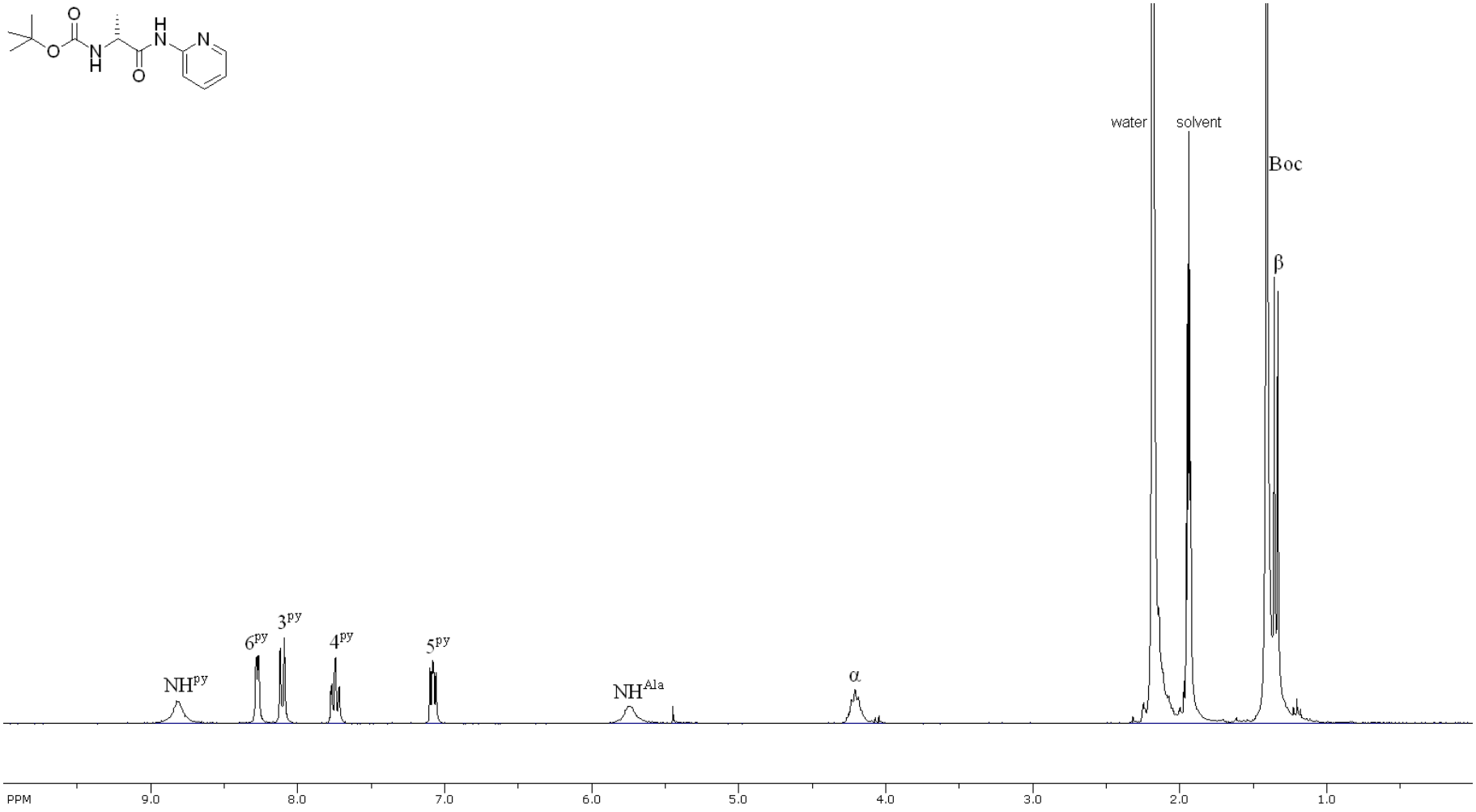

^{1}H NMR ($CDCl_3$) of Boc-D,L-Ala-2ampy

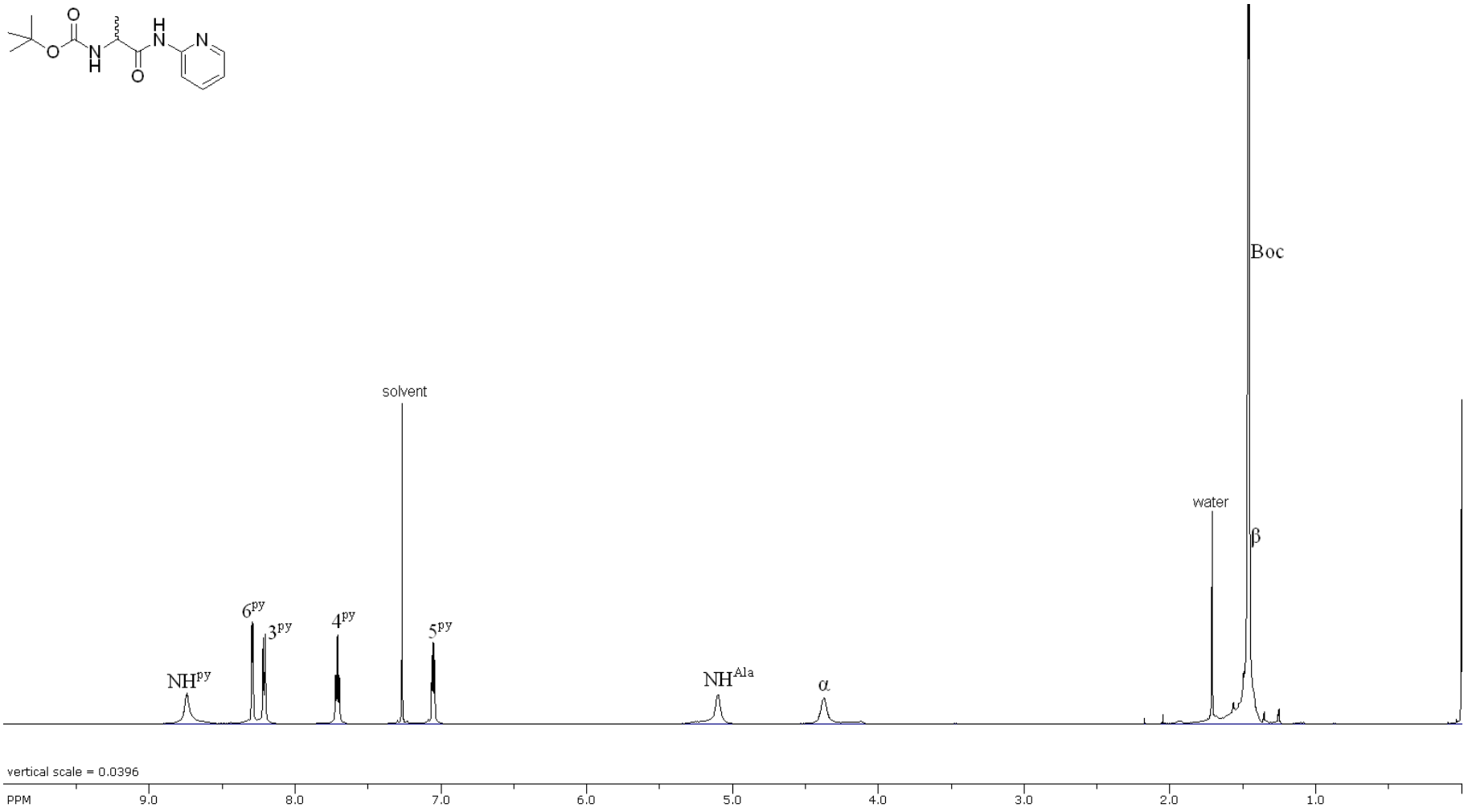

^{1}H NMR ($CDCl_3$) of **1a**, Me_2BTC-L-Ala-2ampy

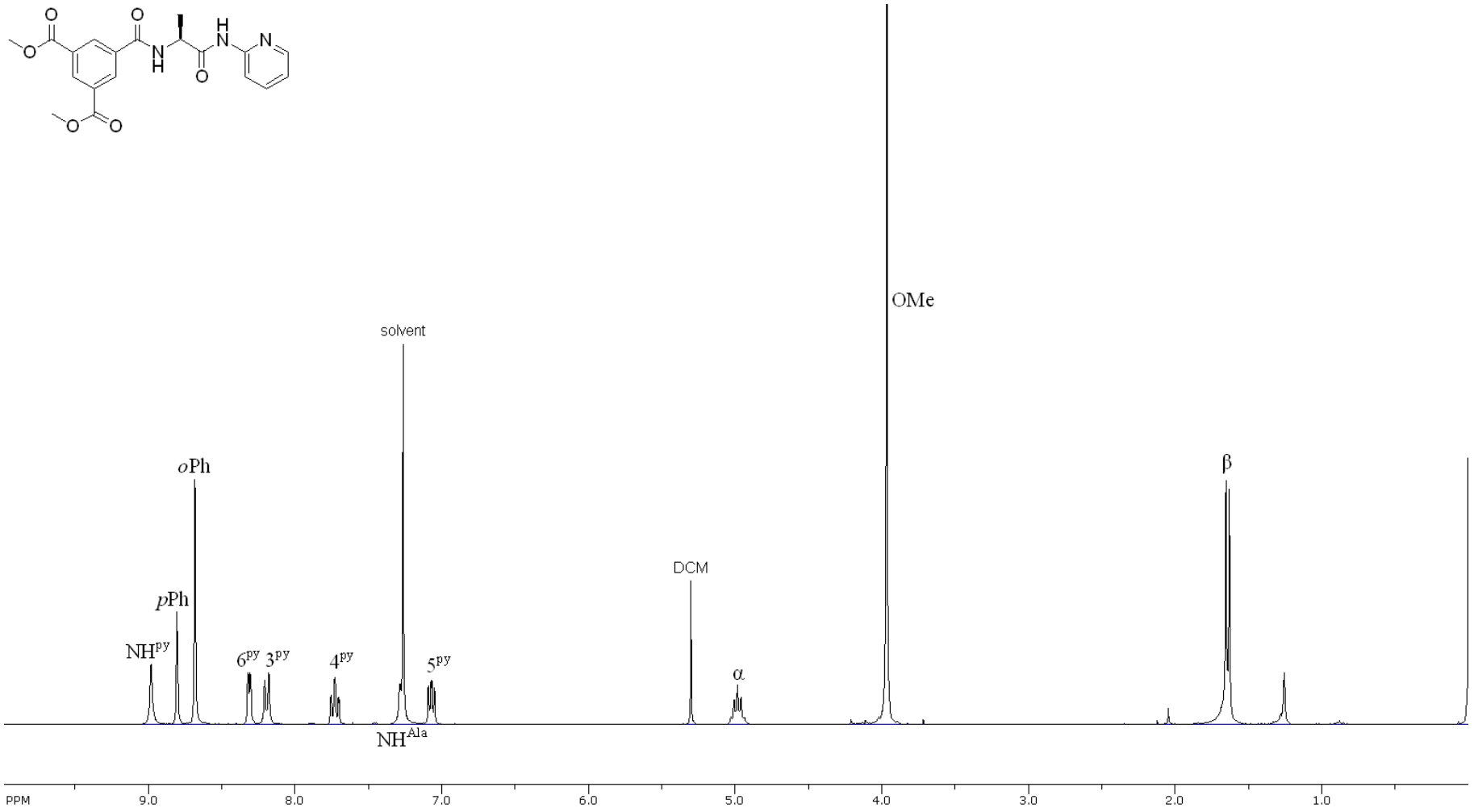

^{13}C NMR ($CDCl_3$) of **1a**, Me_2BTC-L-Ala-2ampy

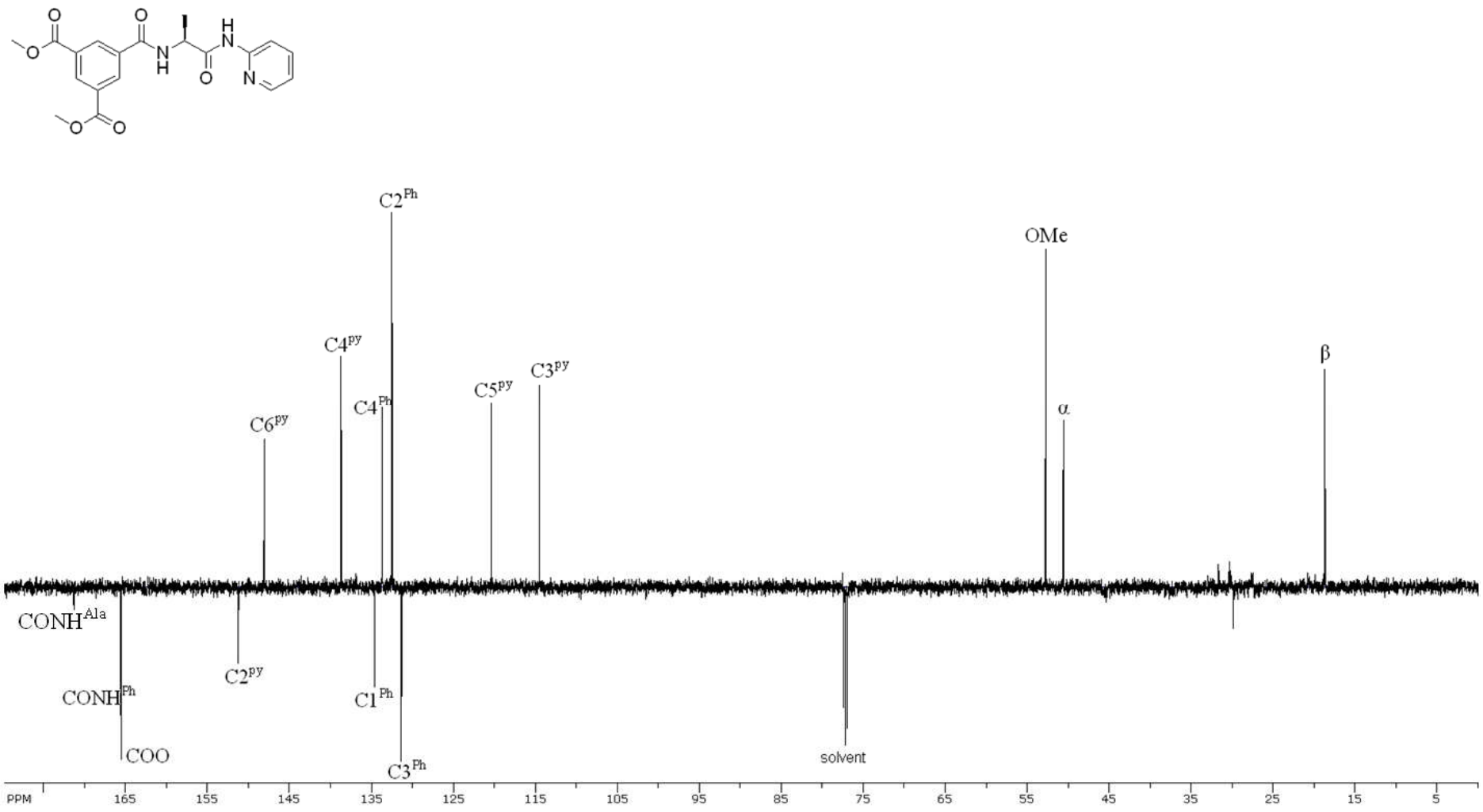

^{13}C NMR (acetonitrile-d_3) of **1a**, Me_2BTC-L-Ala-2ampy

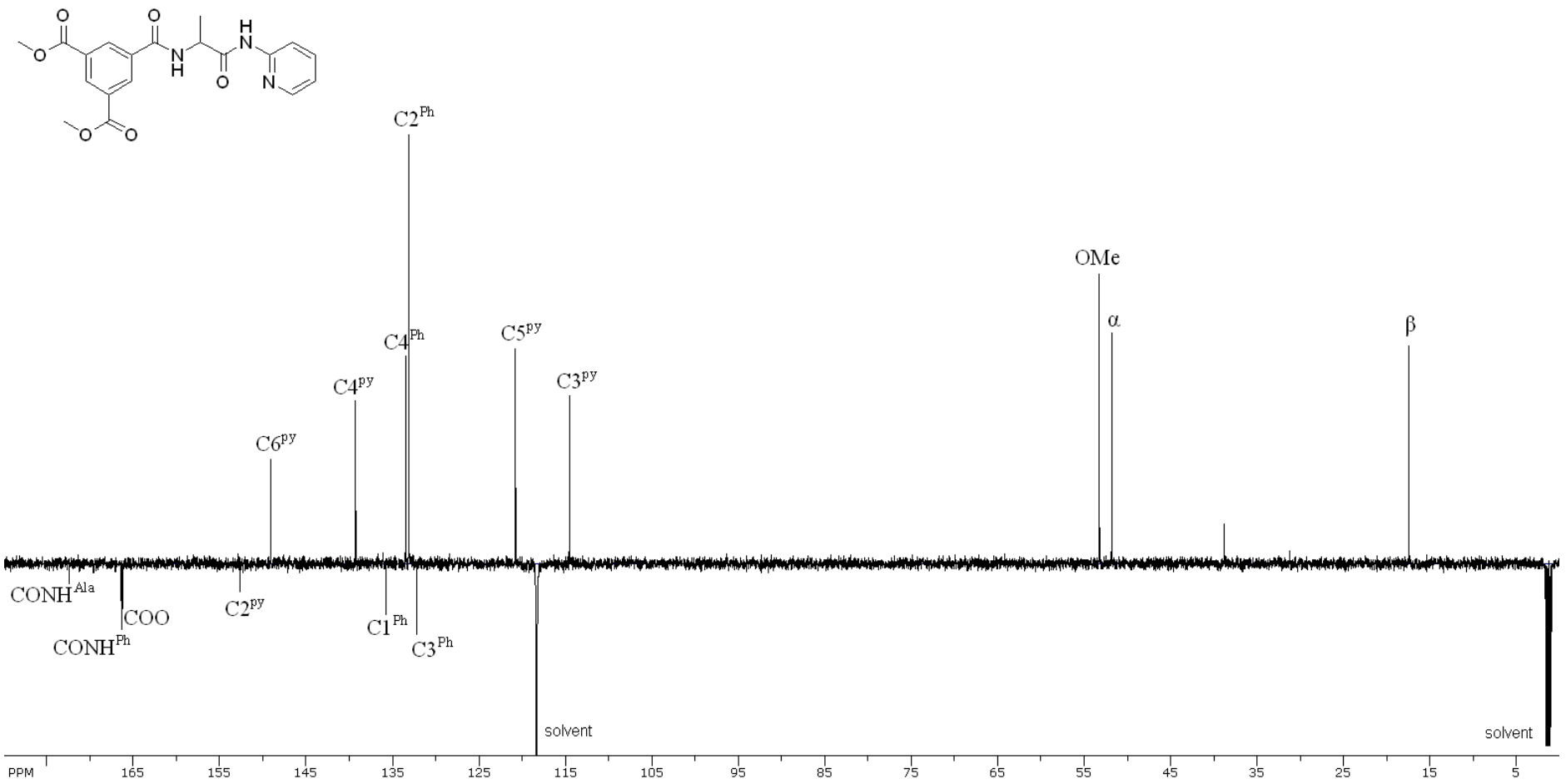

^{1}H NMR (acetonitrile-d_3) of D-**1a**, Me_2BTC-D-Ala-2ampy

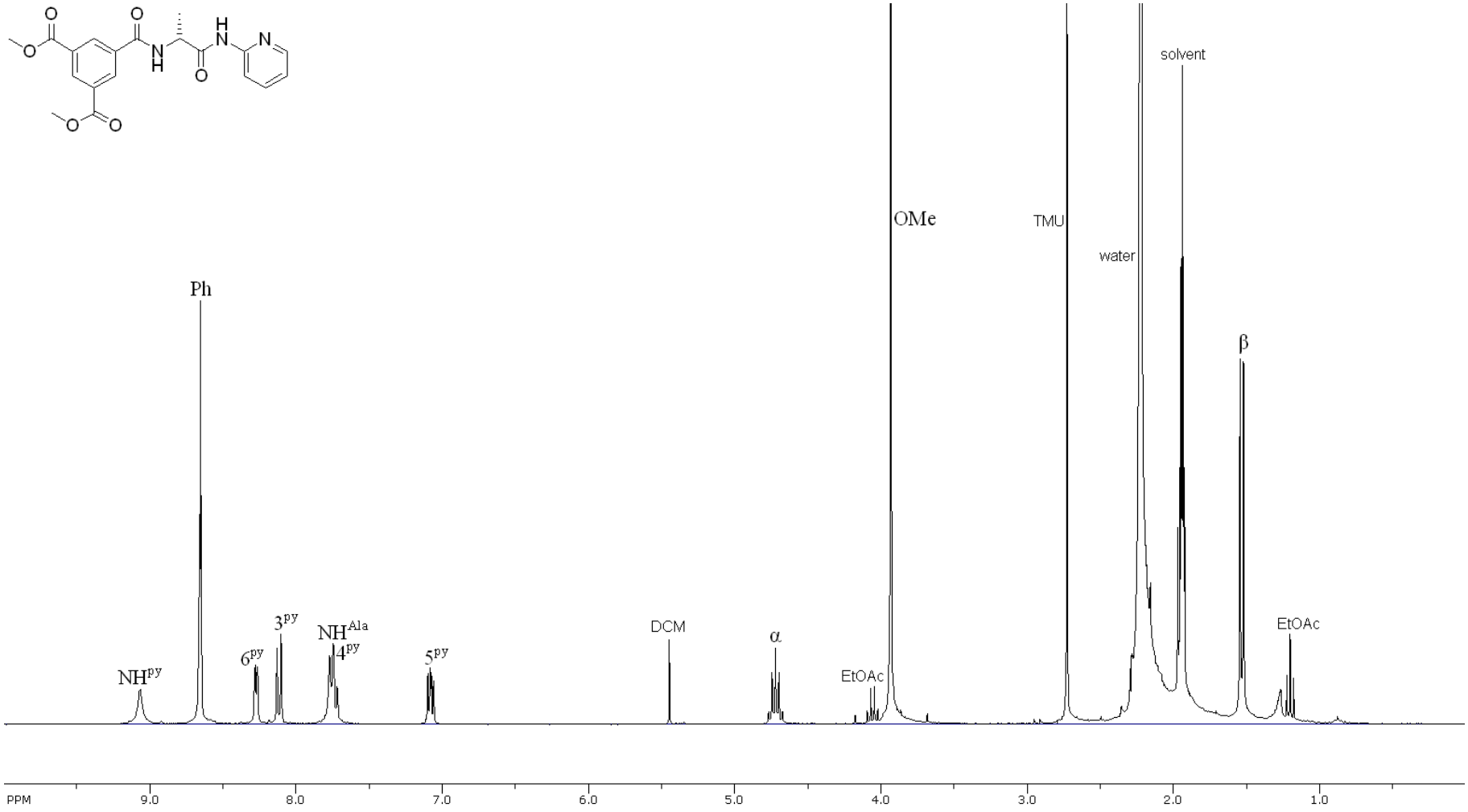

^{1}H NMR ($CDCl_3$) of rac-**1a**, Me_2BTC-D,L-Ala-2ampy

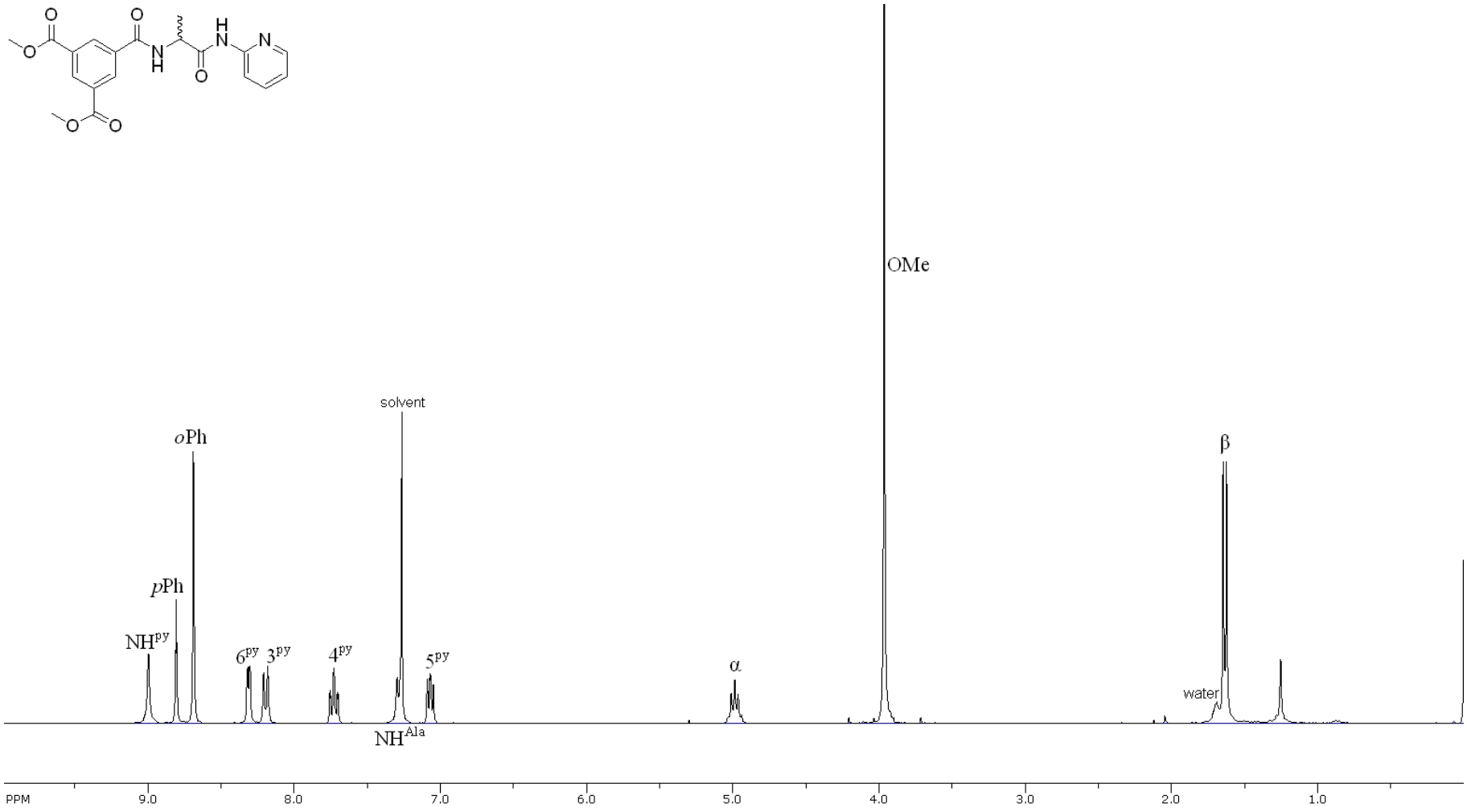

^{1}H NMR ($CDCl_3$) of **1b**, Me_2BTC-Gly-2ampy

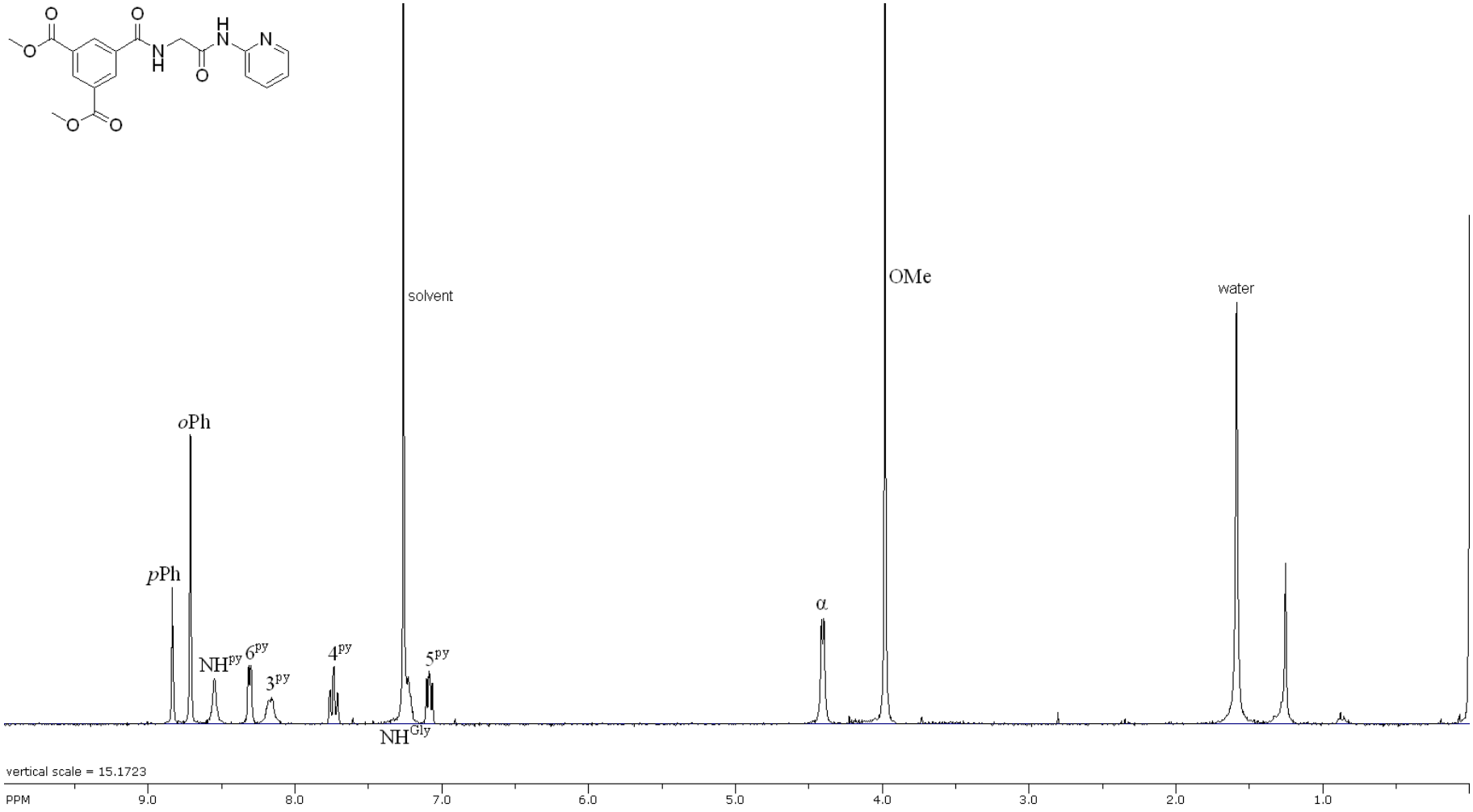

^{1}H NMR (acetonitrile-d_3) of **2a**, [Zn(**1a**)$_2$(NO$_3$)$_2$]

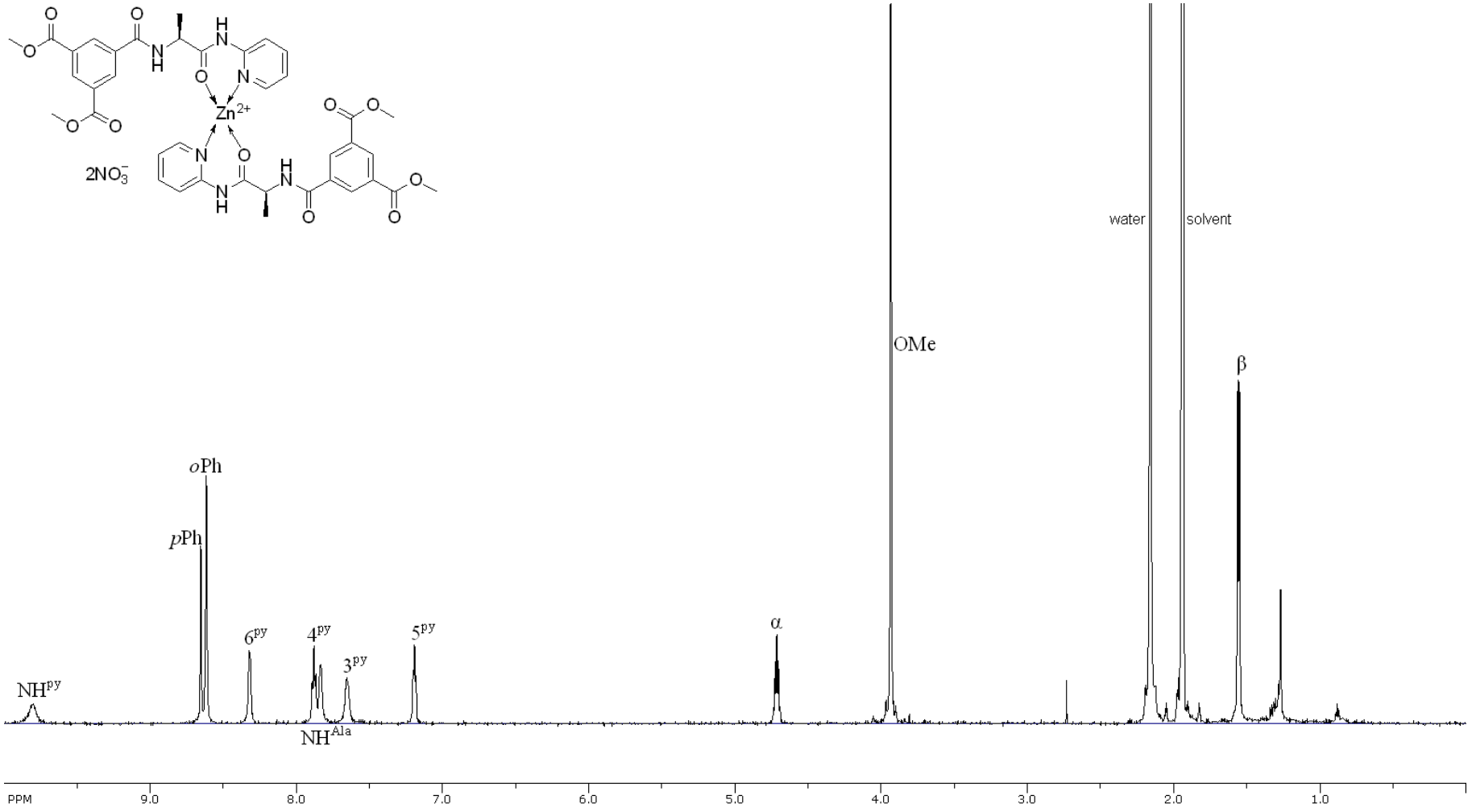

^{13}C NMR (acetonitrile-d_3) of **2a**, [Zn(**1a**)$_2$(NO$_3$)$_2$]

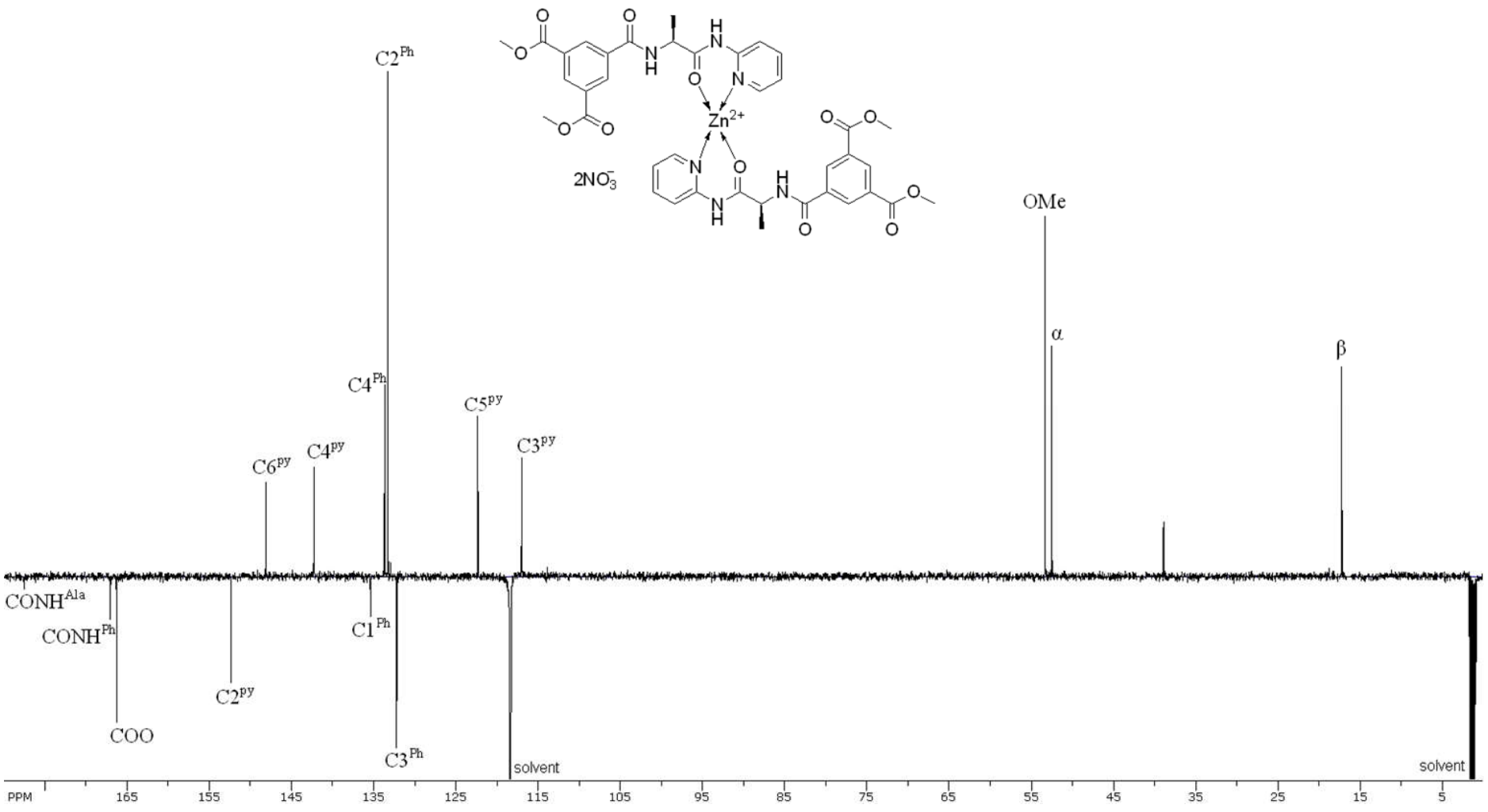

^{1}H NMR (acetonitrile-d_3) of **3a**, [Zn(**1a**)$_2$(BF$_4$)$_2$]

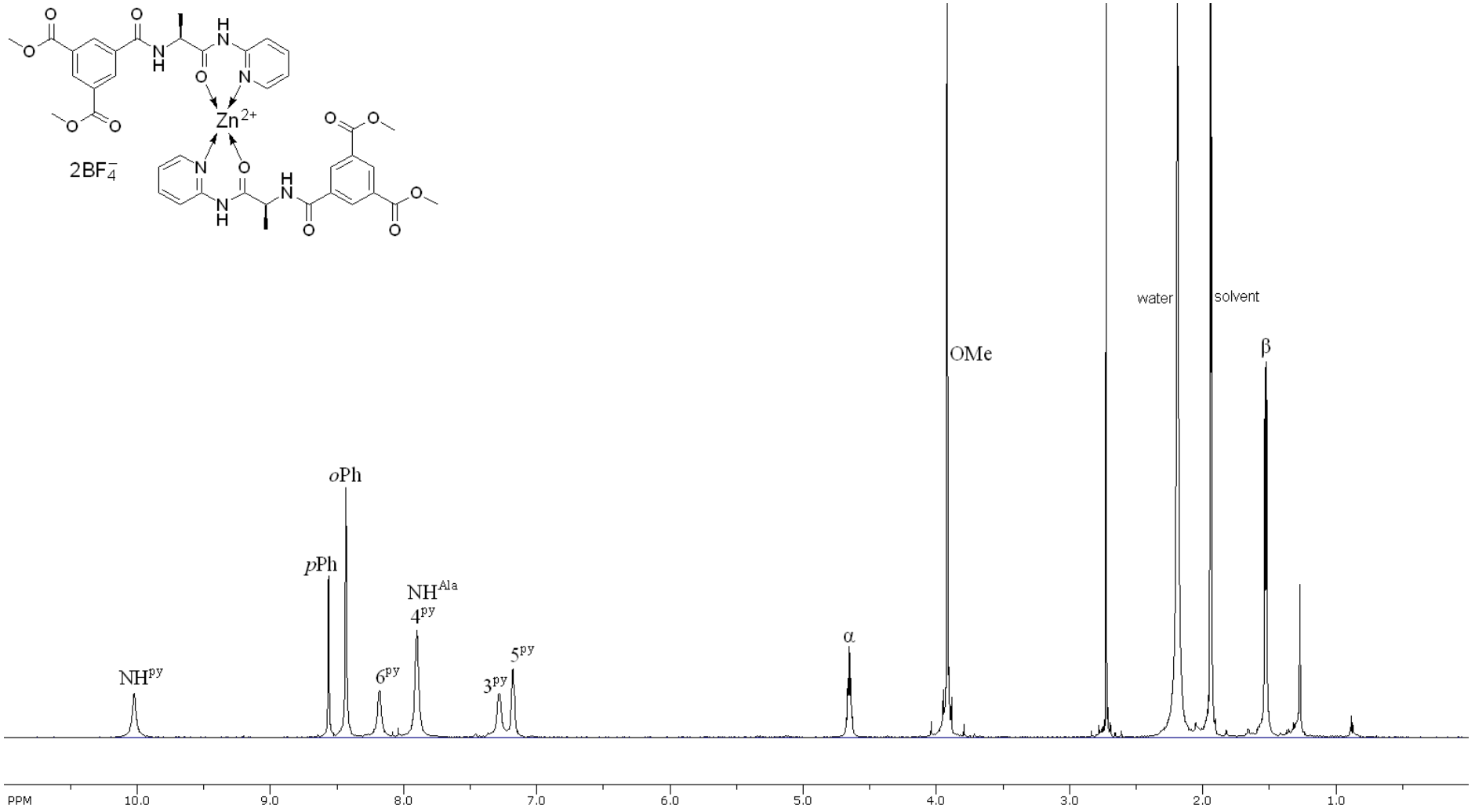

Integrated NMR Spectra

^{1}H NMR ($CDCl_3$) of Me_3BTC

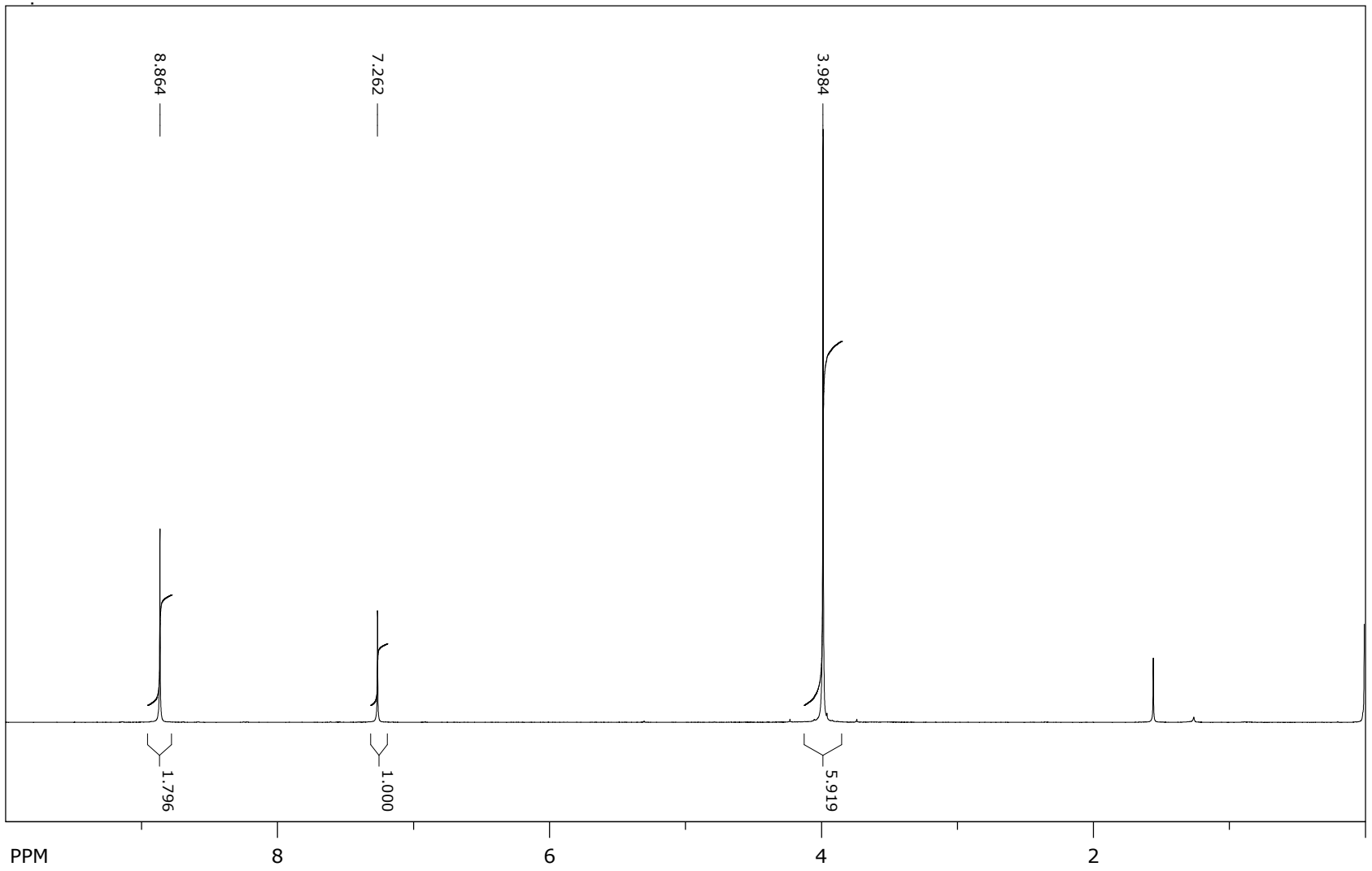

^{1}H NMR (DMSO-d_6) of Me_2BTC-OH

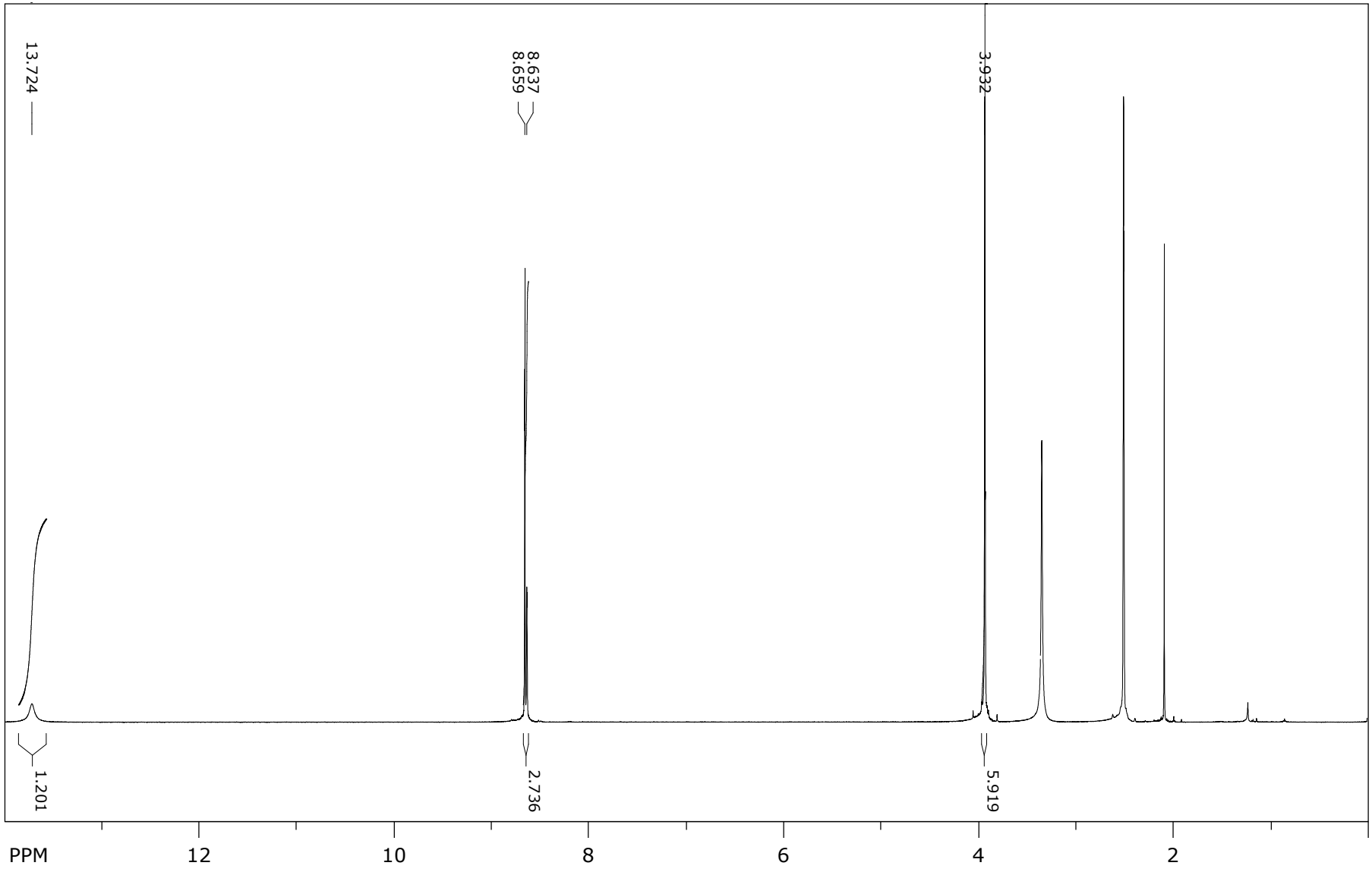

^{1}H NMR (DMSO-d_6) of Boc-D-Ala-OH

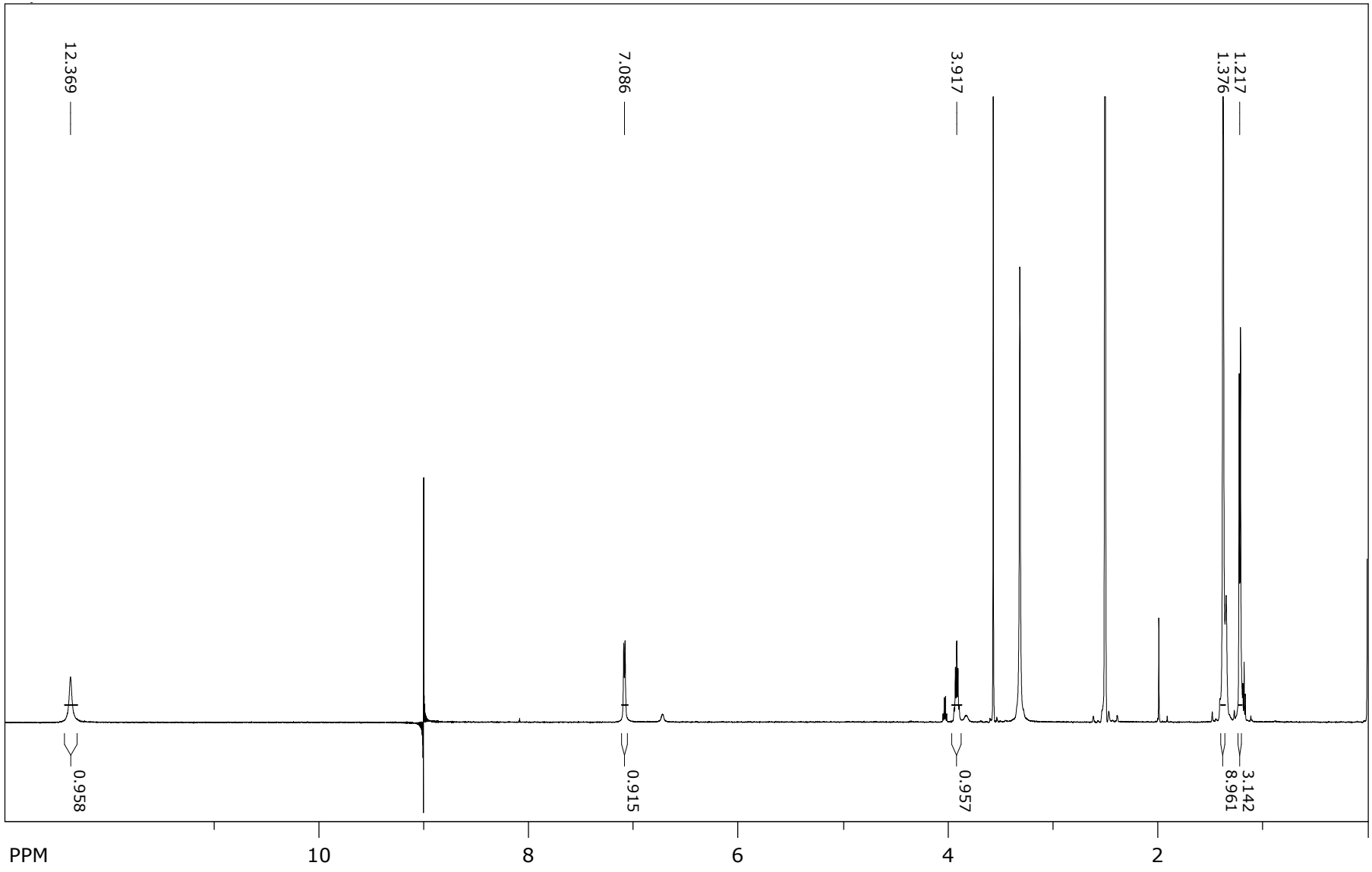

^{1}H NMR (DMSO-d_6) of Boc-D,L-Ala-OH

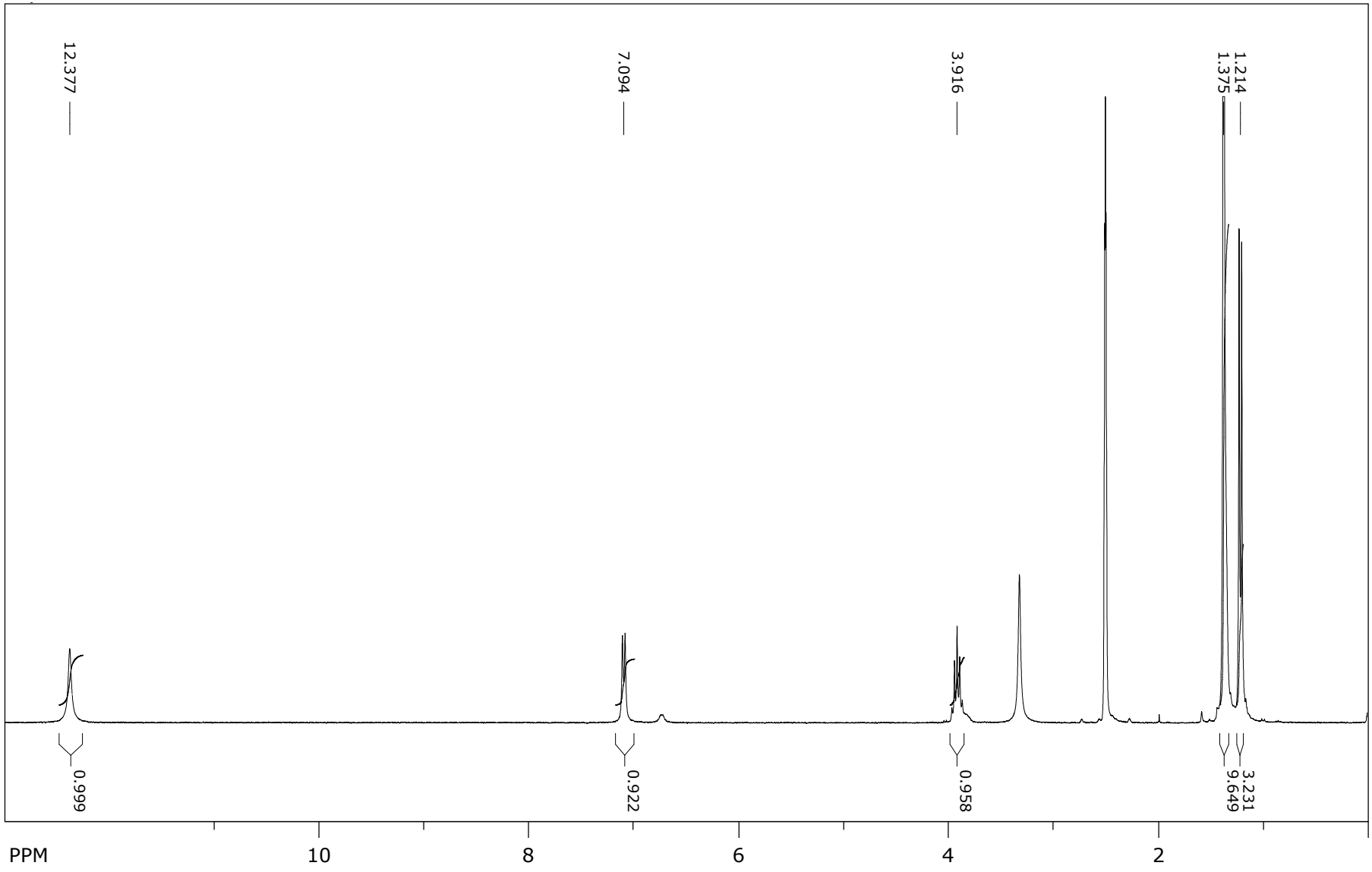

^{1}H NMR ($CDCl_3$) of Boc-Gly-2ampy

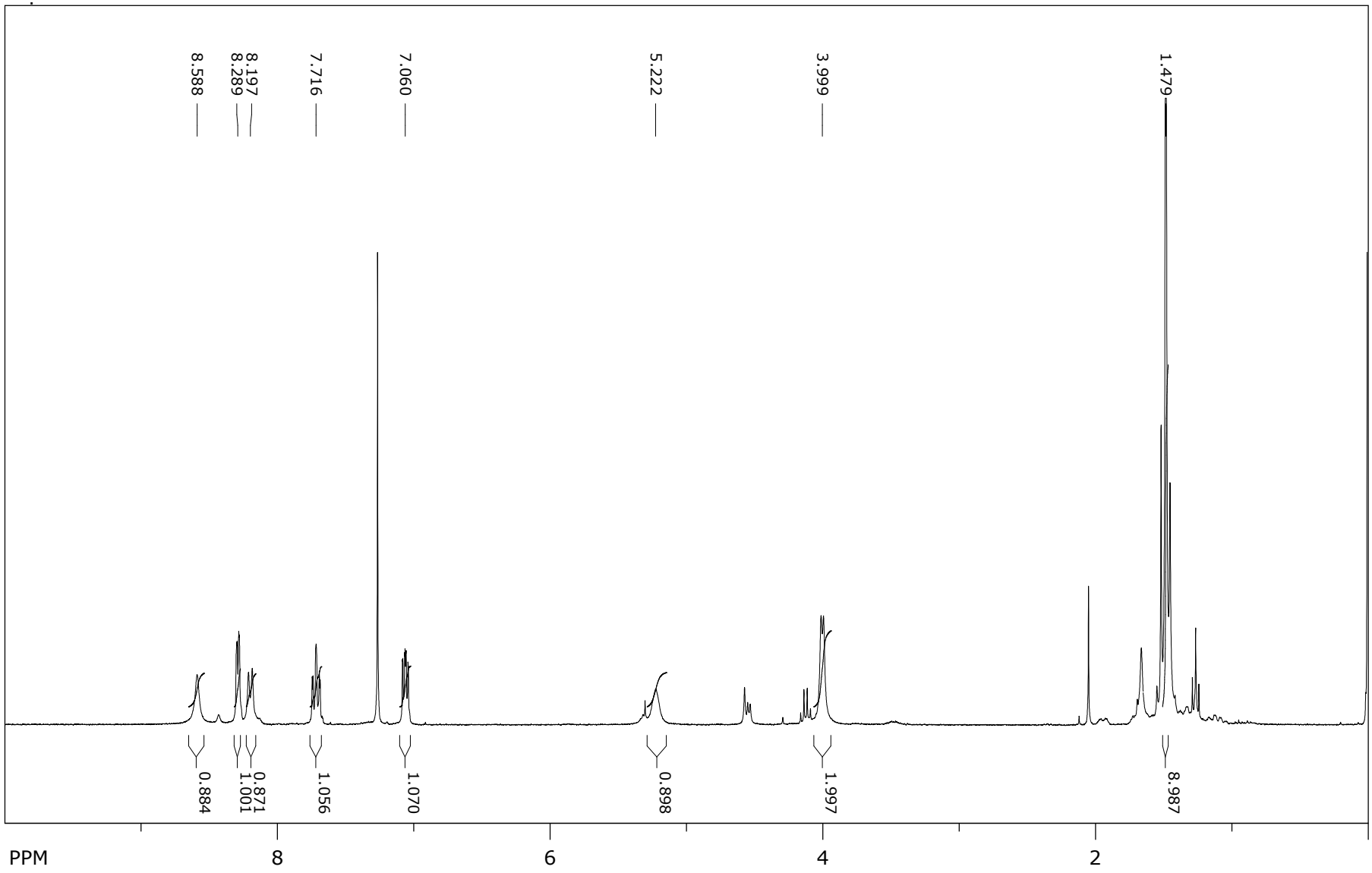

^{1}H NMR ($CDCl_3$) of Boc-L-Ala-2ampy

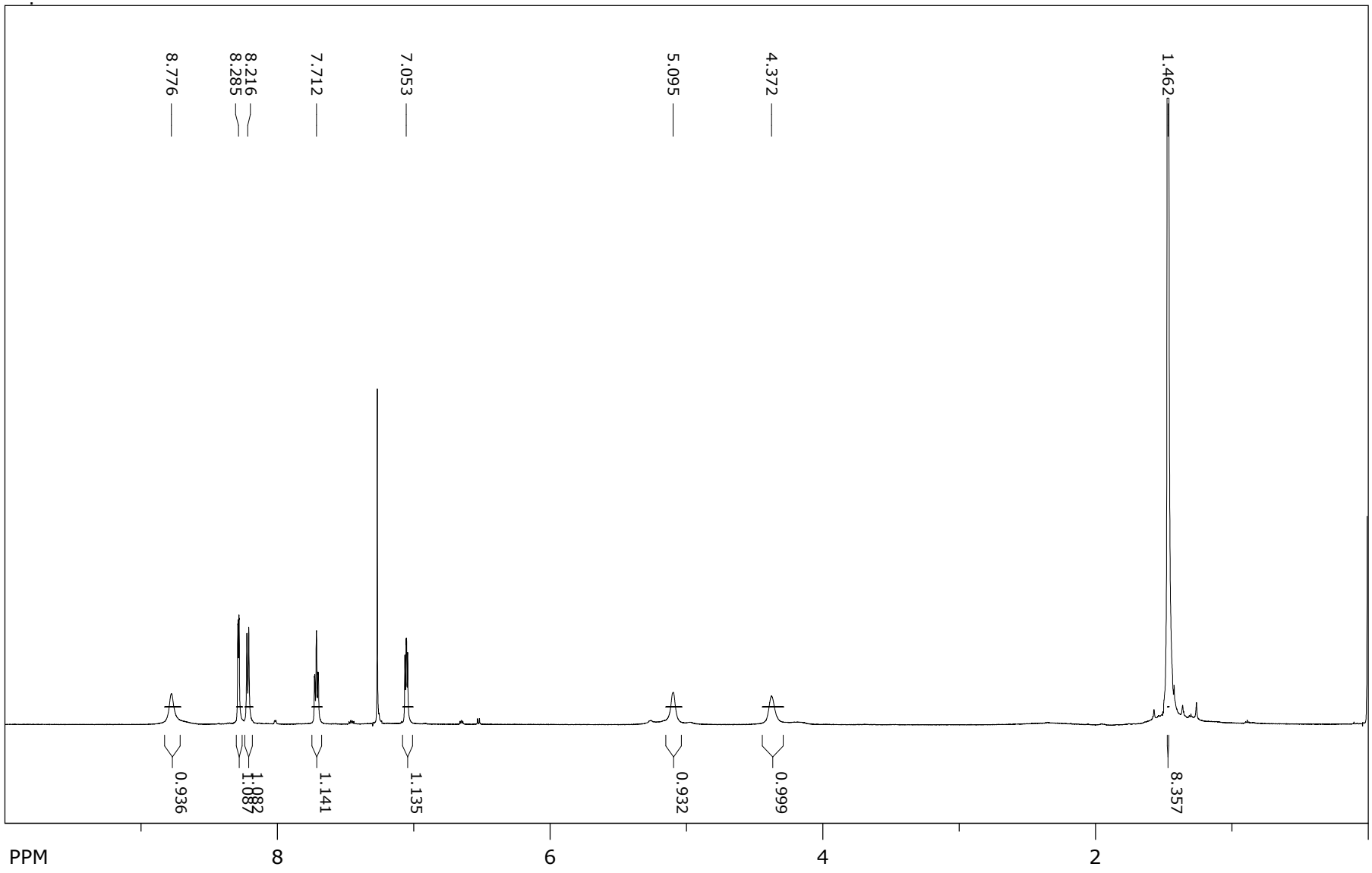

^{1}H NMR (CD_3CN) of Boc-D-Ala-2ampy

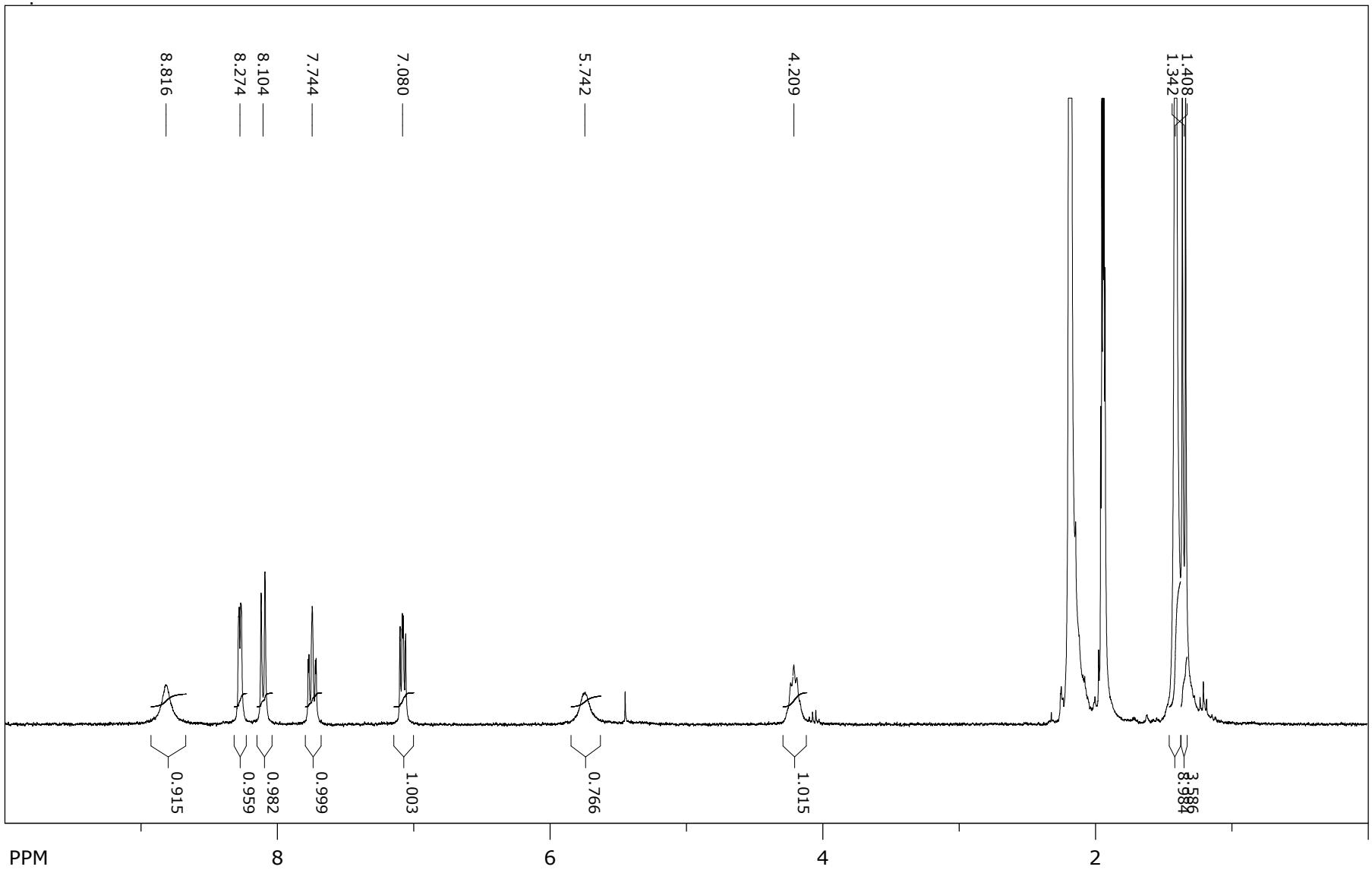

^{1}H NMR ($CDCl_3$) of Boc-D,L-Ala-2ampy

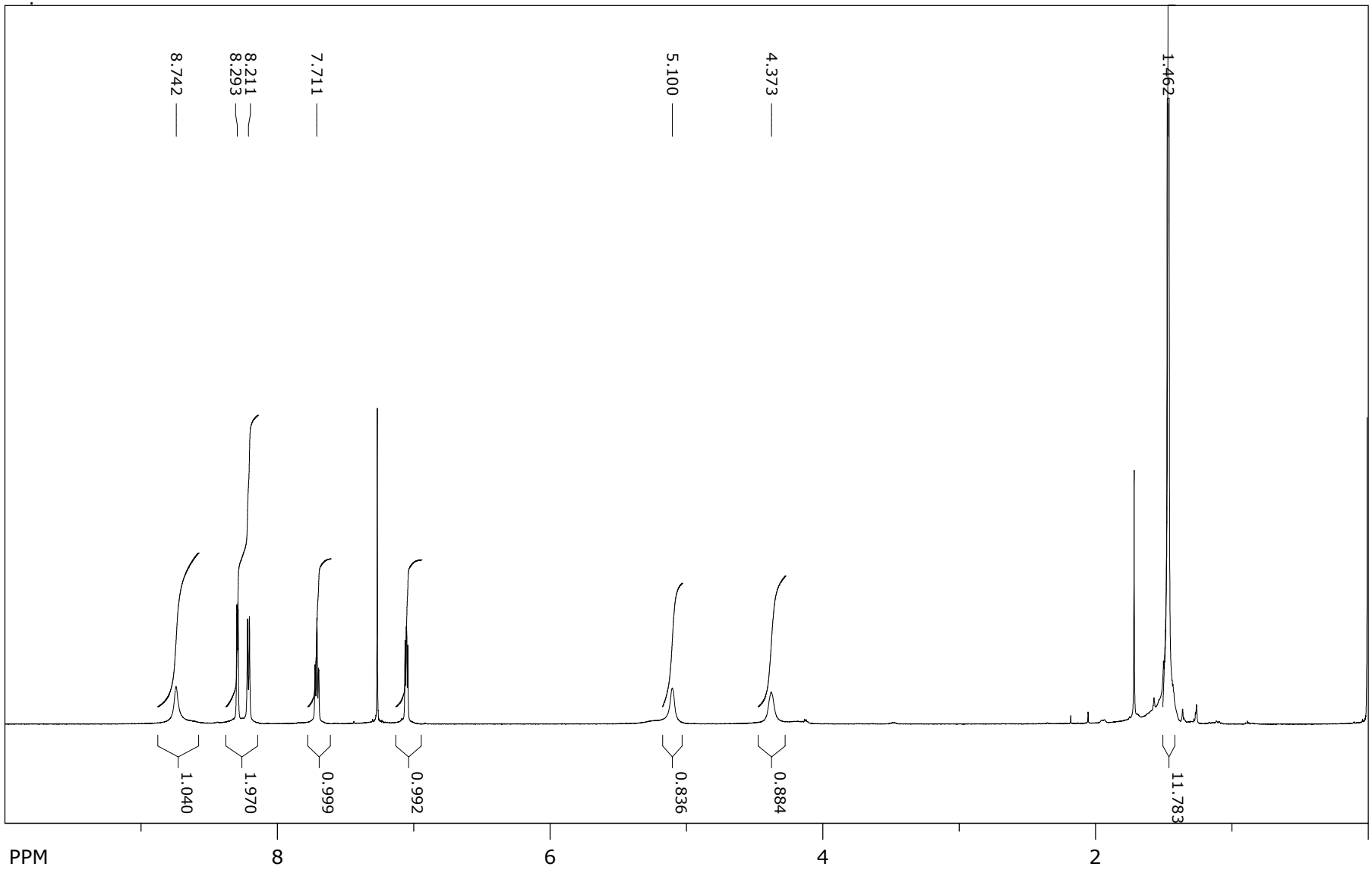

^{1}H NMR ($CDCl_3$) of **1a**, Me_2BTC-L-Ala-2ampy

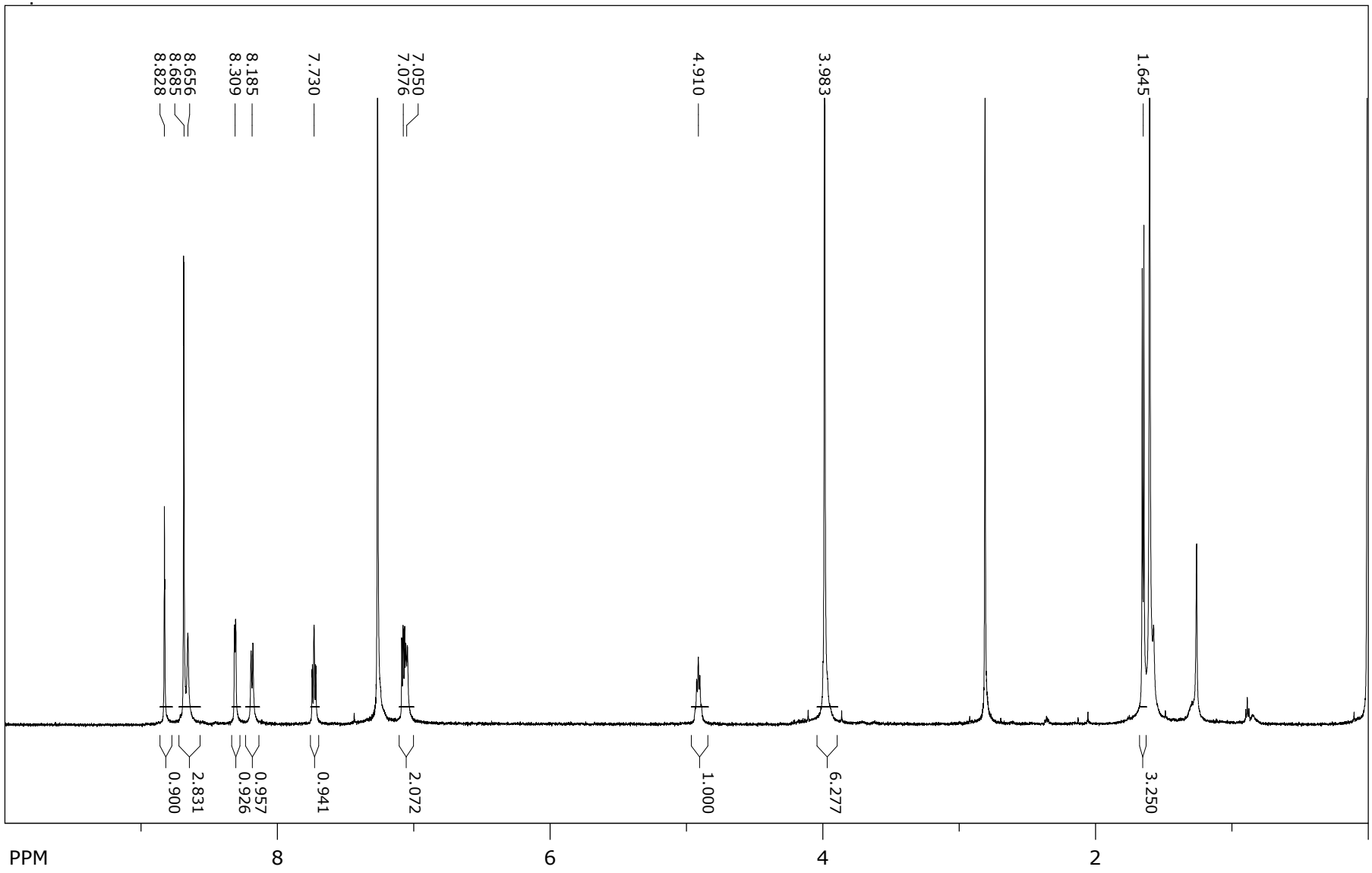

^{1}H NMR (acetonitrile-d_3) of D-**1a**, Me_2BTC-D-Ala-2ampy

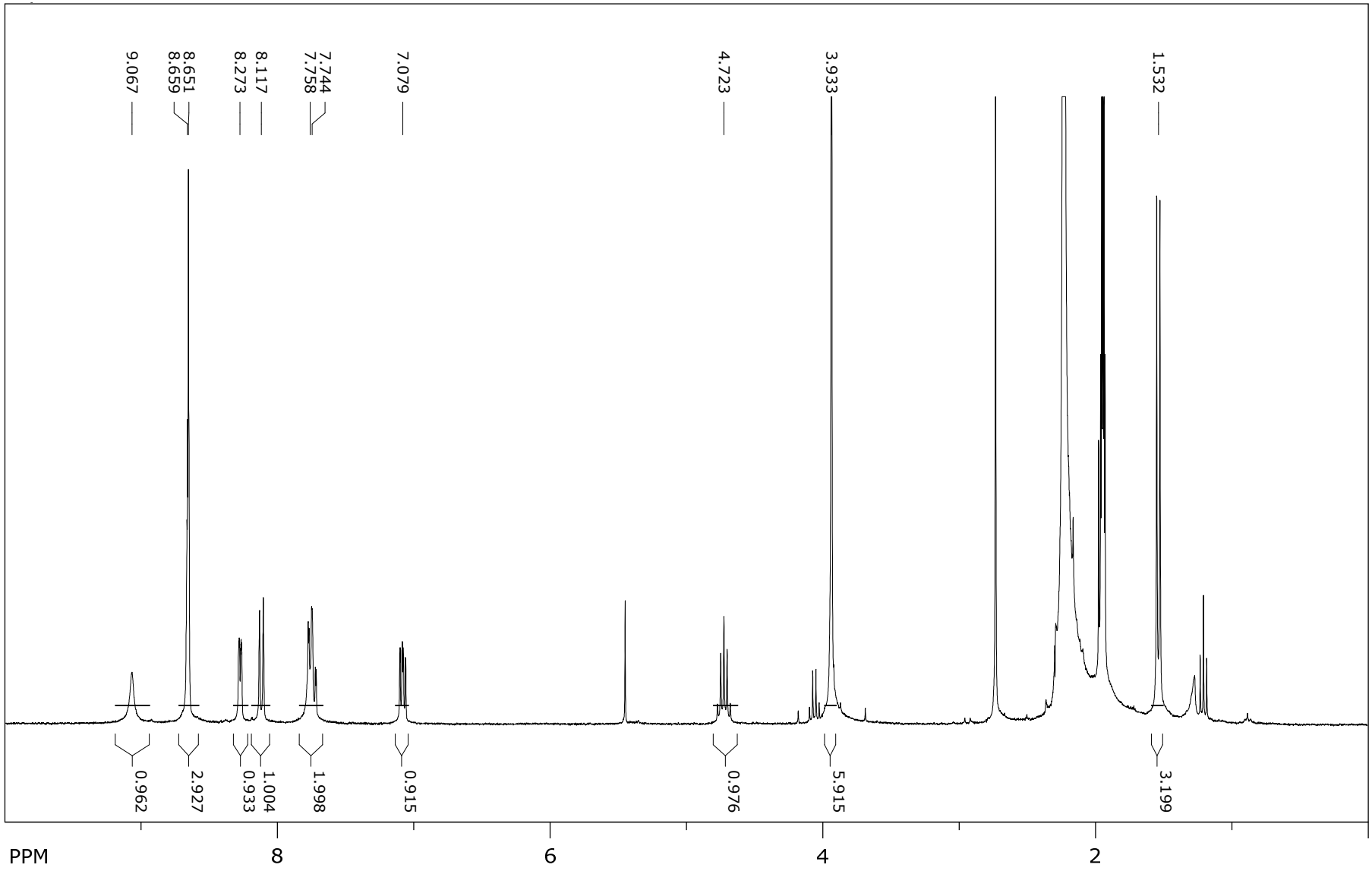

^{1}H NMR ($CDCl_3$) of rac-**1a**, Me_2BTC-D,L-Ala-2ampy

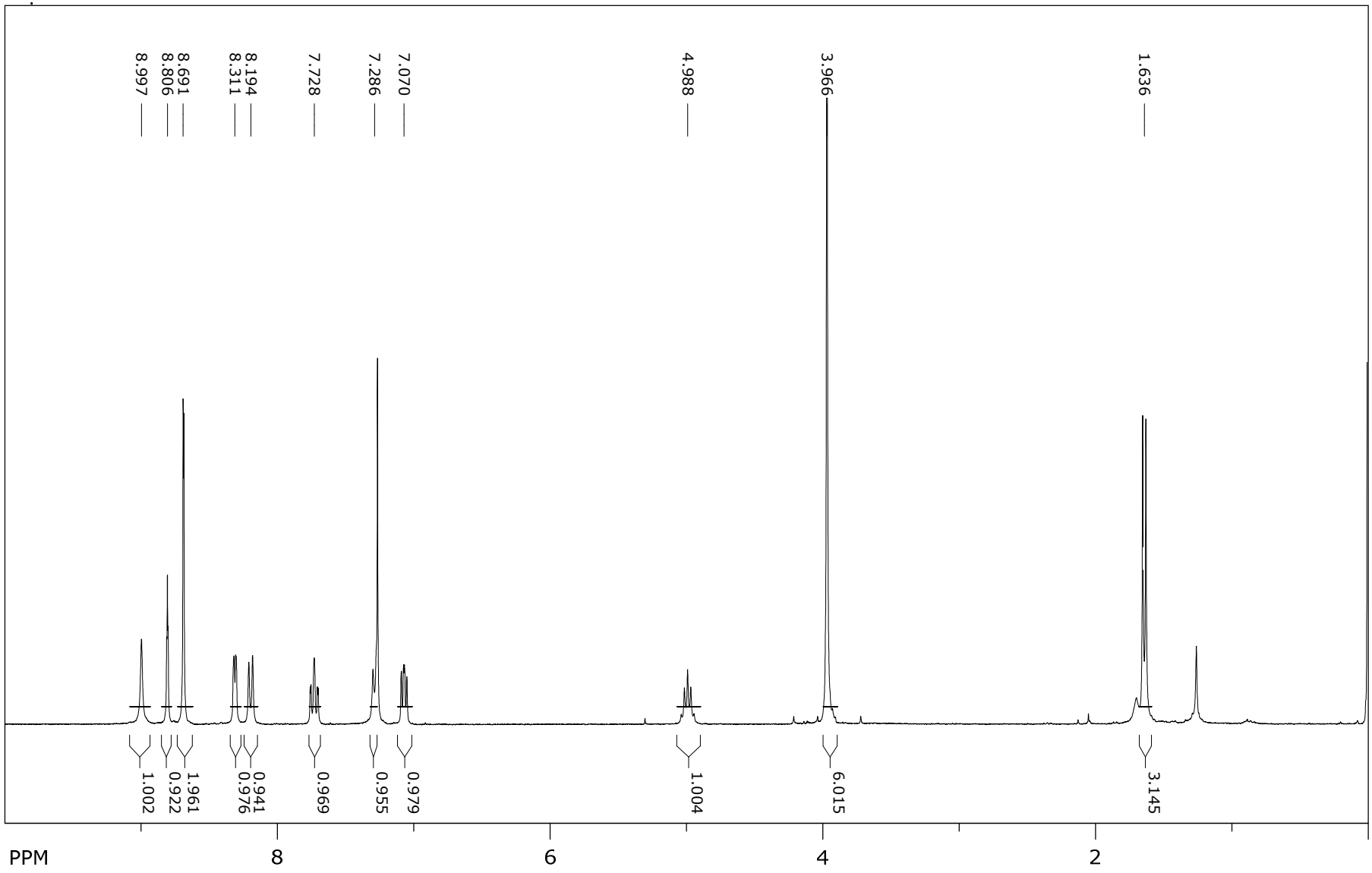

^{1}H NMR ($CDCl_3$) of **1b**, Me_2BTC-Gly-2ampy

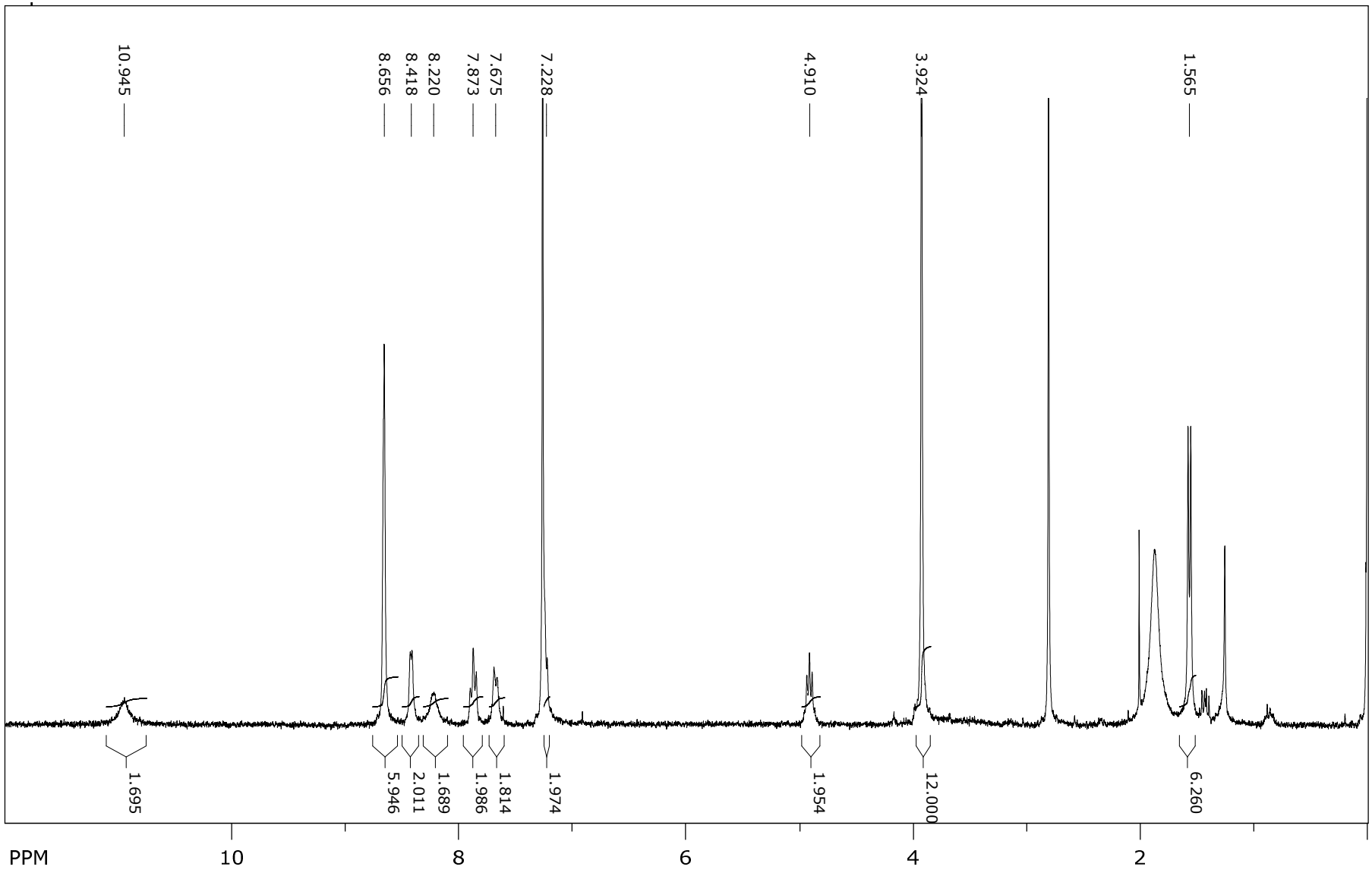

^{1}H NMR (acetonitrile-d_3) of **2a**, [Zn(**1a**)$_2$(NO$_3$)$_2$]

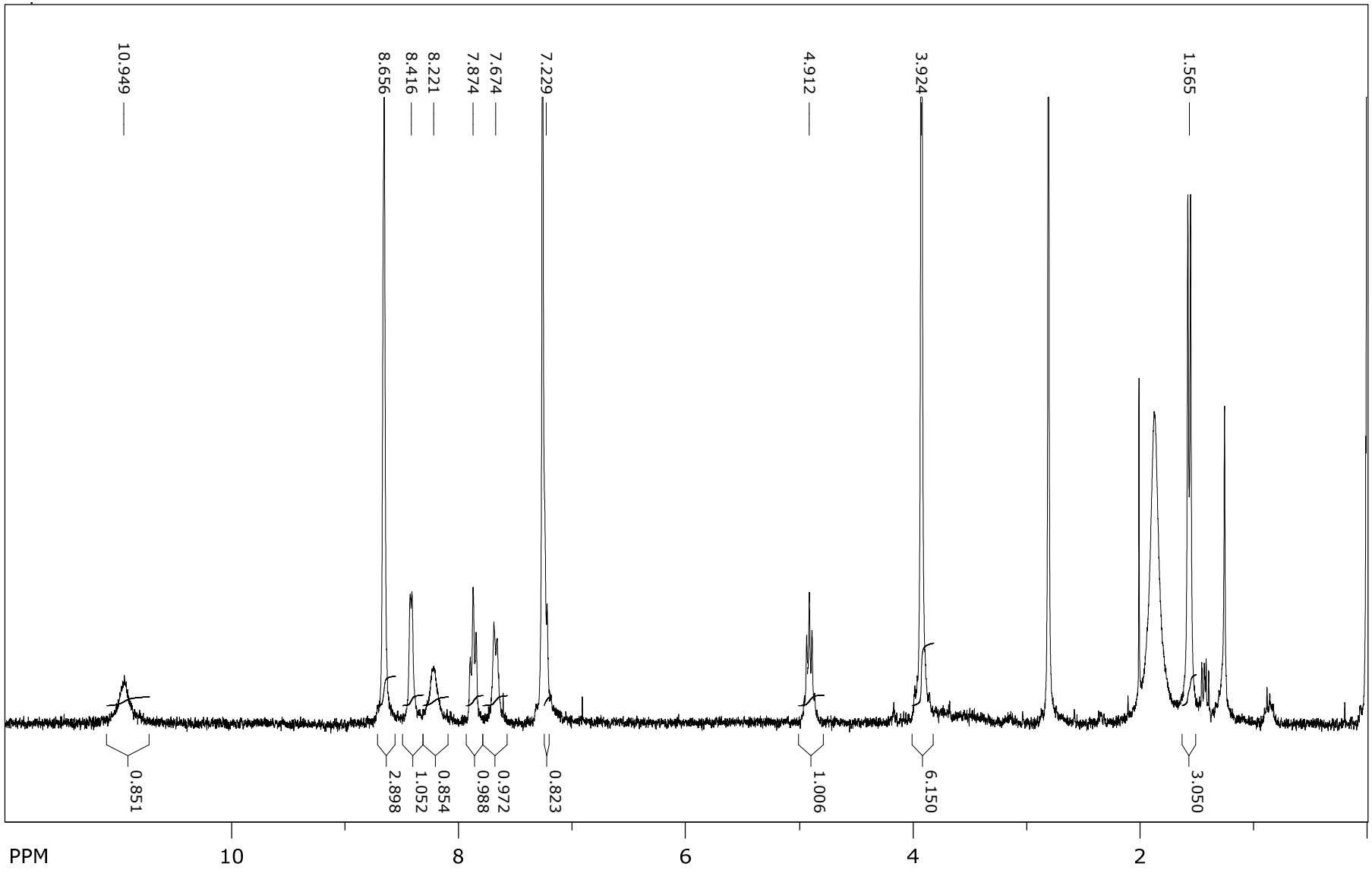

^{1}H NMR (acetonitrile-d_3) of **3a**, [Zn(**1a**)$_2$(BF$_4$)$_2$]

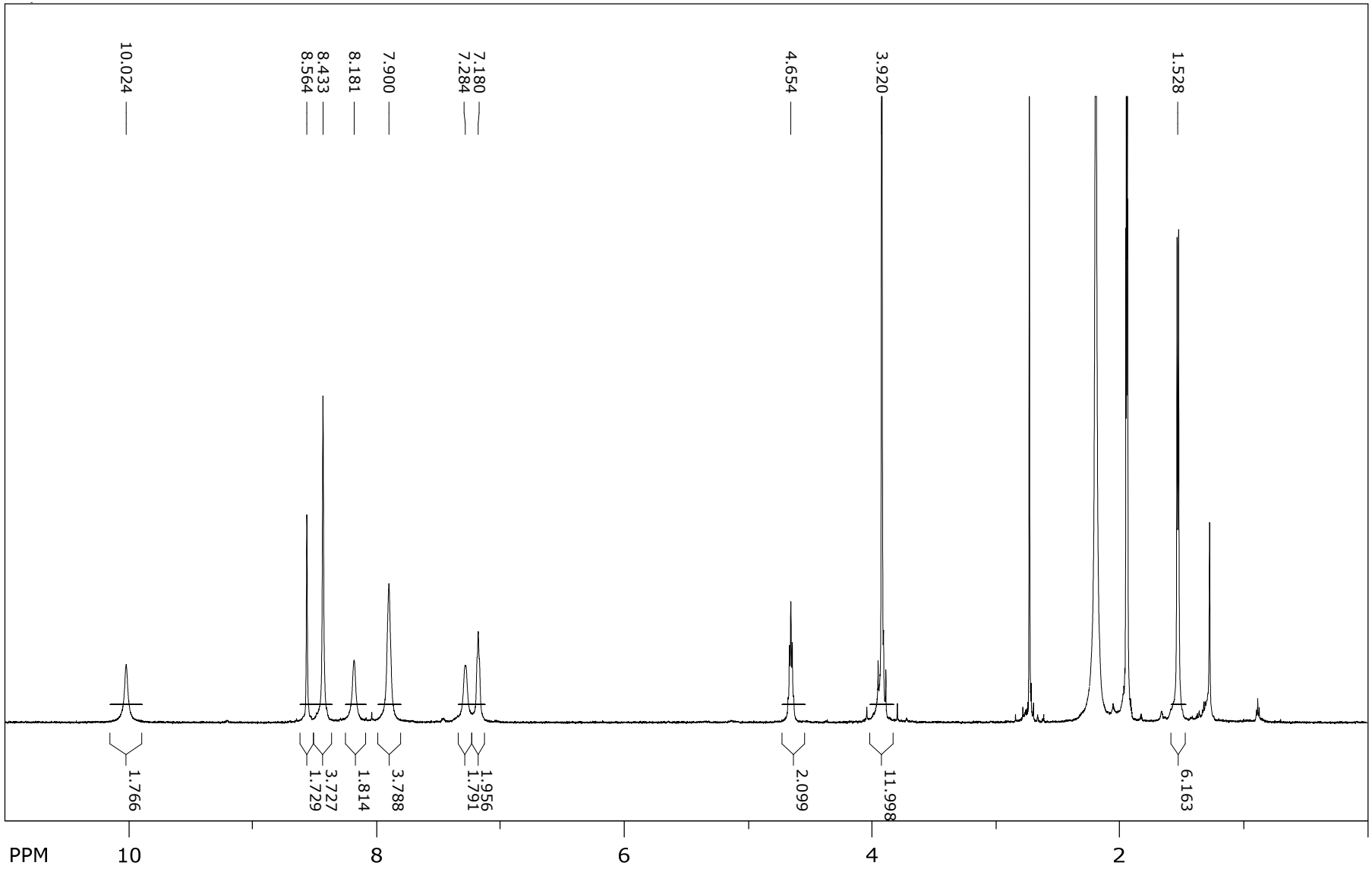

X-Ray Structure

Table S 1: X-ray diffraction experimental data for D-**1a**.

Chemical Formula	$C_{19}H_{19}N_3O_6$
Formula Weight (g mol^{-1})	385.37
Crystal System	orthorhombic
Space Group	$P2_12_12_1$
a (Å)	14.2548 (8)
b (Å)	24.6361 (14)
c (Å)	25.1330 (16)
V (Å^3)	8826.3 (9)
Z	16
D_c (g cm^{-3})	1.160
Temperature (K)	293
λ (Å)	1.54184
Θ range (^{o})	3.5–75.1
hkl range	−17→15, −30→30, −31→31
Reflns. collected	83588
Independ. reflns.	17527
R_{int}	0.117
parameters/restraints/constraints	1009/ 408/0
$R[I> 2\sigma(I)]$[a]	0.088
wR_2 (all data)[b]	0.277
Goof, S[c]	0.90
max./min. res. el. den. (e Å^{-3})	0.22/−0.26
Flack parameter	0.3 (3)

[a] $R = \sum||F_o| - |F_c||/\sum|F_o|$

[b] $wR_2 = \{\sum[w(F_o^2 - F_c^2)^2]/\sum[w(F_o^2)^2]\}^{1/2}$ where $w = 1/[\sigma^2(F_o^2) + (0.1153P)^2]$ and $P = (F_o^2 + 2F_c^2)/3$

[c] $S = \{\sum[w(F_o^2 - F_c^2)^2]/(n-p)\}^{1/2}$ where n is number of reflections and p is the total number of parameters refined.

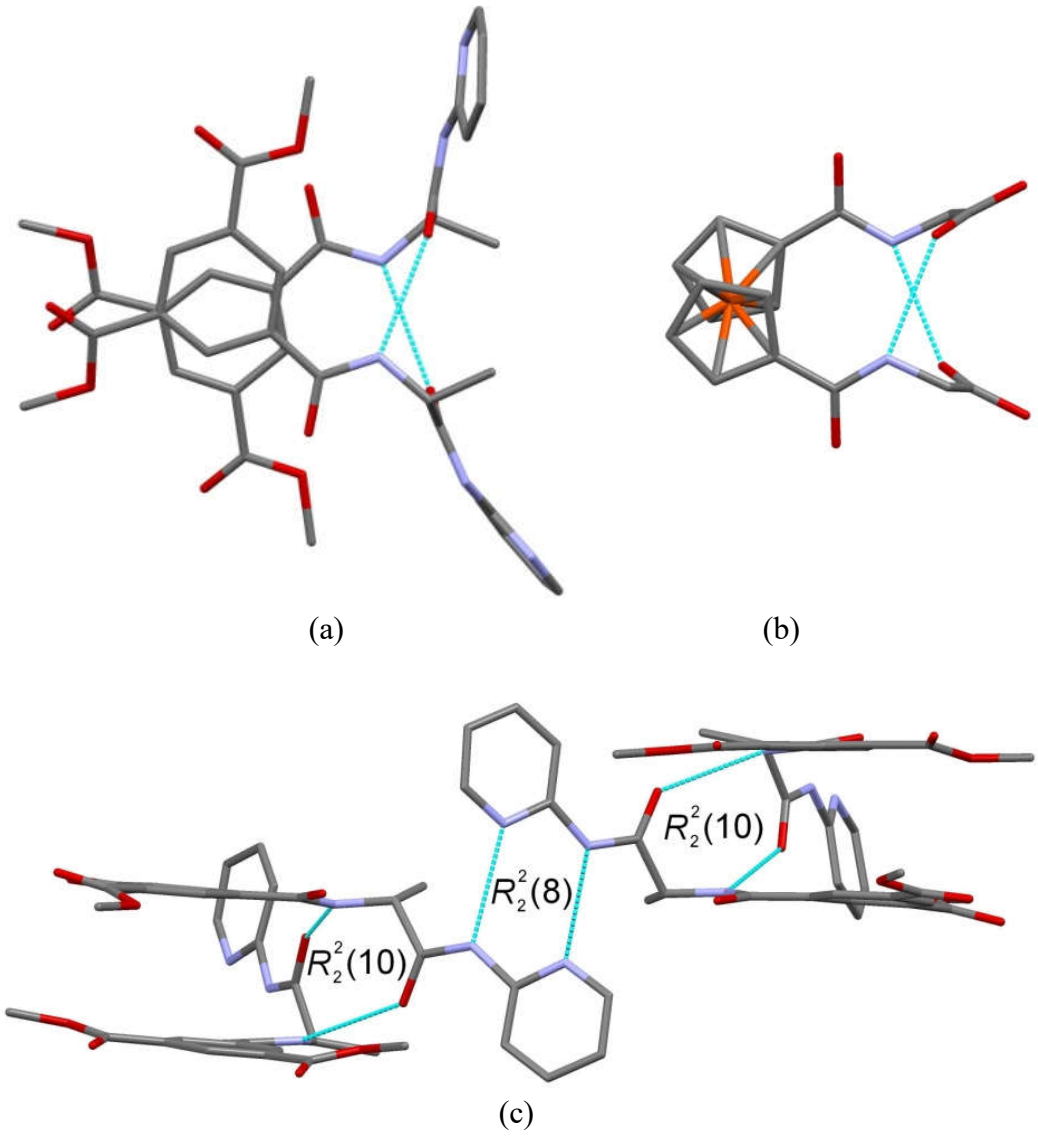

Figure S 1. Supramolecular "Herrick conformation" in the single crystal structures of: (a) D-**1a** compared to (b) bis(glycyl)ferrocene bio-conjugate[S20]; (b) four symmetry non-equivalent molecules of D-**1a** showing alternating hydrogen bonded patterns in the crystal structure.

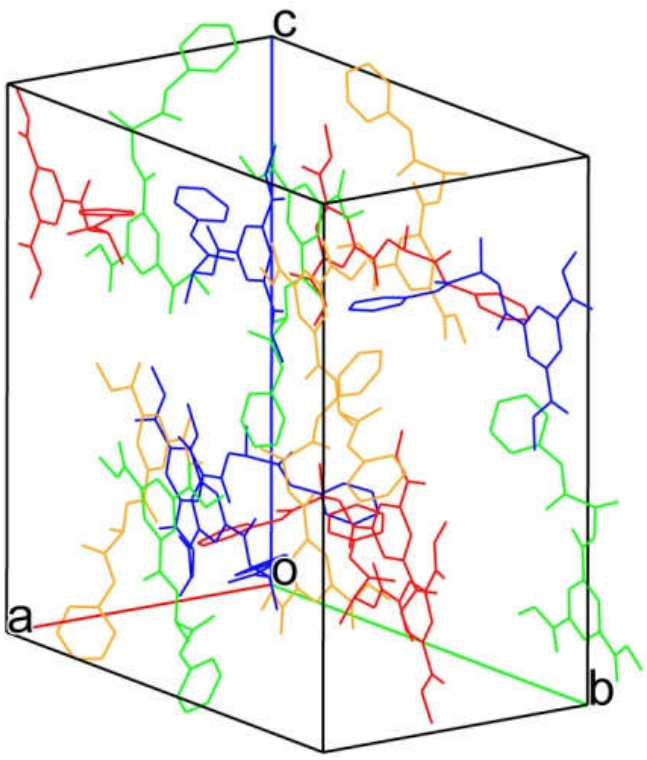

(a)

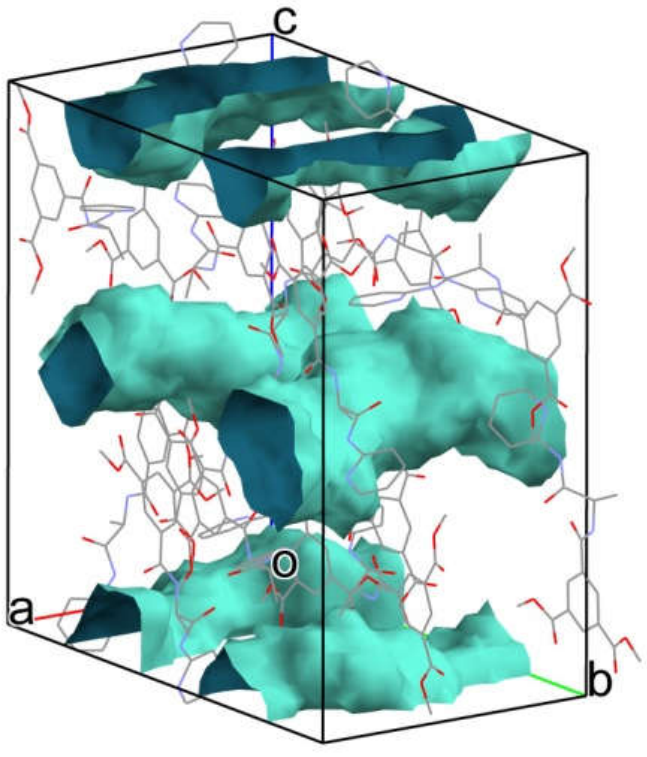

(b)

Figure S 2. Unit cell of D-**1a** (a) coloured by symmetry equivalence and (b) 1D-voids (blue coloured area) in the crystal structure. Electron density in these voids is treated by SQUEEZE procedure.[S3]

Molecular Dynamics Simulations

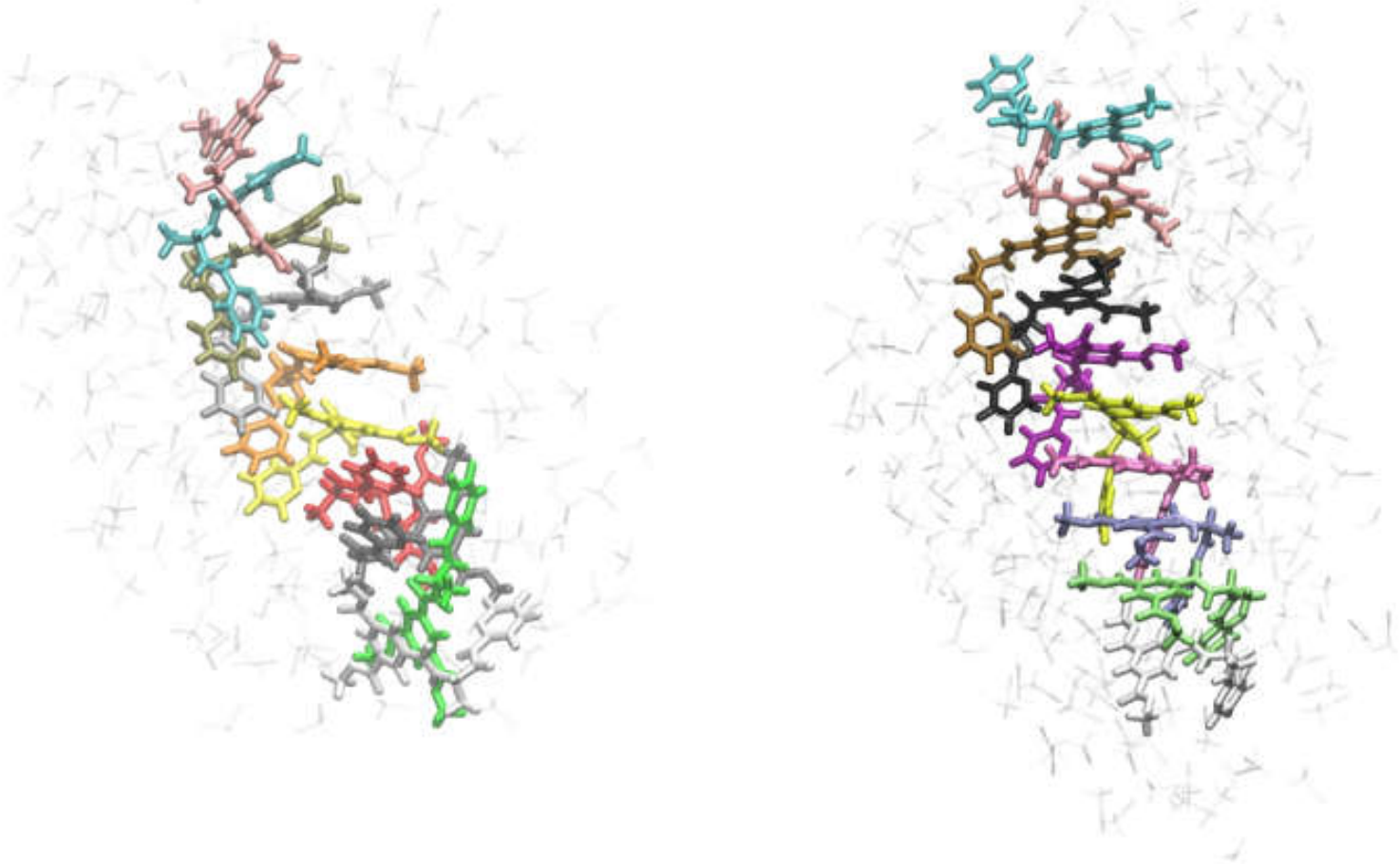

(a) (b)

Figure S 3. Representative snapshots from MD simulations of **1a** in (a) chloroform and (b) acetonitrile. Solvent molecules within 10 Å from **1a** molecules are shown transparent.

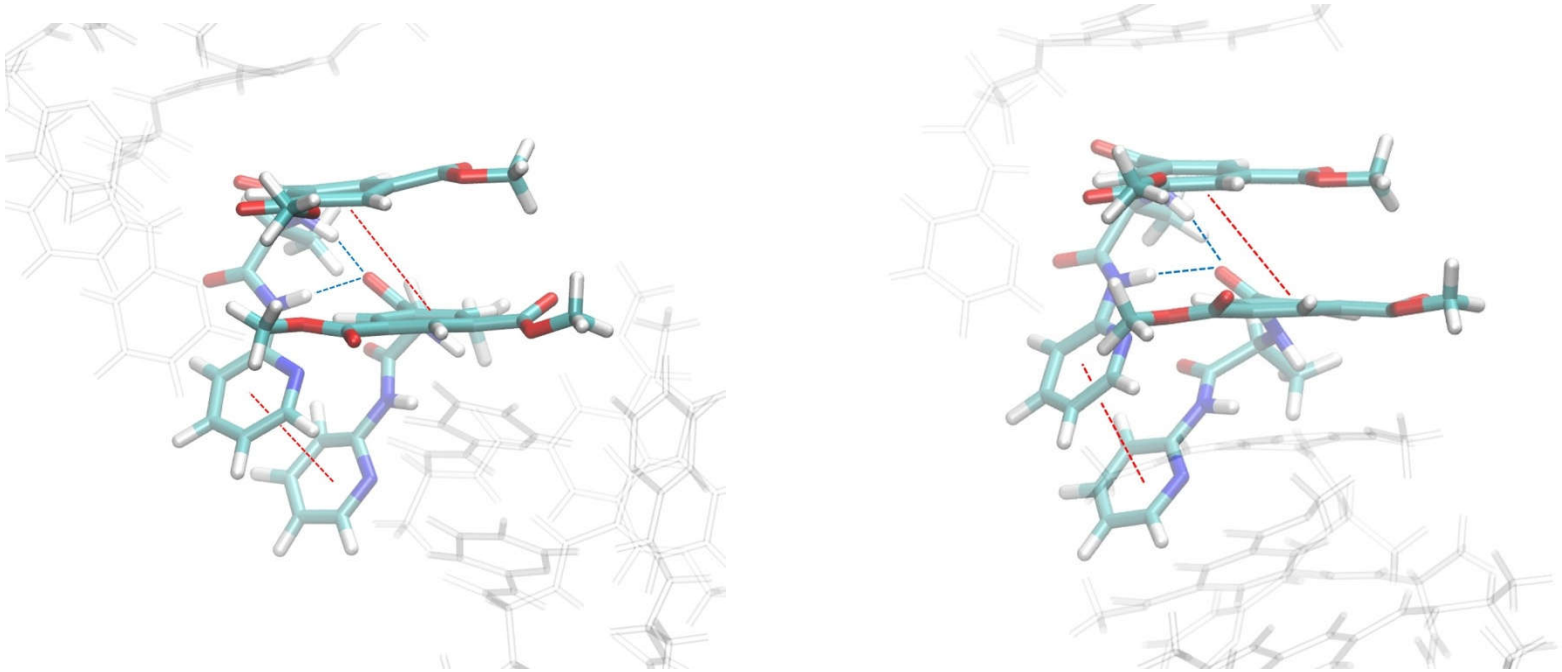

(a) (b)

Figure S 4. Representative snapshots from Molecular Dynamics Simulations of **1a** linear aggregates in (a) chloroform and (b) acetonitrile showing hydrogen bonding and π- π stacking (indicated with blue and red dashed lines, respectively). Solvent molecules are omitted for clarity.

NMR Measurements

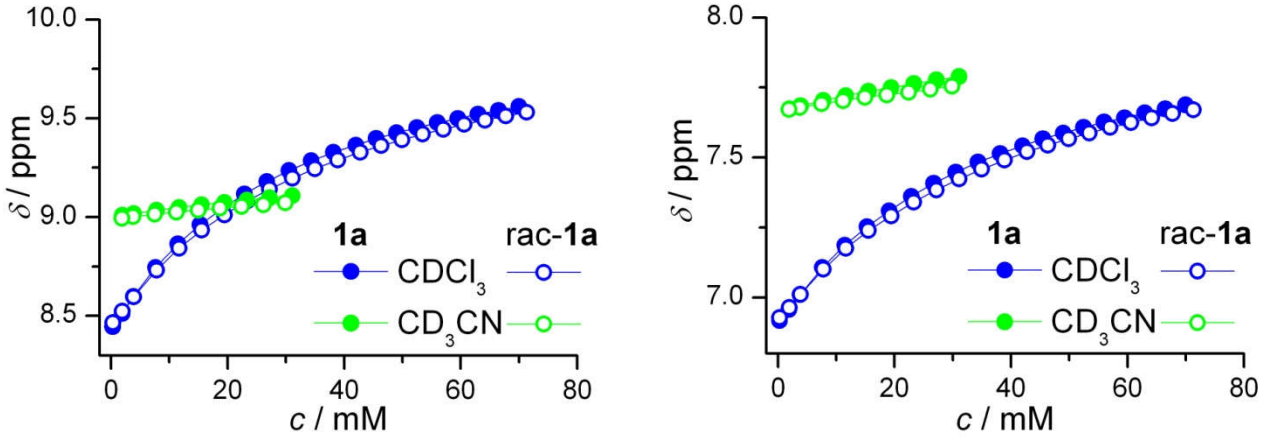

(a) (b)

Figure S 5. Variable concentration ^{1}H NMR chemical shifts of (a) Alanyl and (b) pyridyl amide protons of **1a** and rac-**1a** in acetonitrile-d_3 or chloroform-d_1. It is worth noting that the variable concentration and temperature ^{1}H NMR measurements of rac-**1a** have identical features as chiral **1a**, indicating that the racemic ligand also forms supramolecular assemblies, and in addition exhibits molecular recognition which is common in racemic hydrogen-bonded systems.[S21]

Table S 2. Amide proton ^{1}H NMR temperature coefficients (ppb K^{-1}). The fitted data deviate slightly from linearity.

Compound	chloroform-d_1		acetonitrile-d_3	
	NH^{py}	NH^{Ala}	NH^{py}	NH^{Ala}
1a	–11.1	–7.1	–3.4	–3.7
rac-**1a**	–10.6	–6.8	–3.2	–3.4
2a	–14.1	–18.6	–13.5	–6.2

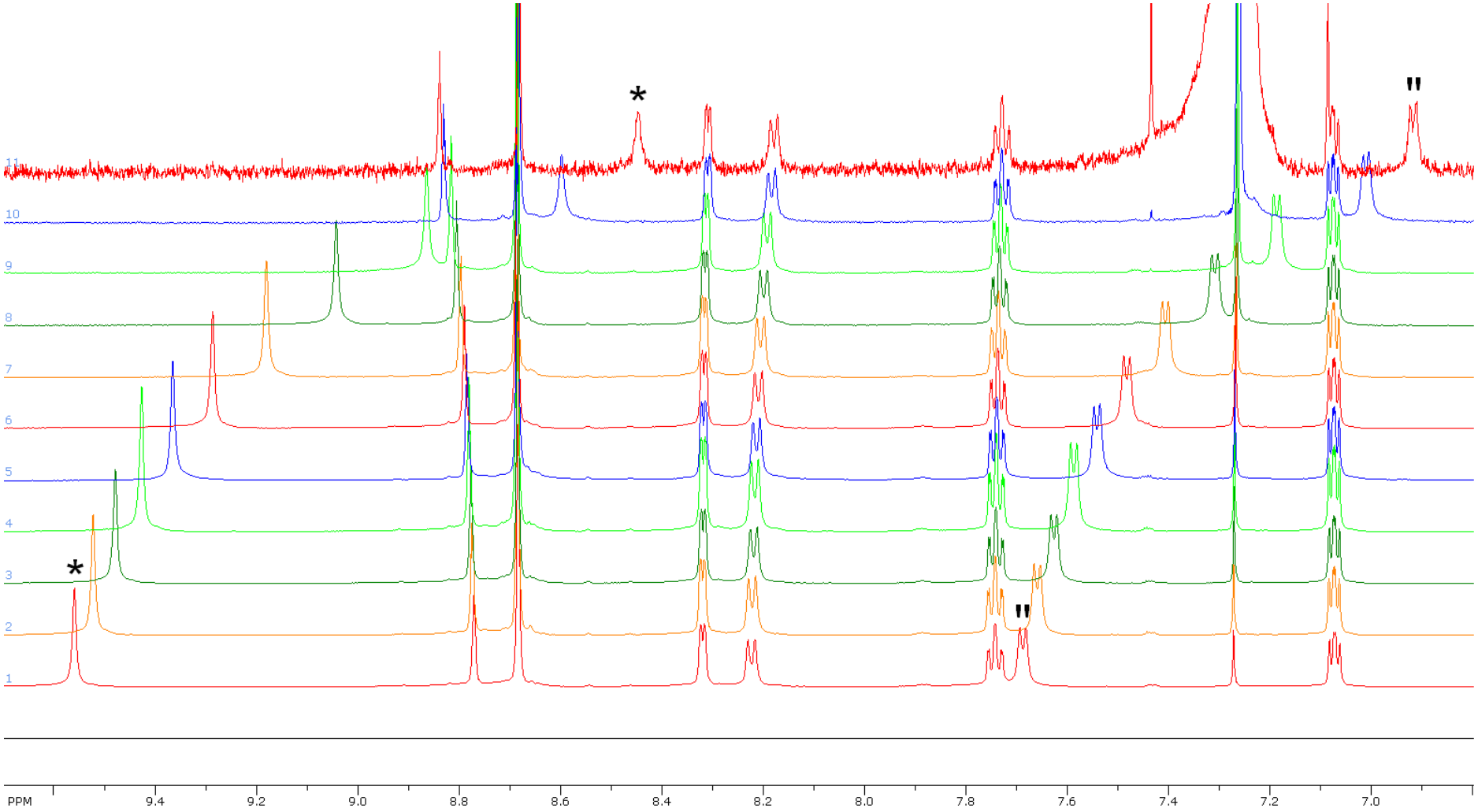

Figure S 6. Variable concentration ^{1}H NMR spectra (0.26–70 mM, top to bottom) of **1a**, in chloroform-d_1. Alanyl (") and pyridyl (*) amide protons are accented.

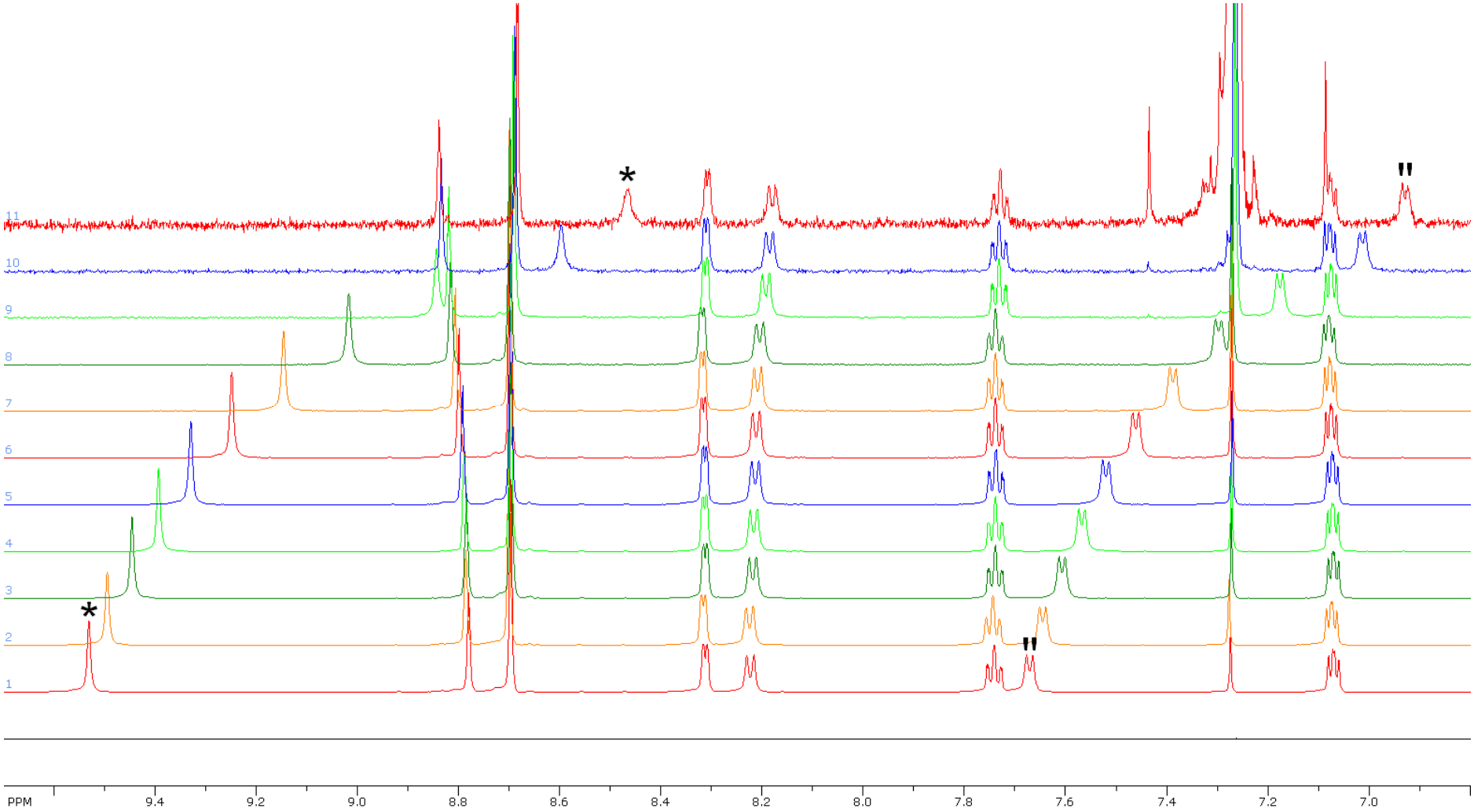

Figure S 7. Variable concentration ^{1}H NMR spectra (0.29–71.3 mM, top to bottom) of rac-**1a**, in chloroform-d_1. Alanyl (") and pyridyl (*) amide protons are accented.

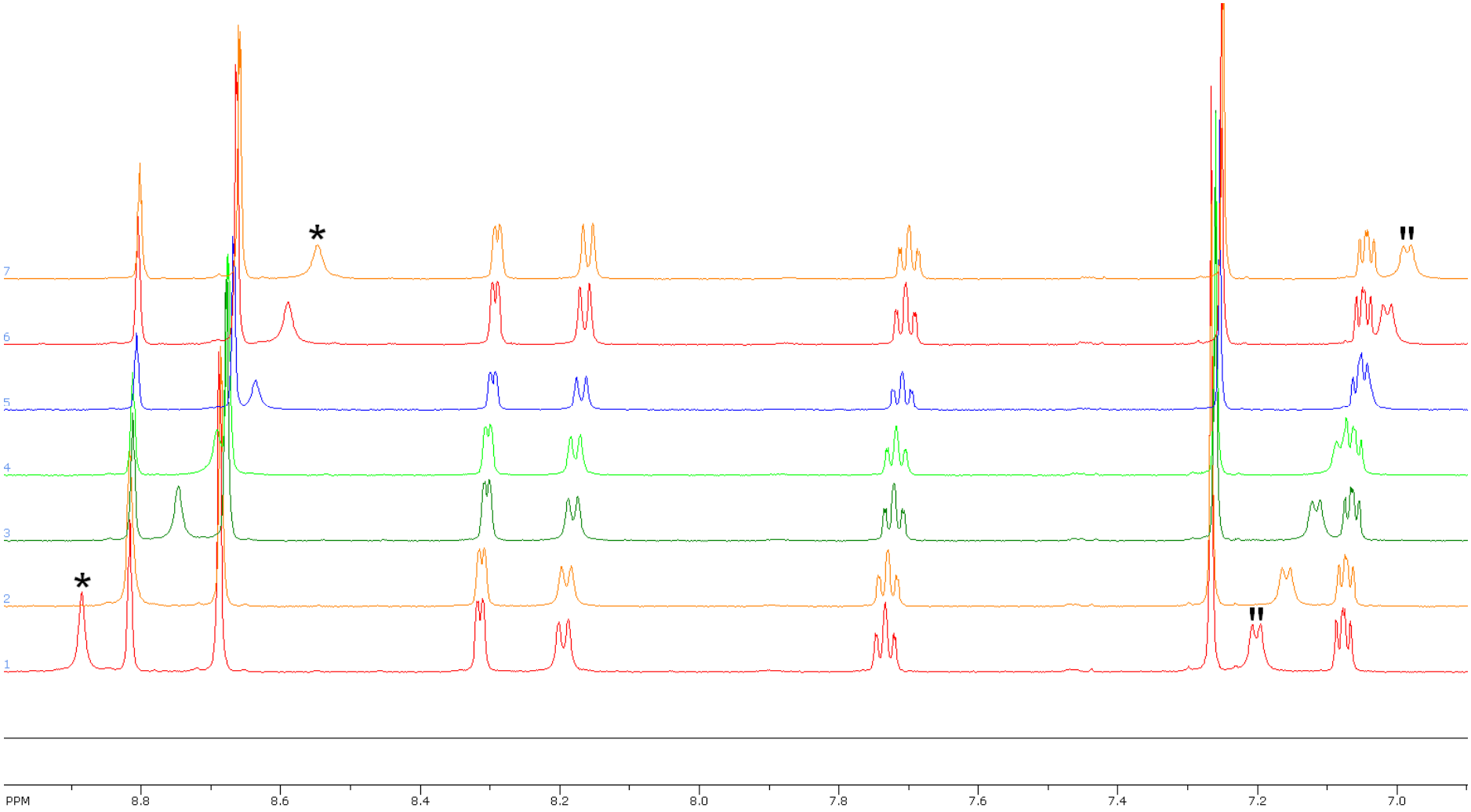

Figure S 8. Variable temperature ^{1}H NMR spectra (55–25 °C, top to bottom) of **1a**, in chloroform-d_1. Alanyl (") and pyridyl (*) amide protons are accented.

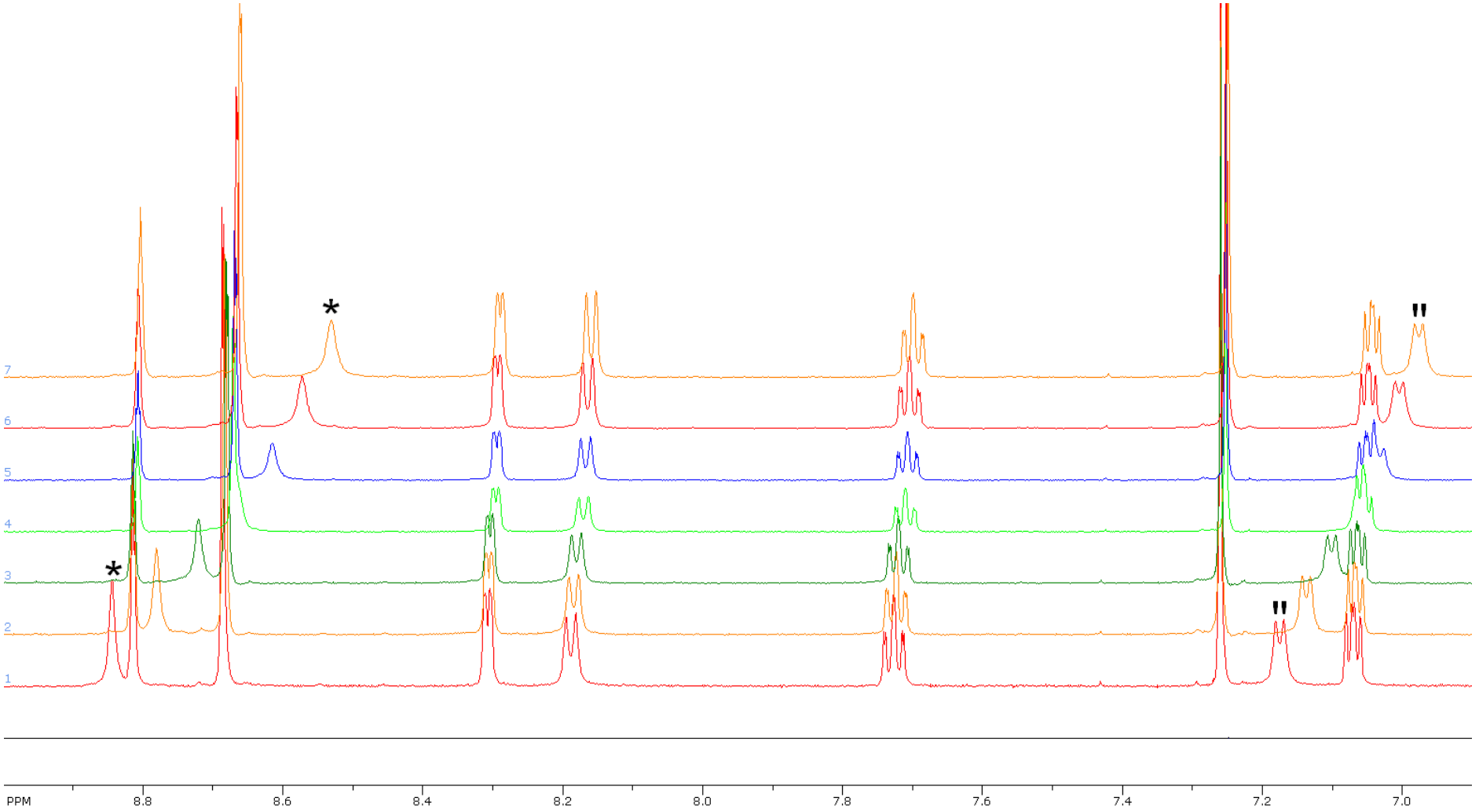

Figure S 9. Variable temperature ^{1}H NMR spectra (55–25 °C, top to bottom) of rac-**1a**, in chloroform-d_1. Alanyl (") and pyridyl (*) amide protons are accented.

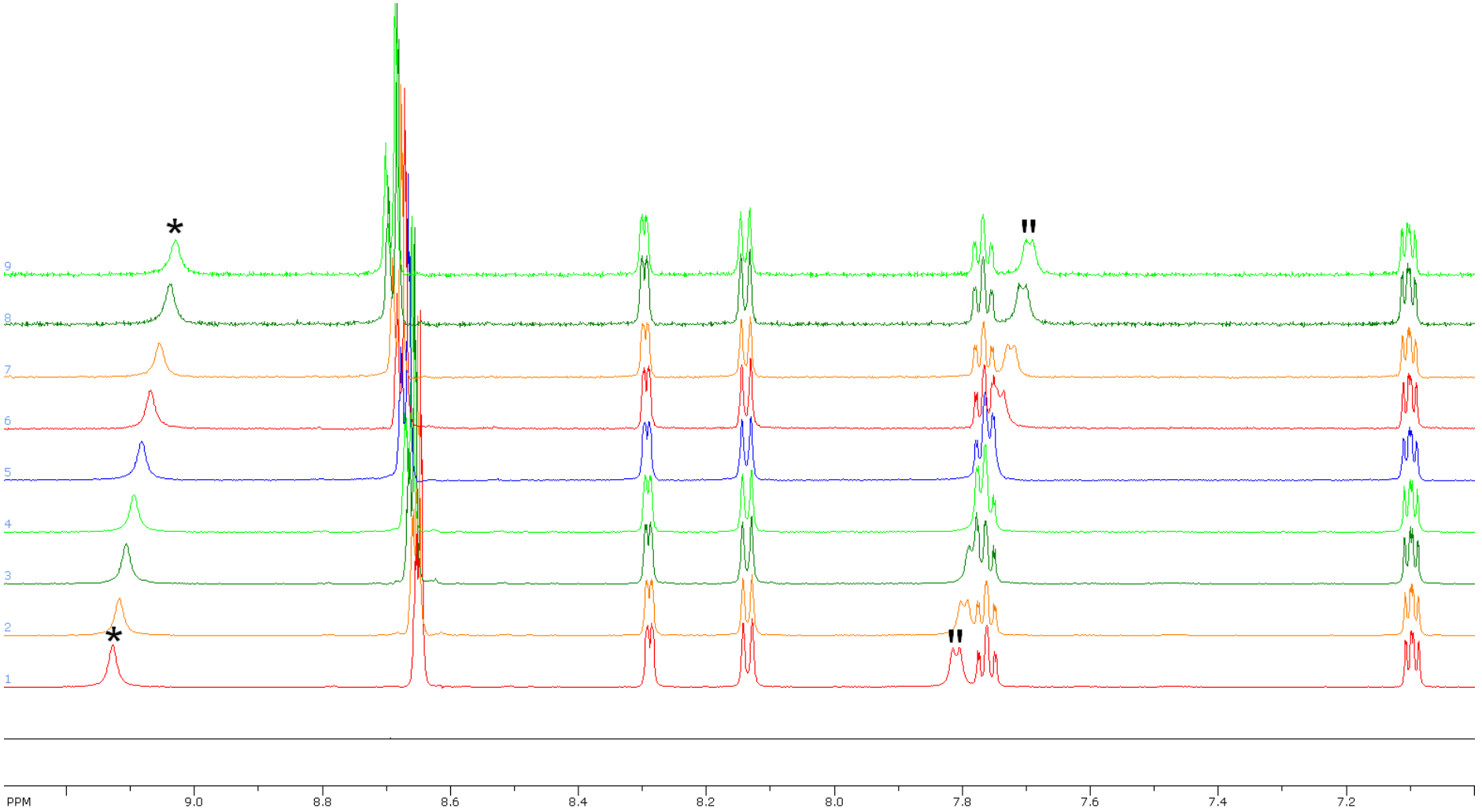

Figure S 10. Variable concentration ^{1}H NMR spectra (1.9–31.1 mM, top to bottom) of **1a**, in acetonitrile-d_3. Alanyl (") and pyridyl (*) amide protons are accented.

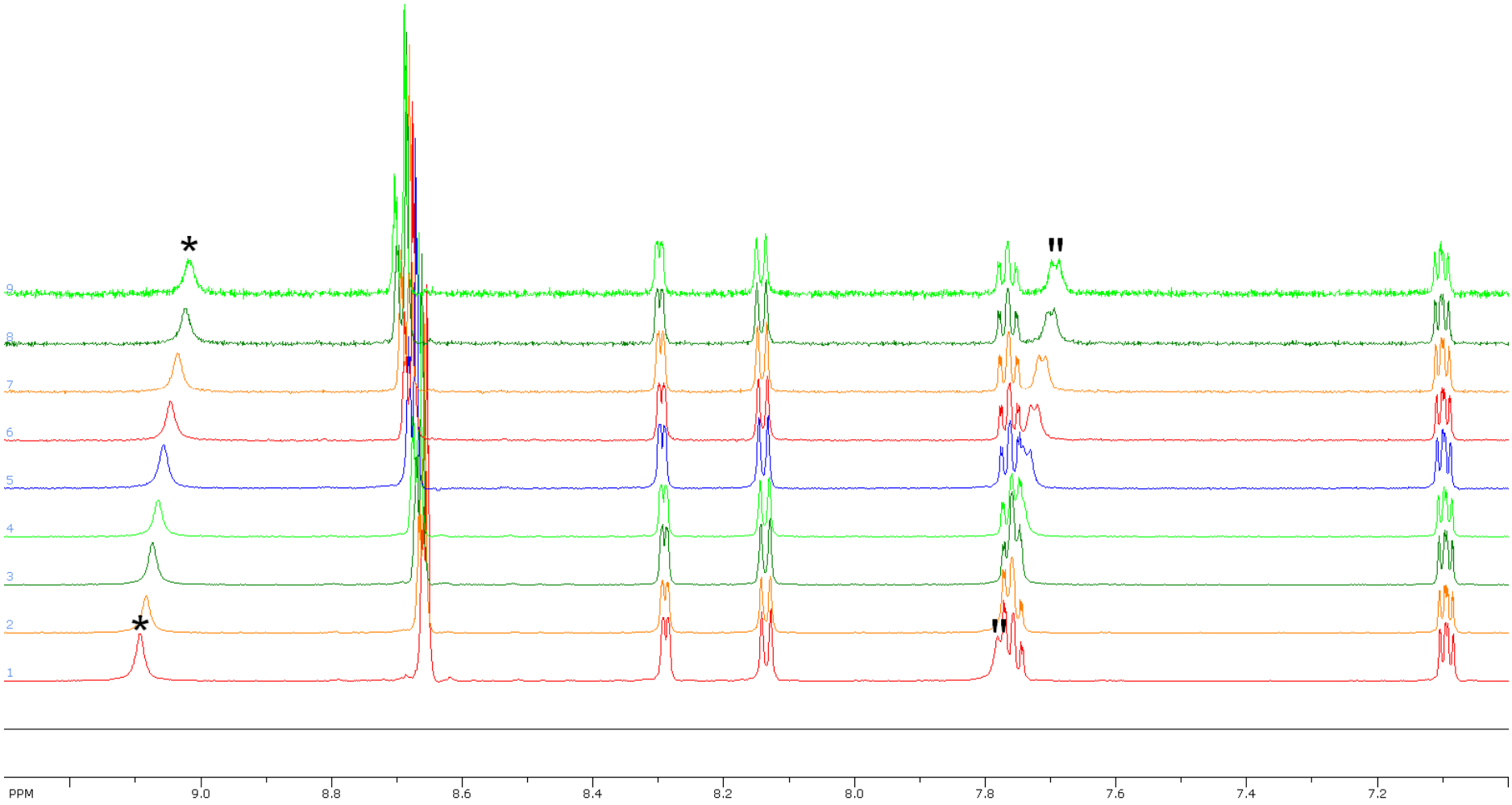

Figure S 11. Variable concentration ^{1}H NMR spectra (1.9–29.9 mM, top to bottom) of rac-**1a**, in acetonitrile-d_3. Alanyl (") and pyridyl (*) amide protons are accented.

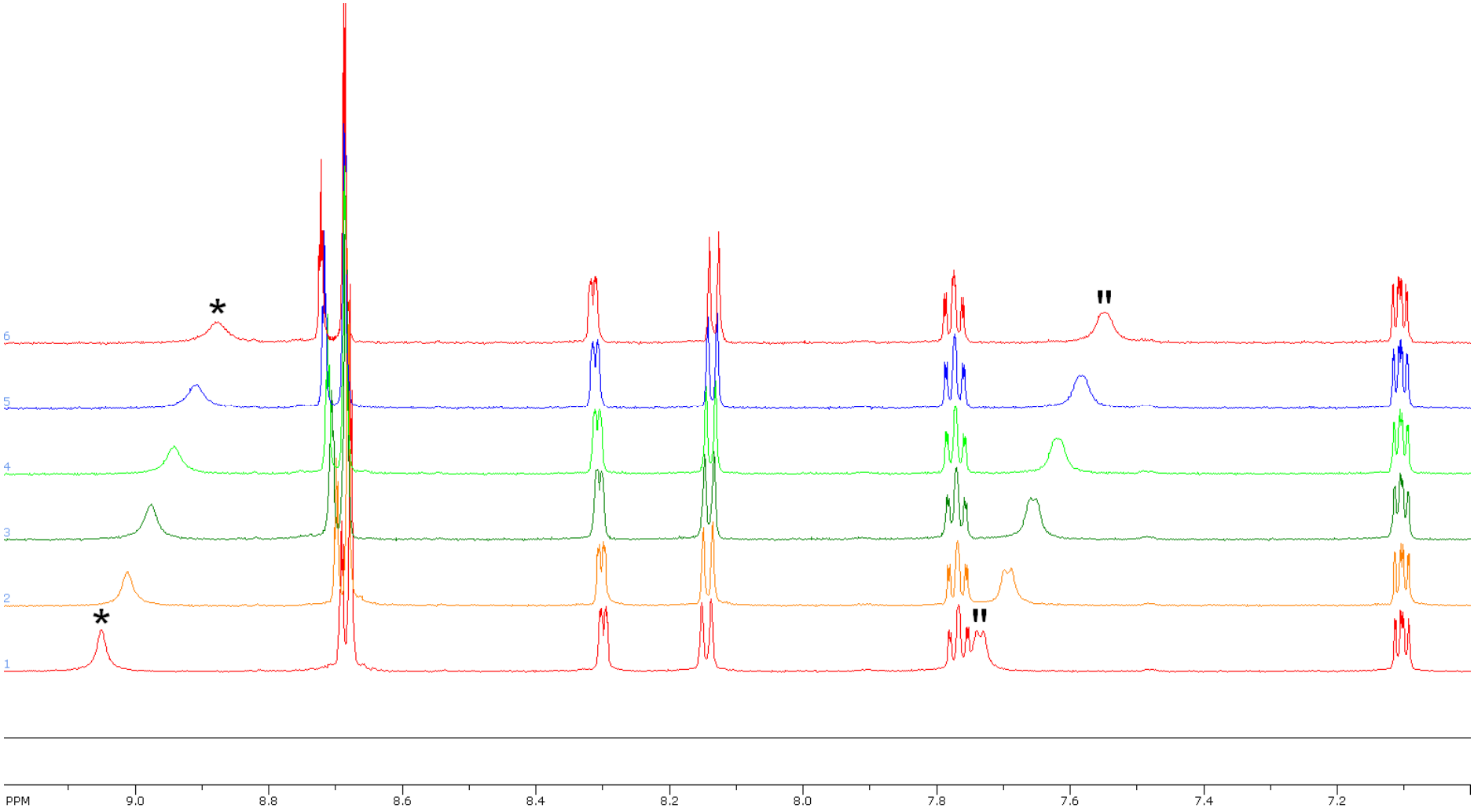

Figure S 12. Variable temperature ^{1}H NMR spectra (75–25 °C, top to bottom) of **1a**, in acetonitrile-d_3. Alanyl (") and pyridyl (*) amide protons are accented.

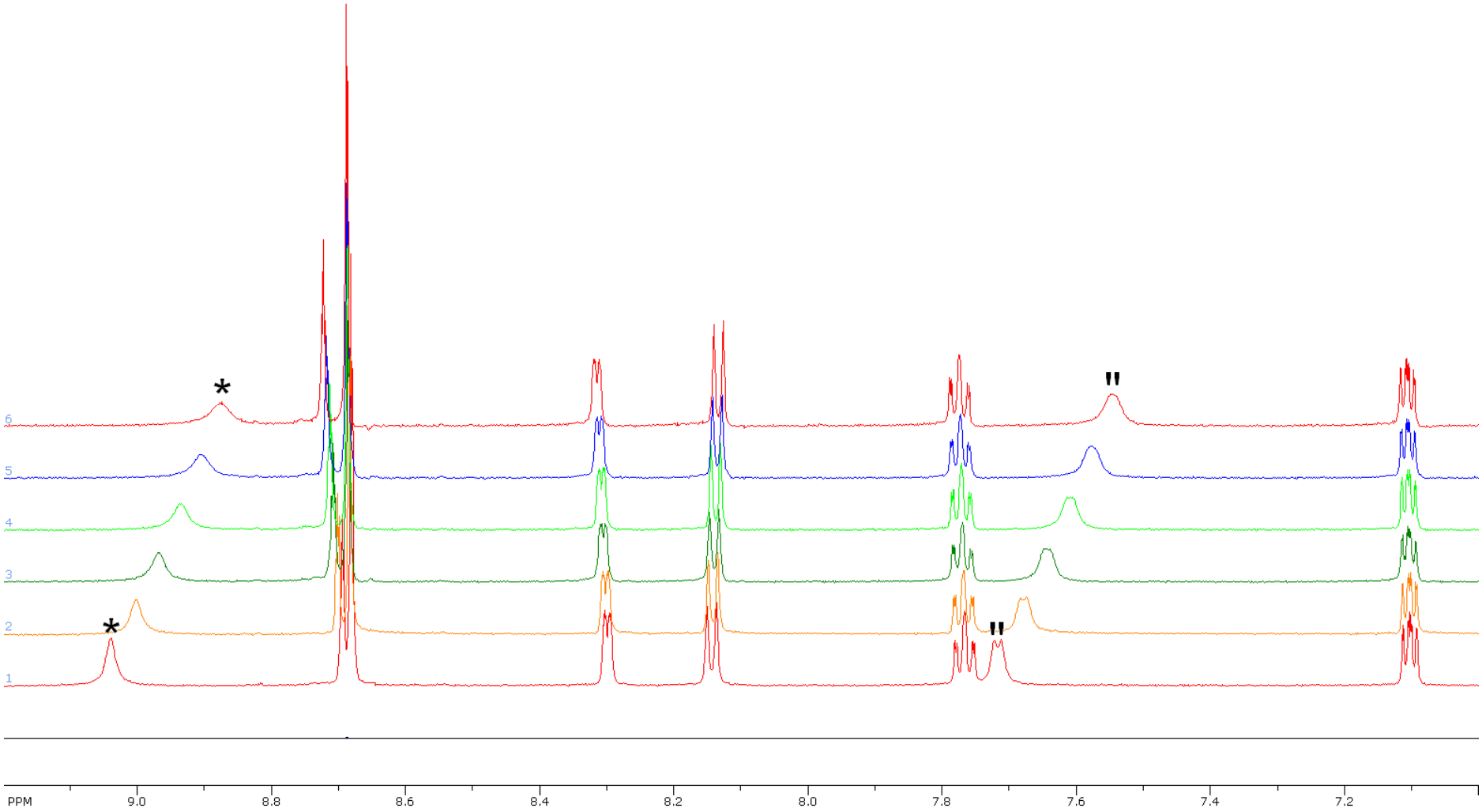

Figure S 13. Variable temperature ^{1}H NMR spectra (75–25 °C, top to bottom) of rac-**1a**, in acetonitrile-d_3. Alanyl (") and pyridyl (*) amide protons are accented.

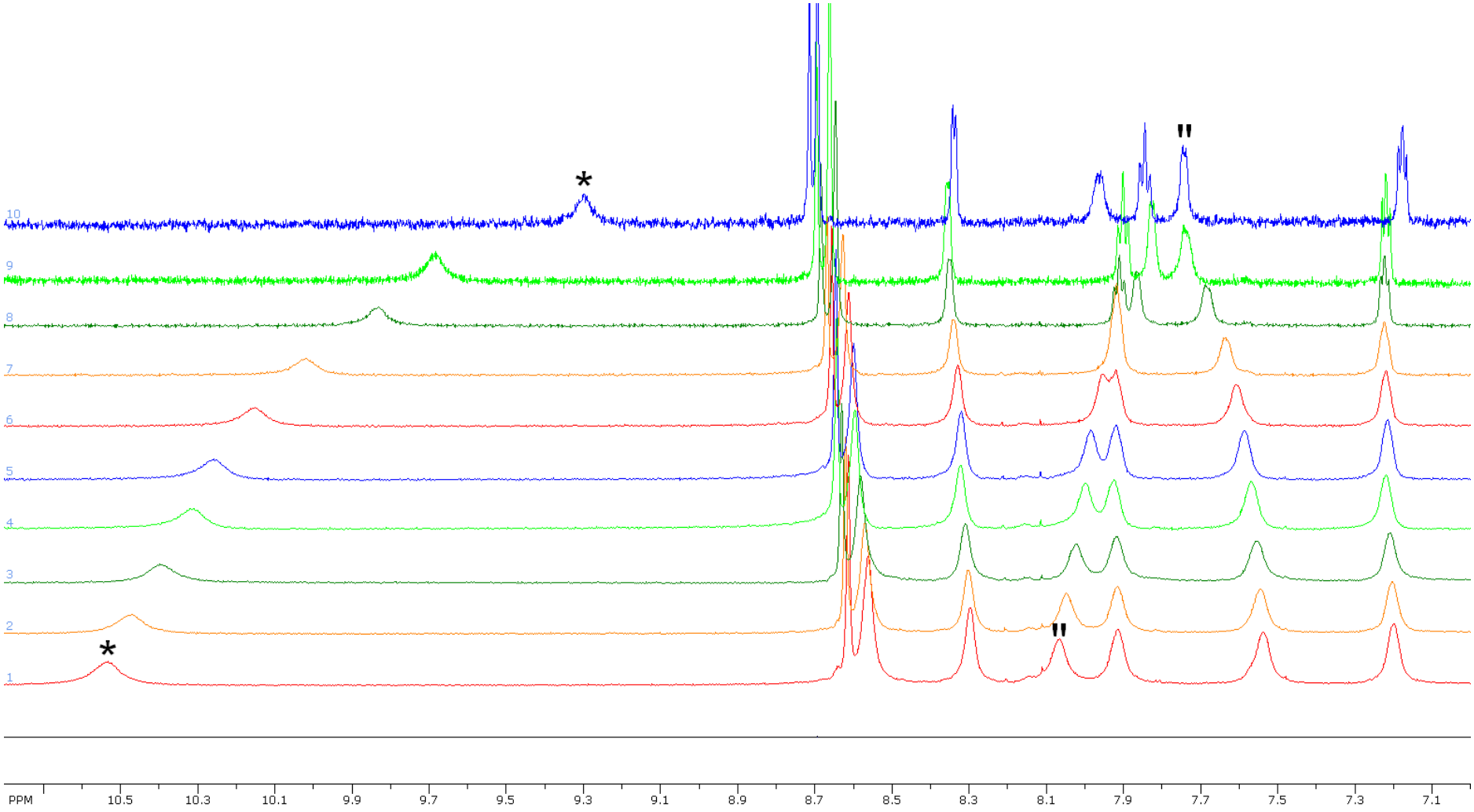

Figure S 14. Variable concentration ^{1}H NMR spectra (0.16–17.4 mM, top to bottom) of **2a**, in acetonitrile-d_3. Alanyl (") and pyridyl (*) amide protons are accented.

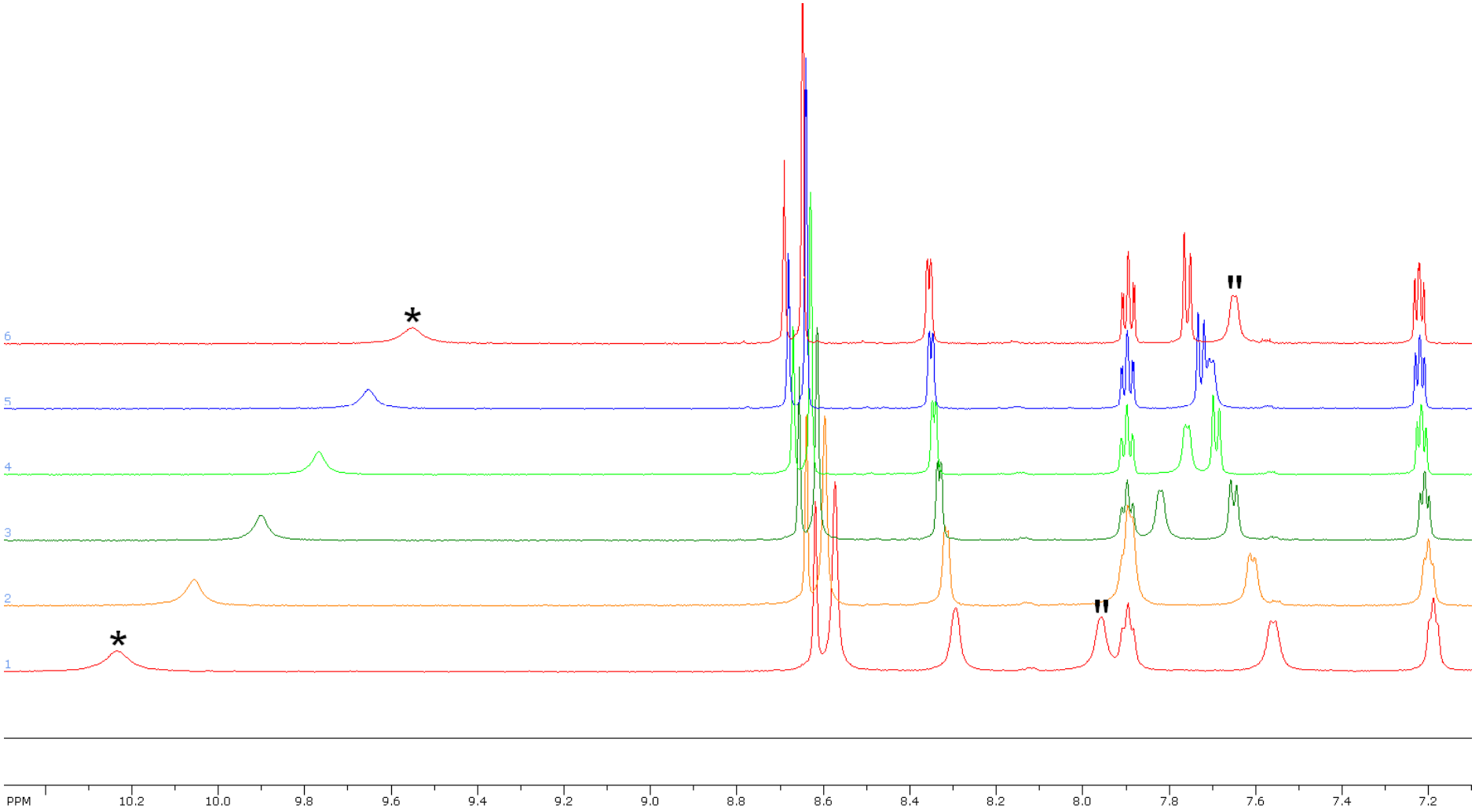

Figure S 15. Variable temperature ^{1}H NMR spectra (75–25 °C, top to bottom) of **2a**, in acetonitrile-d_3. Alanyl (") and pyridyl (*) amide protons are accented.

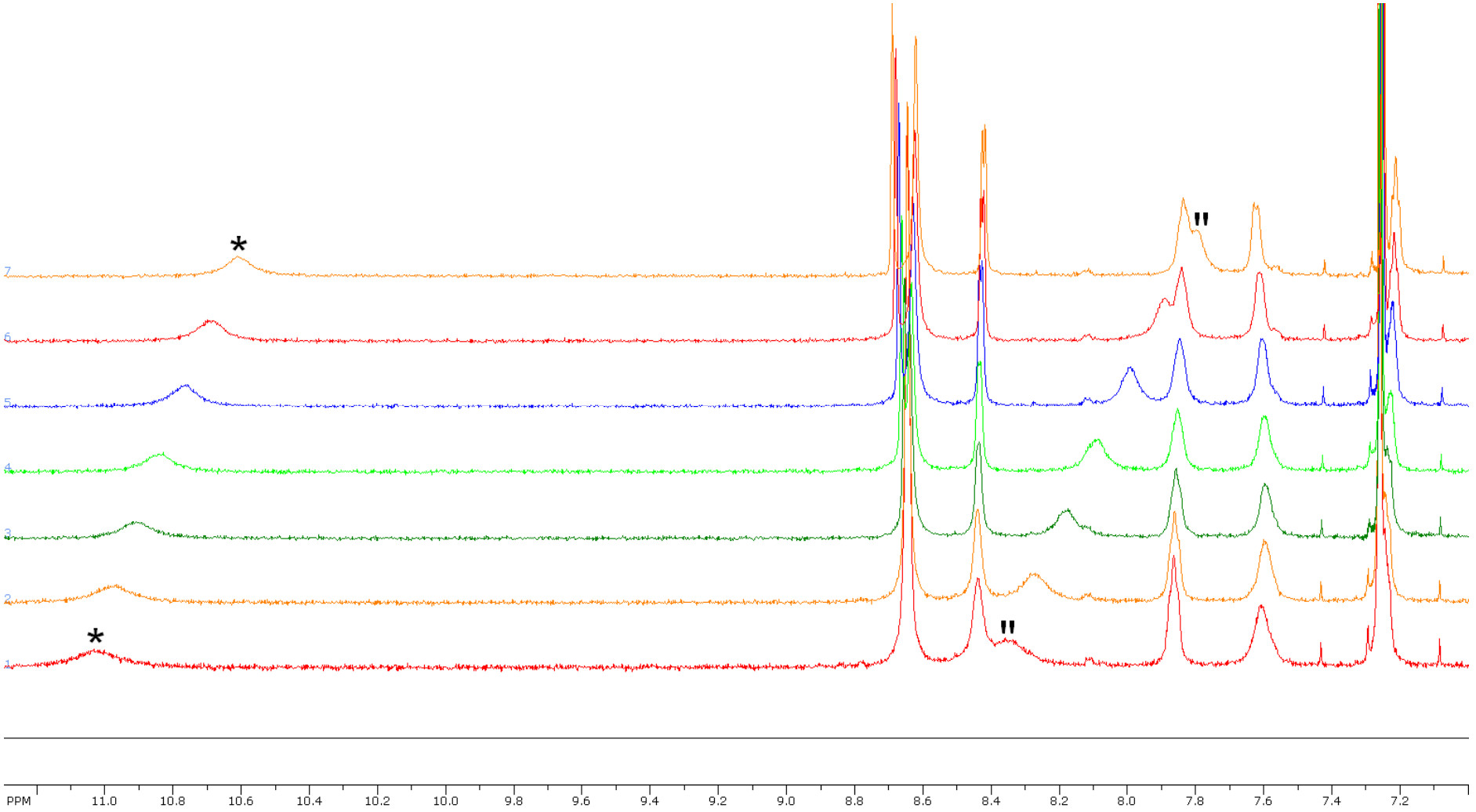

Figure S 16. Variable temperature ^{1}H NMR spectra (55–25 °C, top to bottom) of **2a**, in chloroform-d_1. Alanyl (") and pyridyl (*) amide protons are accented.

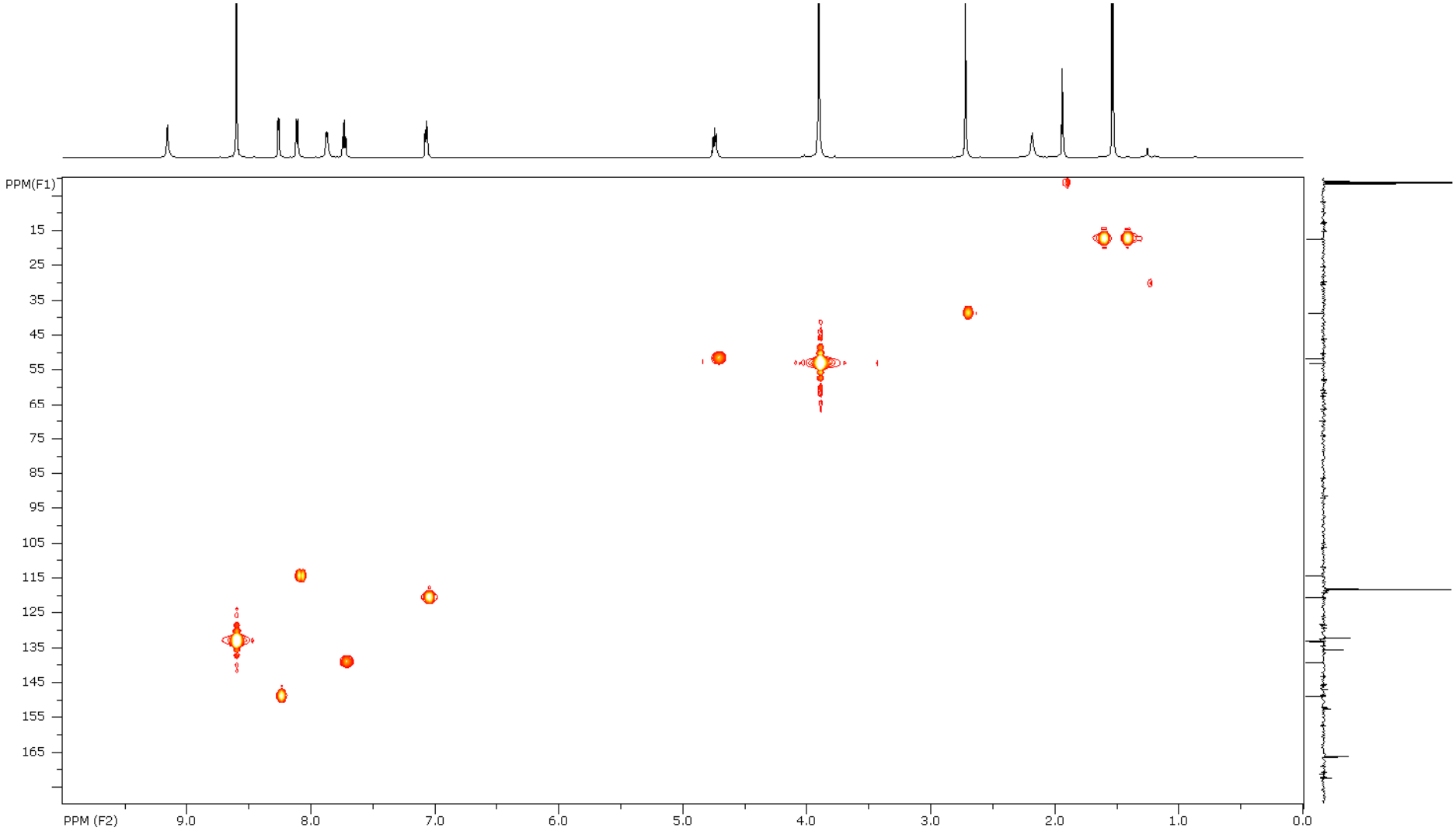

Figure S 17. ^{1}H-^{13}C HMQC spectrum of **1a** in acetonitrile-d_3.

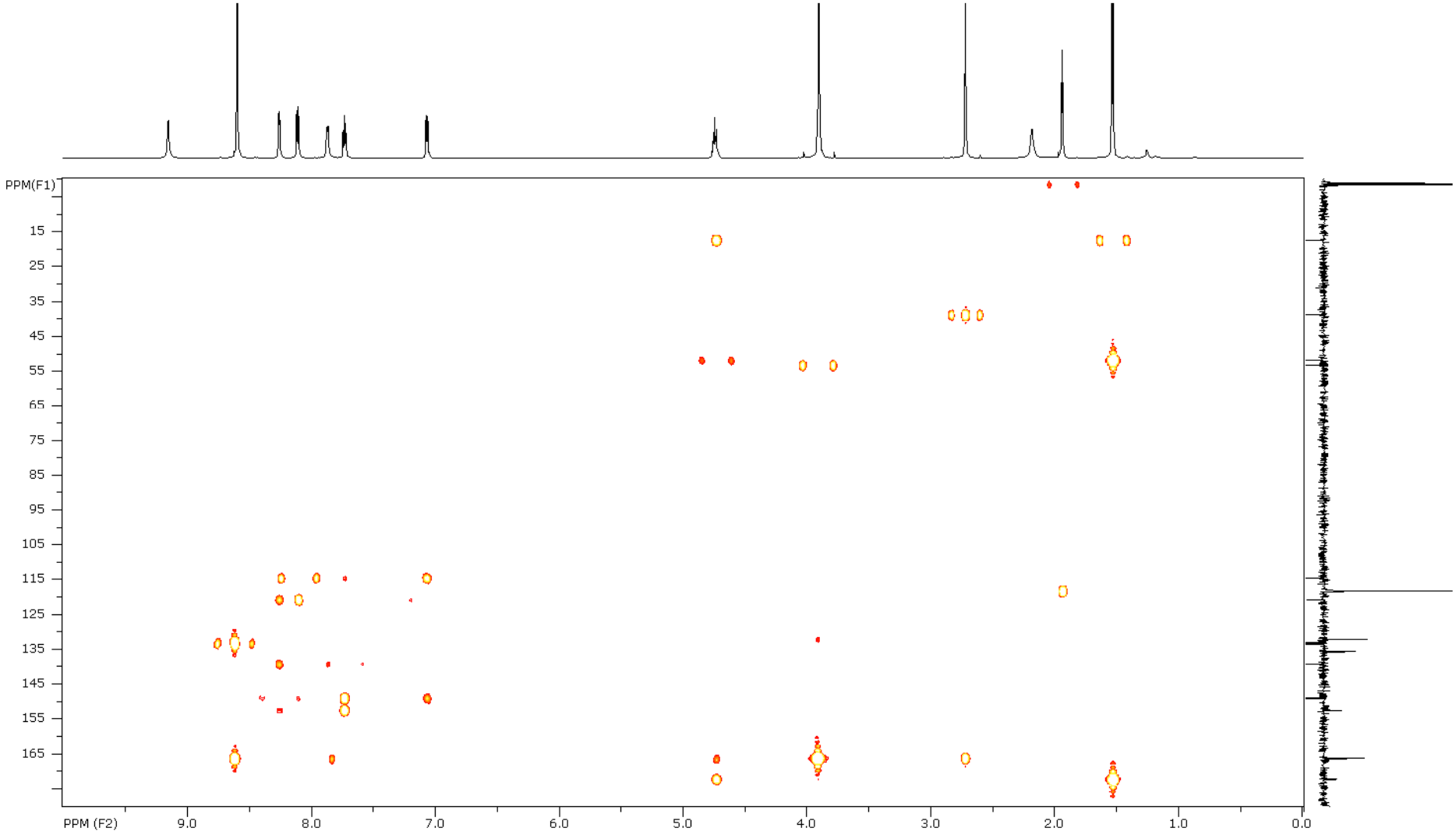

Figure S 18. ^{1}H-^{13}C HMBC spectrum of **1a** in acetonitrile-d_3.

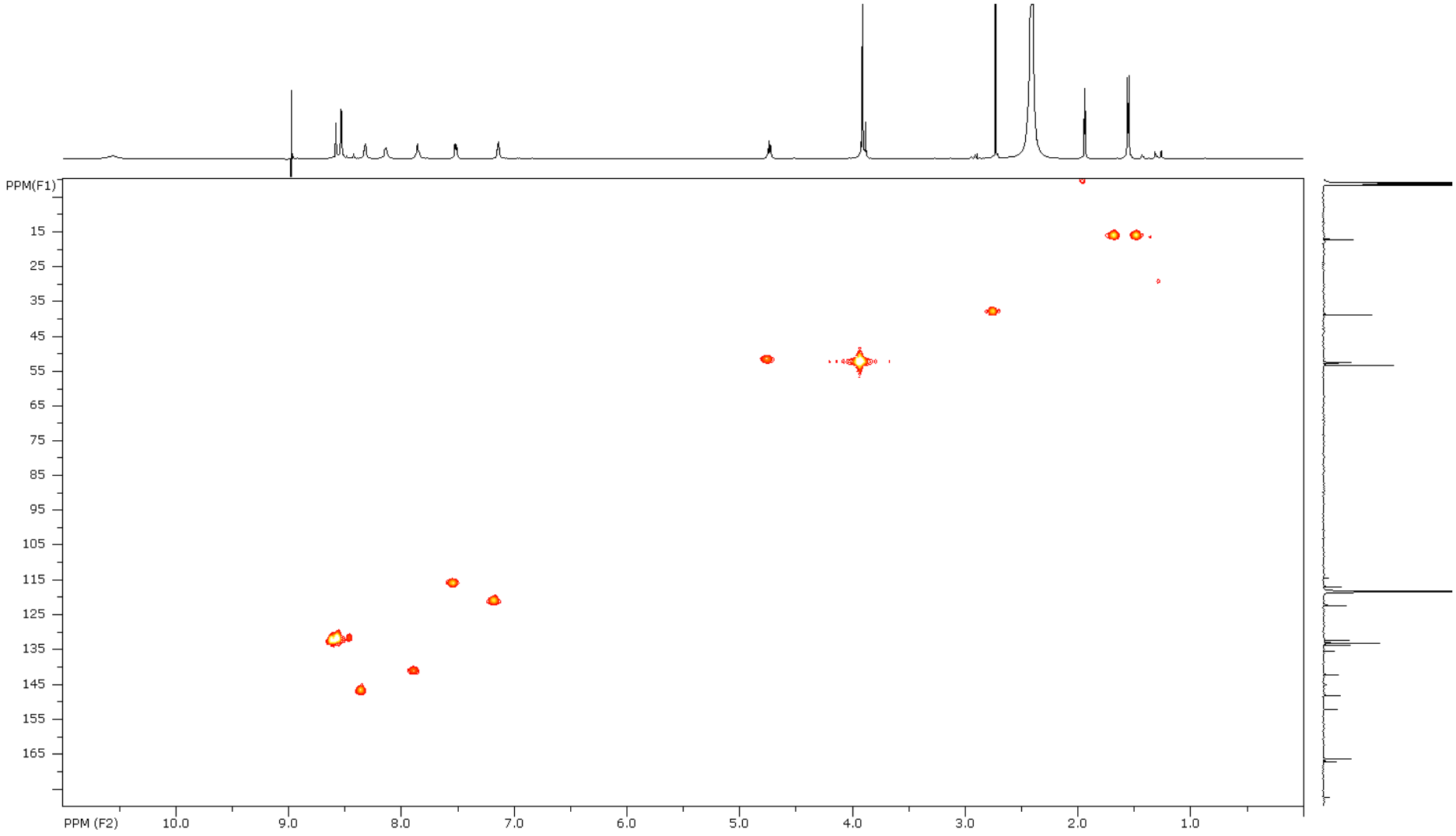

Figure S 19. ^{1}H-^{13}C HMQC spectrum of **2a** in acetonitrile-d_3.

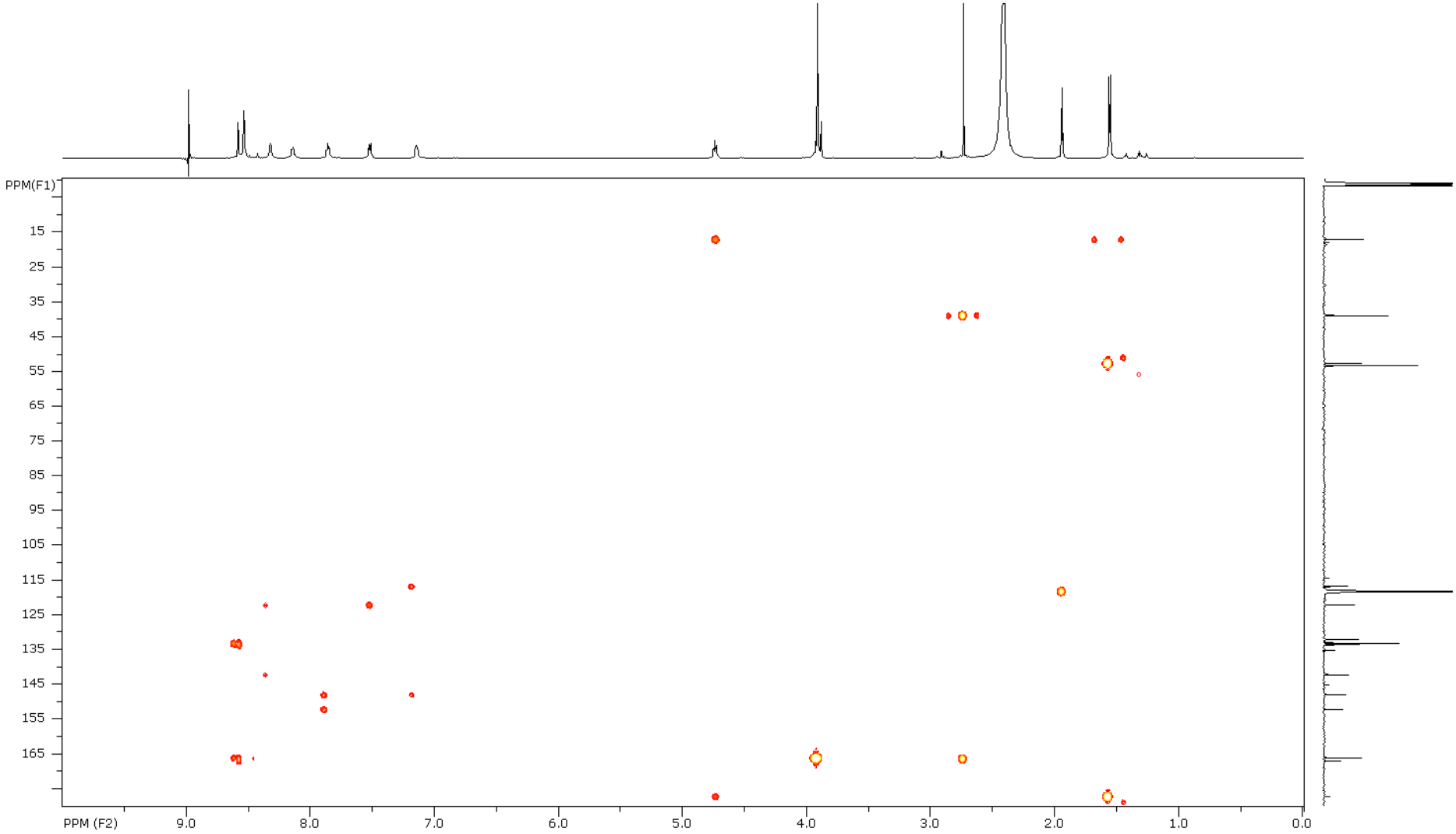

Figure S 20. ^{1}H-^{13}C HMBC spectrum of **2a** in acetonitrile-d_3.

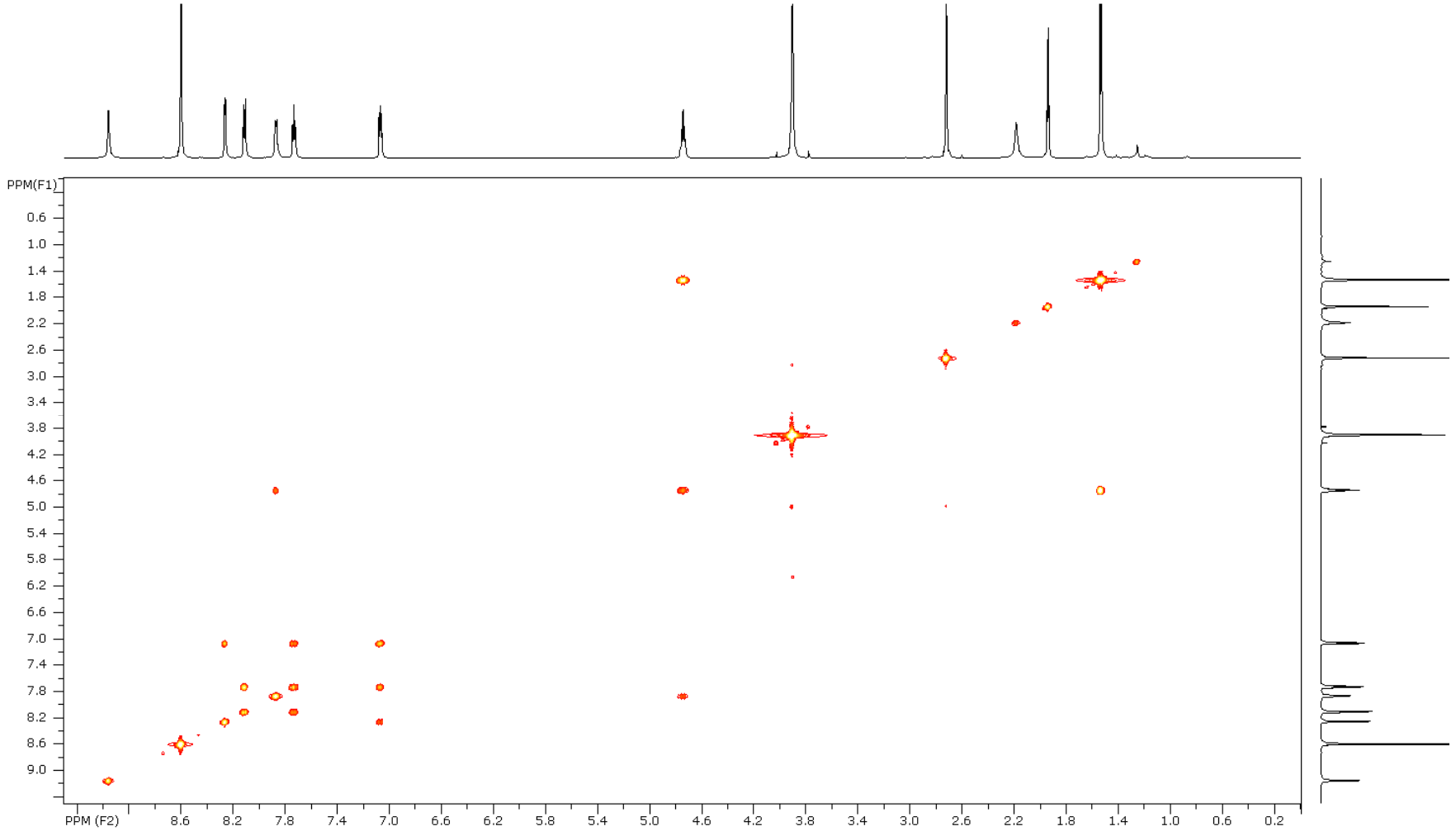

Figure S 21. ^{1}H-^{1}H COSY spectrum of **1a** in acetonitrile-d_3 (40 mM).

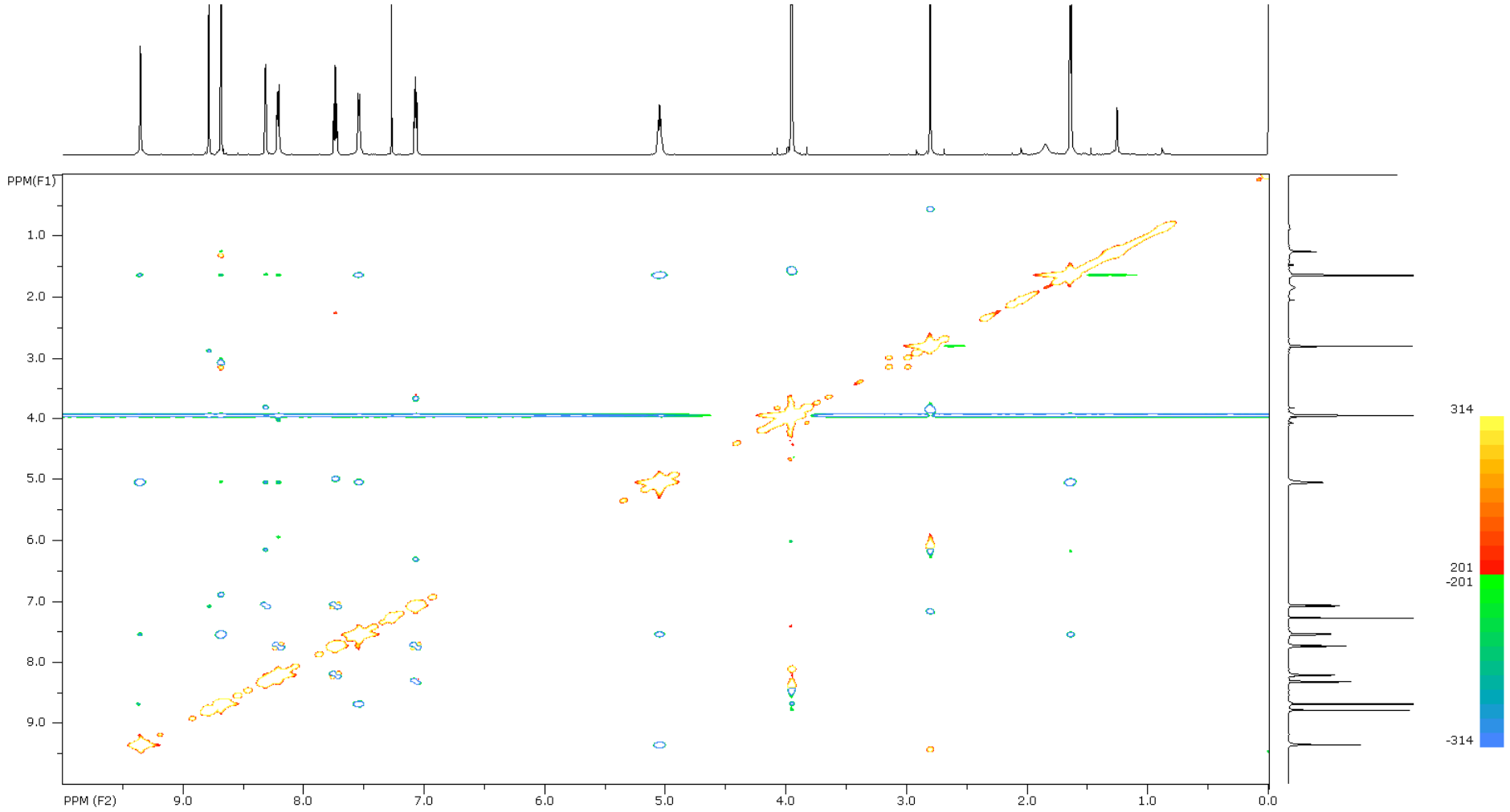

Figure S 22. ^{1}H-^{1}H ROESY spectrum of **1a** in chloroform-d_1 (40 mM).

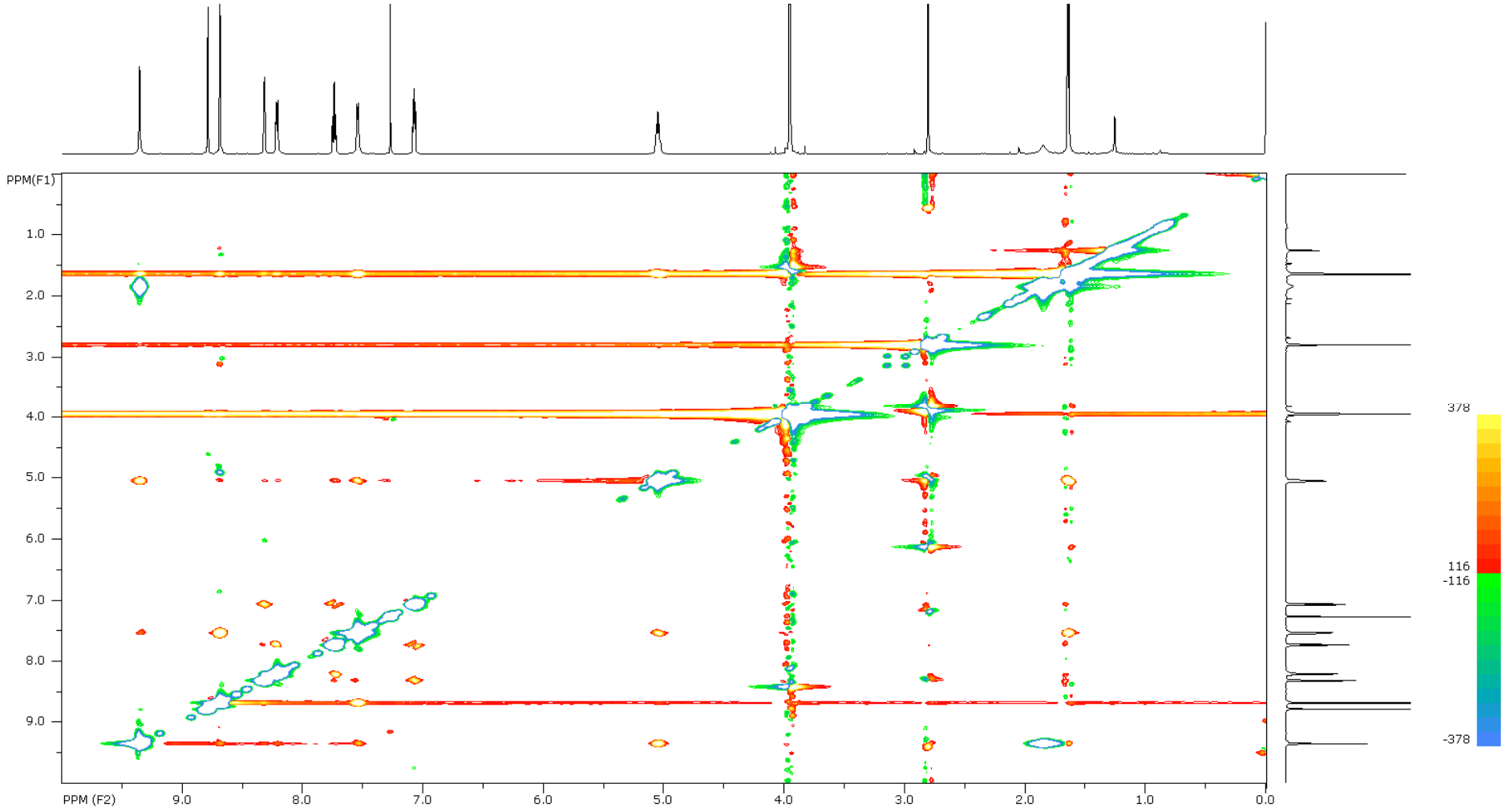

Figure S 23. ^{1}H-^{1}H NOESY spectrum of **1a** in chloroform-d_1 (40 mM).

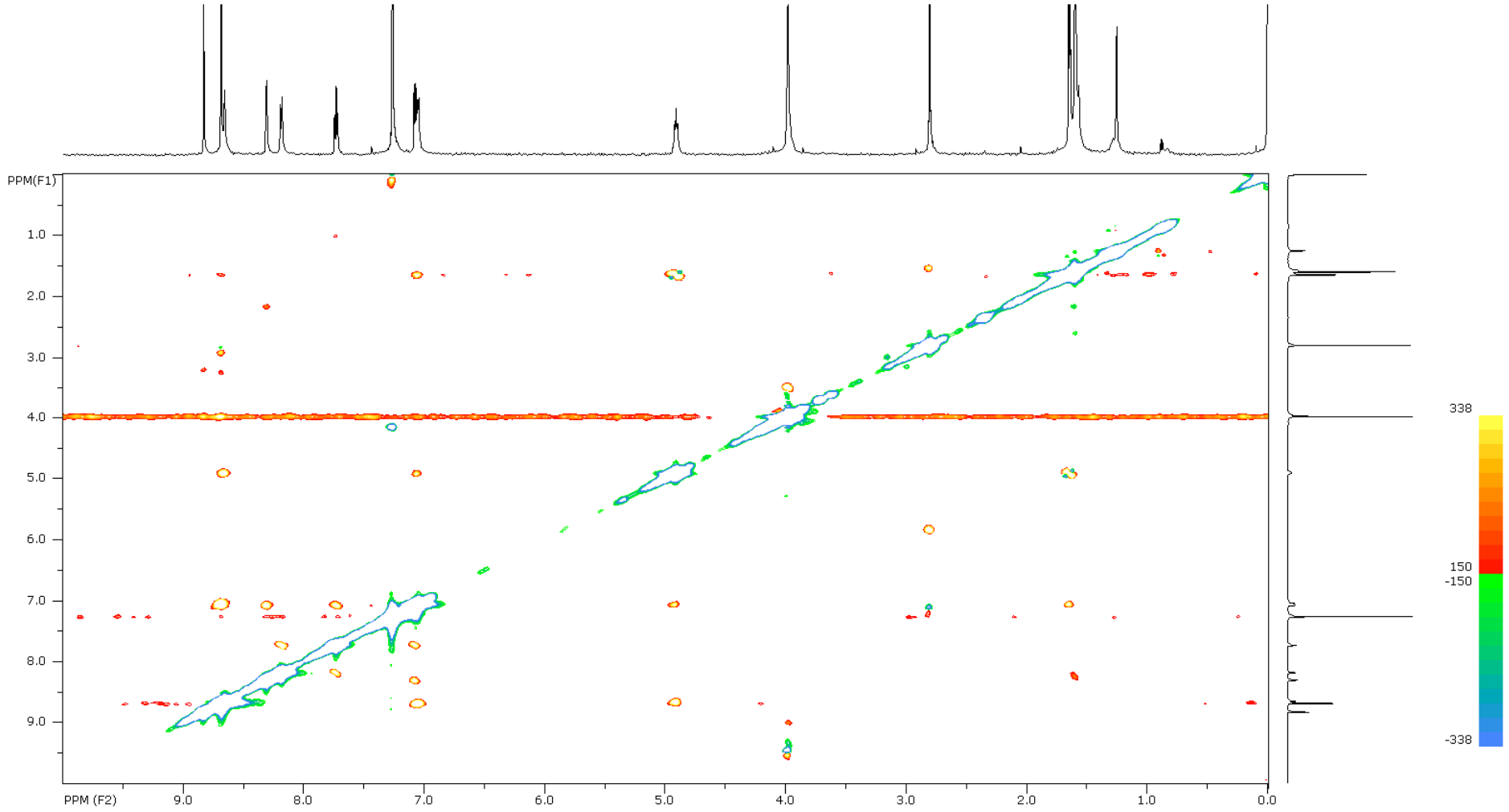

Figure S 24. ^{1}H-^{1}H ROESY spectrum of **1a** in chloroform-d_1 (4 mM).

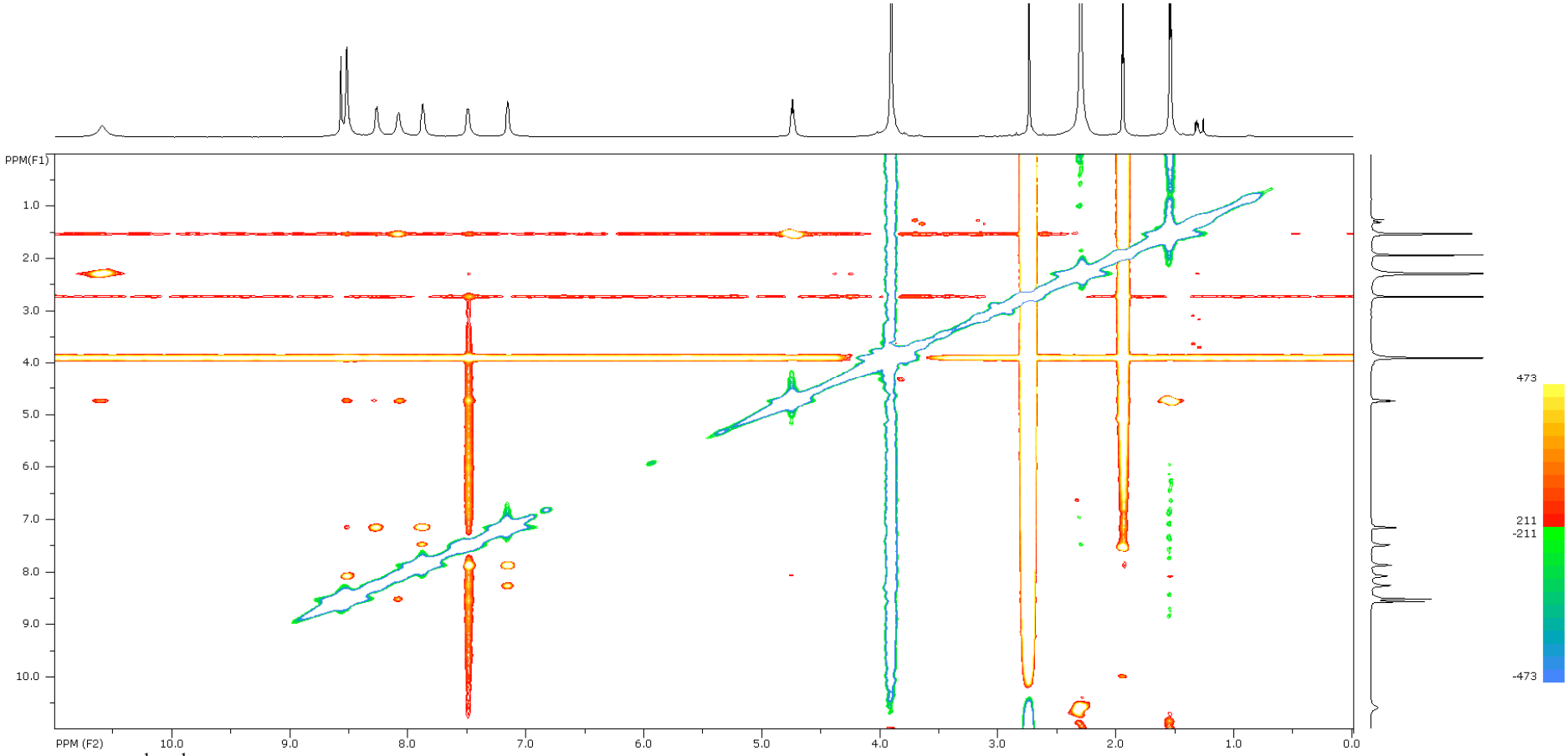

Figure S 25. ^{1}H-^{1}H ROESY spectrum of **2a** in acetonitrile-d_3 (≈ 20 mM).

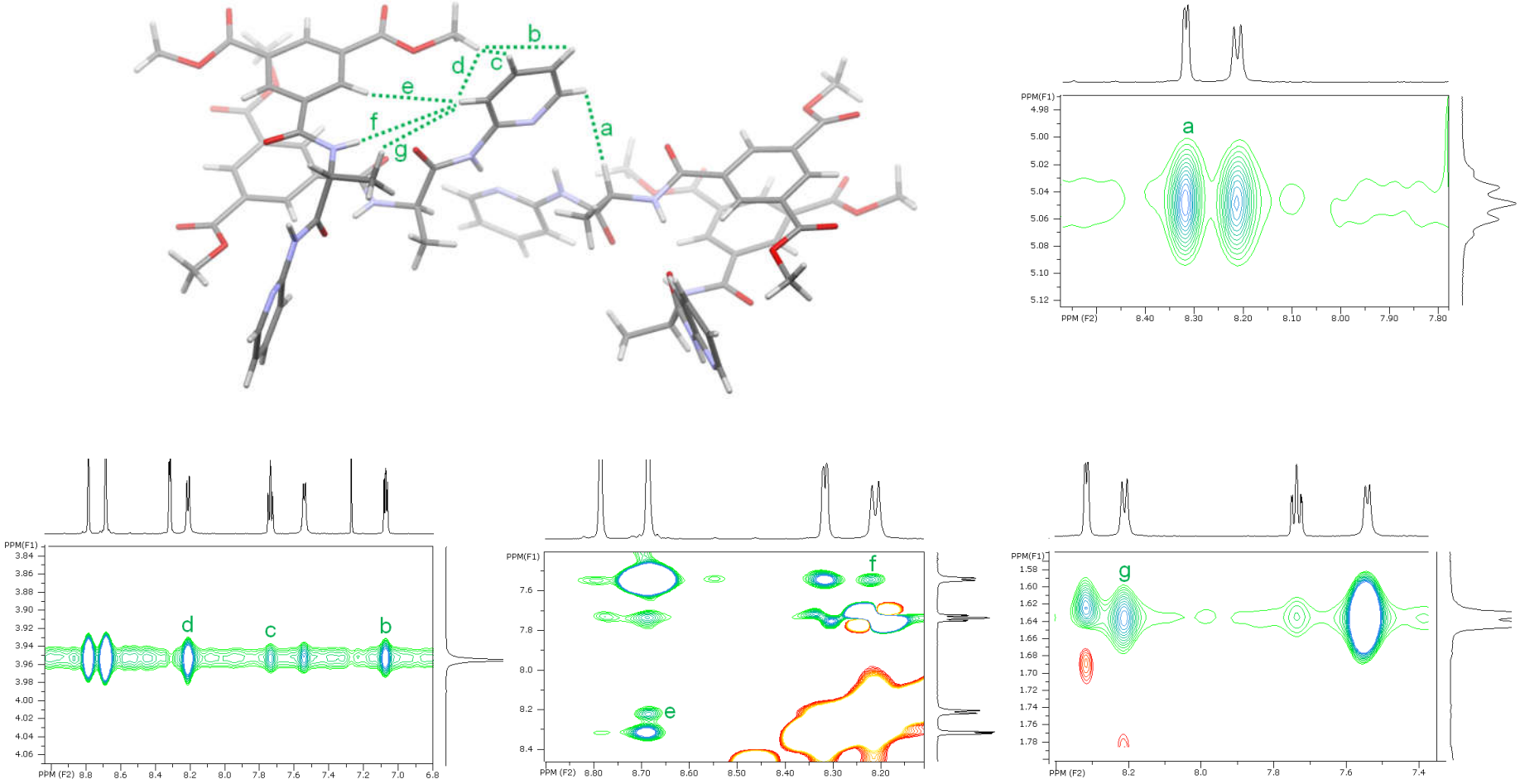

Figure S 26. Molecule arrangement in the crystal structure of **1a**, with intercepts of chosen ROESY contacts in chloroform-d_1 (40 mM), indicating similar molecular arrangements in solution and solid state.

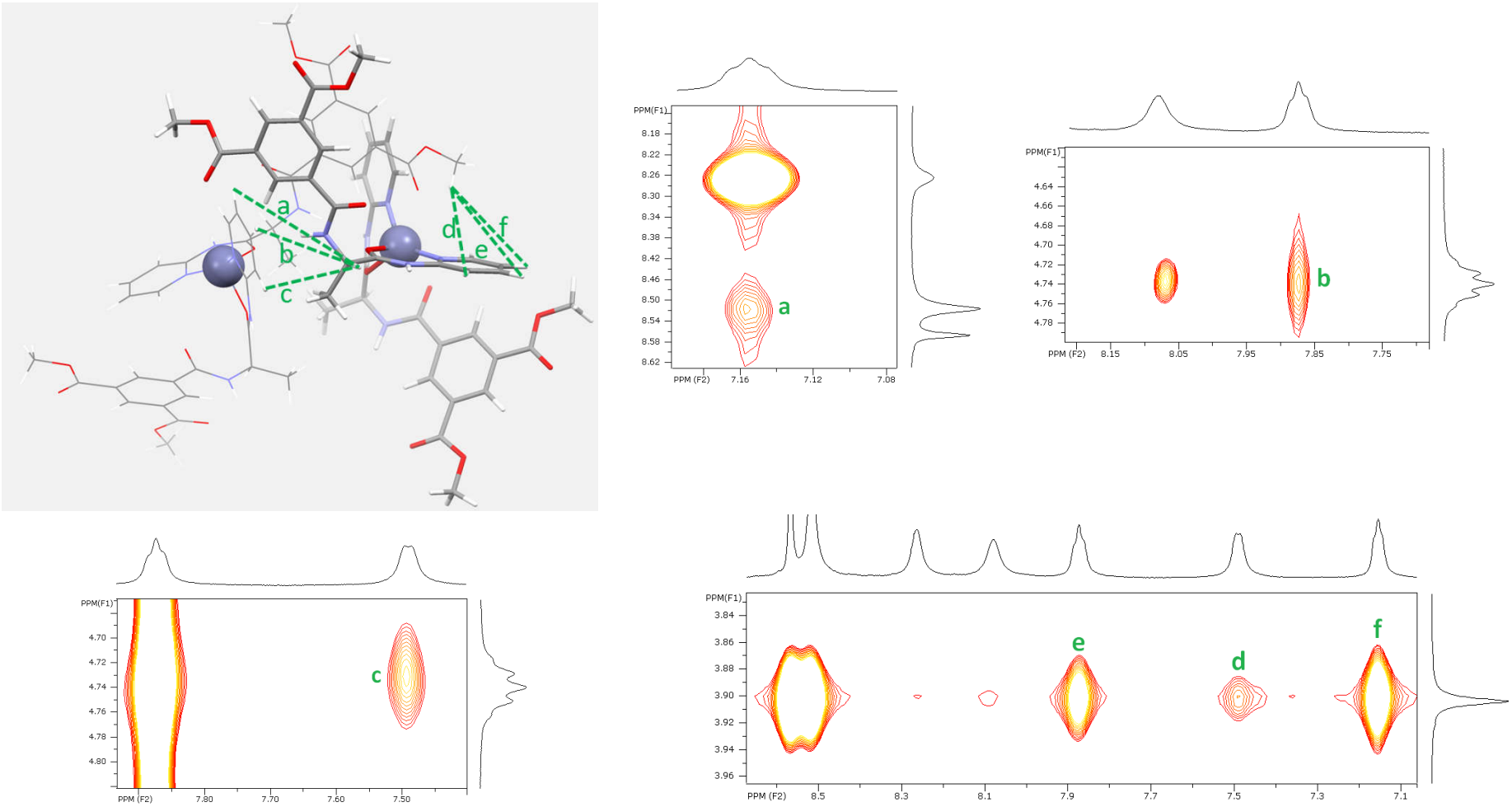

Figure S 27. DFT optimized half-turn structure of **2a**, with intercepts of chosen ROESY contacts in acetonitrile-d_3 (≈ 20 mM), indicating similar molecular arrangement as in **1a**. Two molecules of the complex are shown in different styles for clarity reasons.

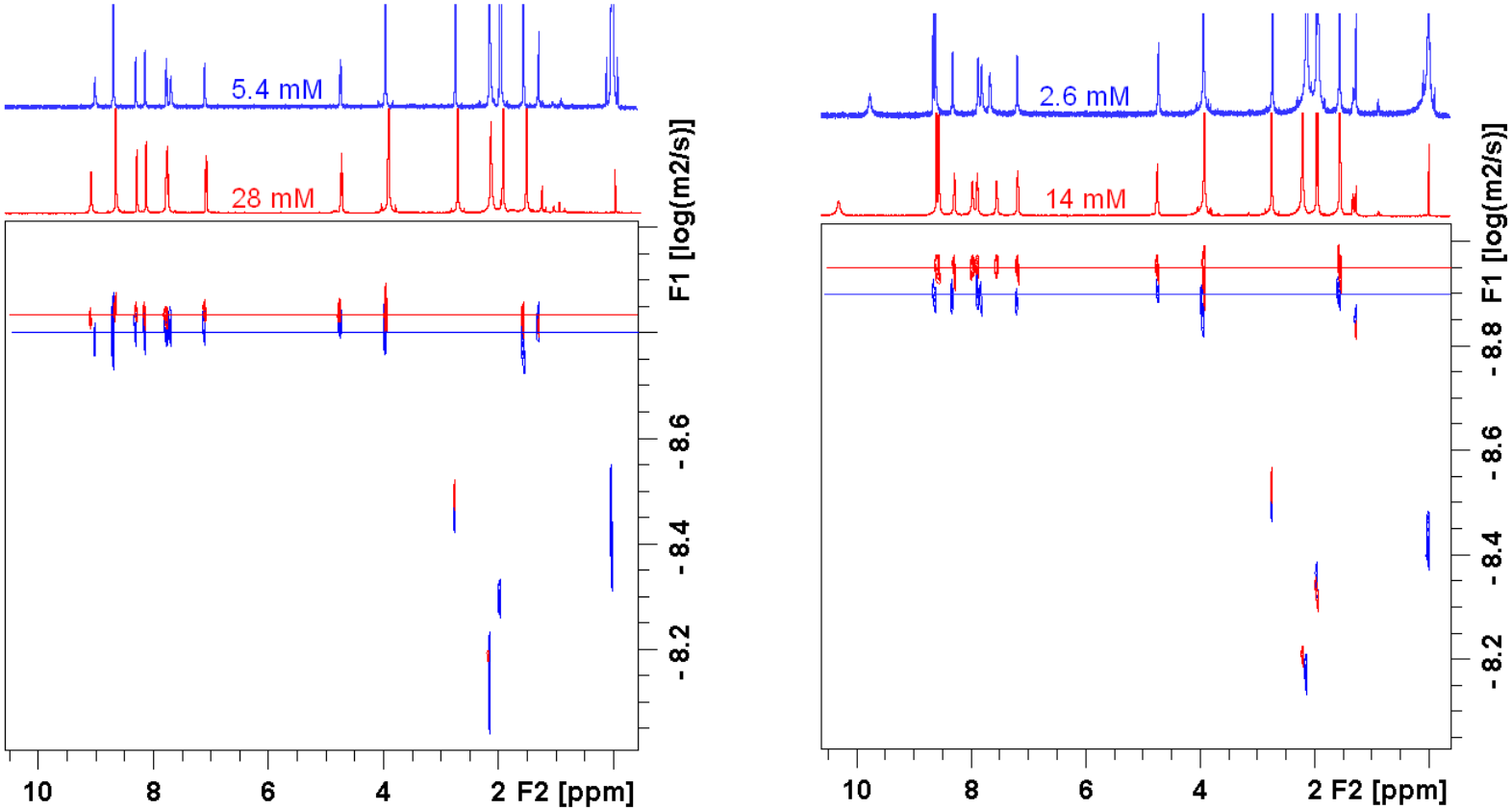

Figure S 28. DOSY spectra of (a) **1a** and (b) **2a** in acetonitrile-d_3 showing reduction of diffusion coefficient at higher concentration, indicating molecular association in both compounds.

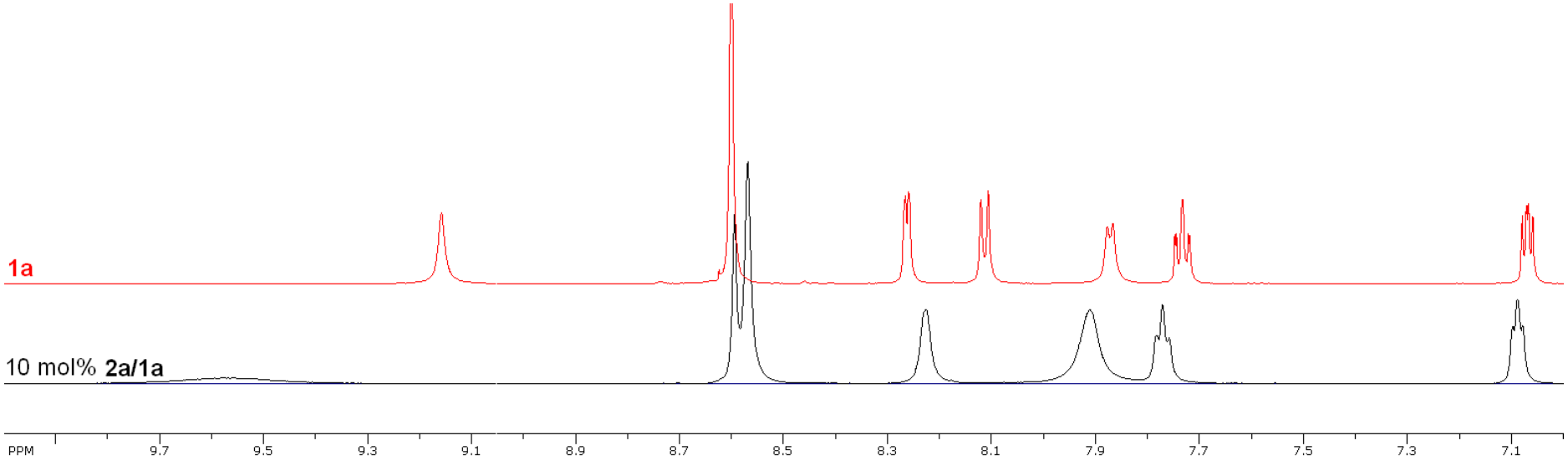

Figure S 29. ^{1}H NMR spectra intercept of **1a** and mixture of **2a**/**1a** in acetonitrile-d_3 showing one set of signals, indicating fast ligand exchange at zinc (at total ligand concentration of 40 mM).

CD Measurements

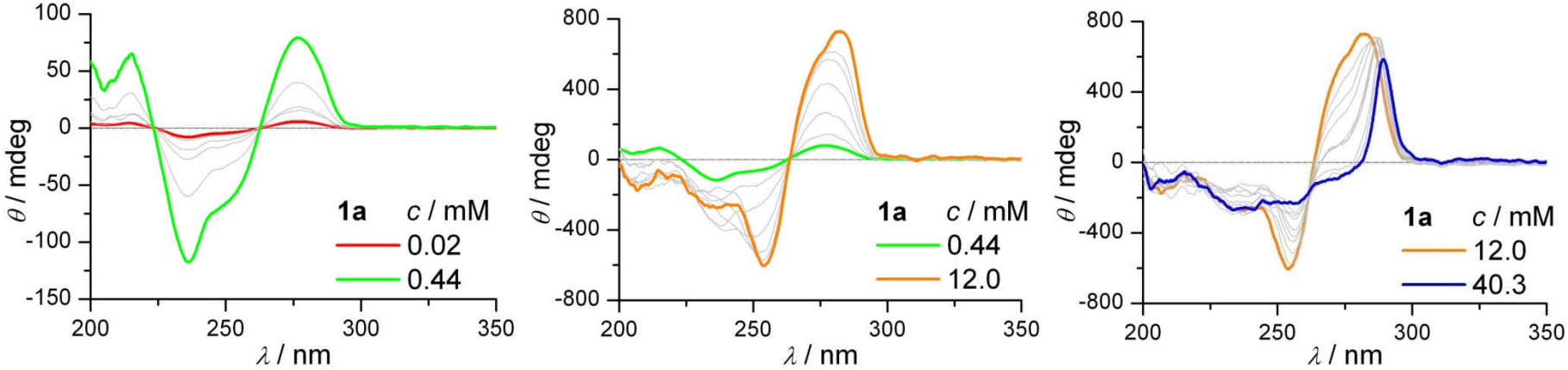

Figure S 30. Variable concentration CD spectra of **1a** in acetonitrile.

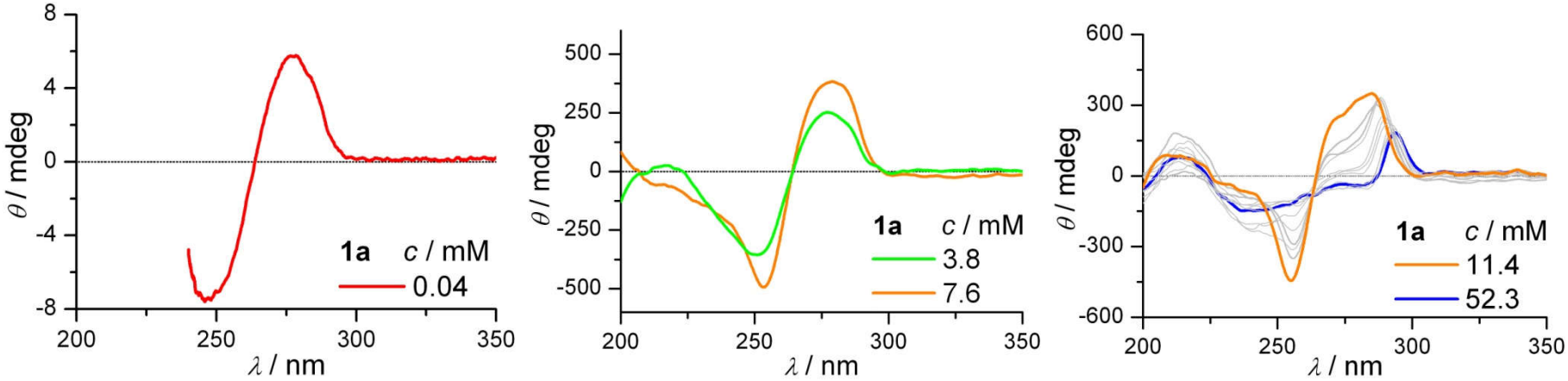

Figure S 31. Variable concentration CD spectra of **1a** in chloroform (3.8–52.3 mM data were smoothed with Savitzky-Golay method).

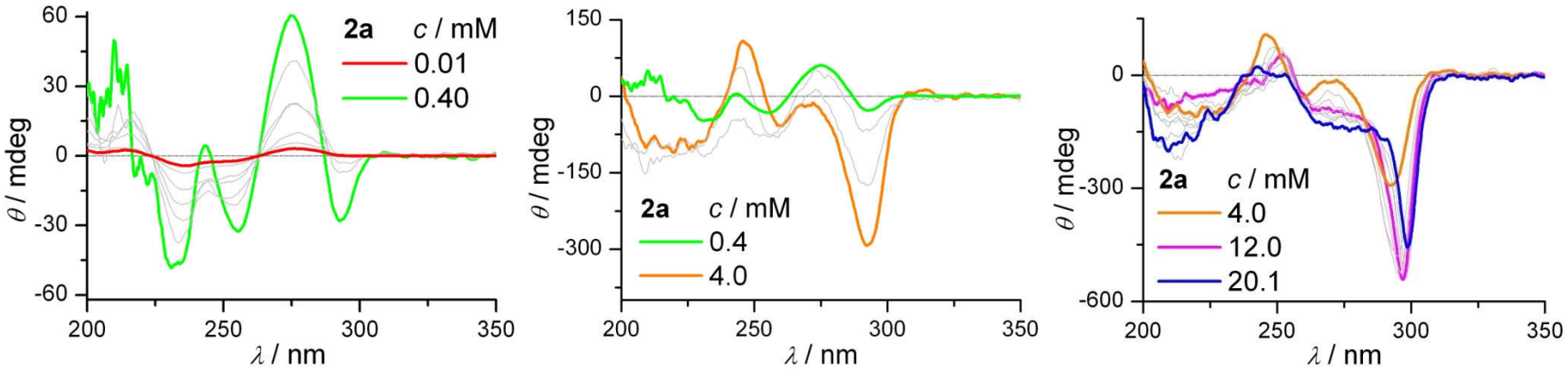

Figure S 32. Variable concentration CD spectra of **2a** in acetonitrile.

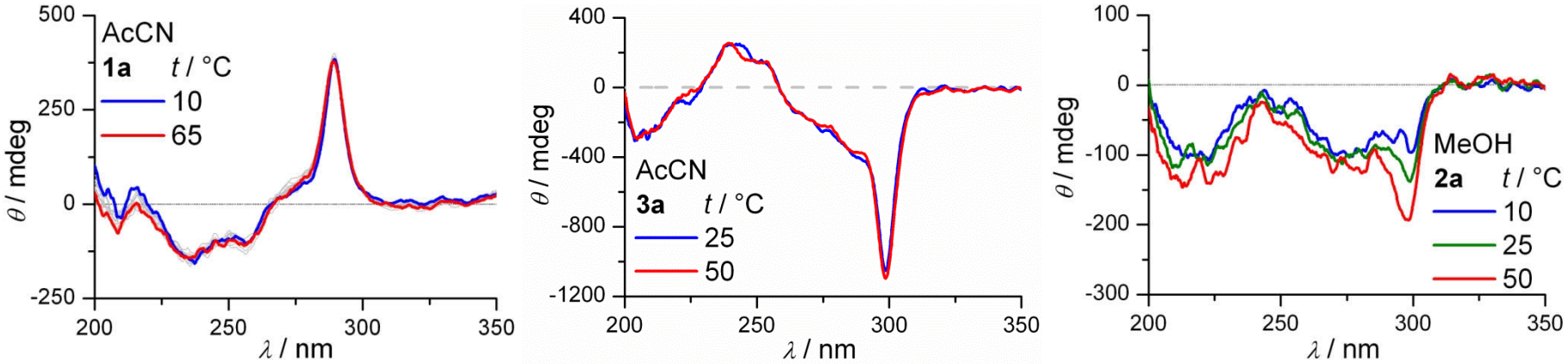

(a) (b) (c)

Figure S 33. Variable temperature CD measurements of (a) **1a** (10–65 °C; step: 5 °C); (b) **3a**; (c) **2a** at total ligand concentration of 40 mM.

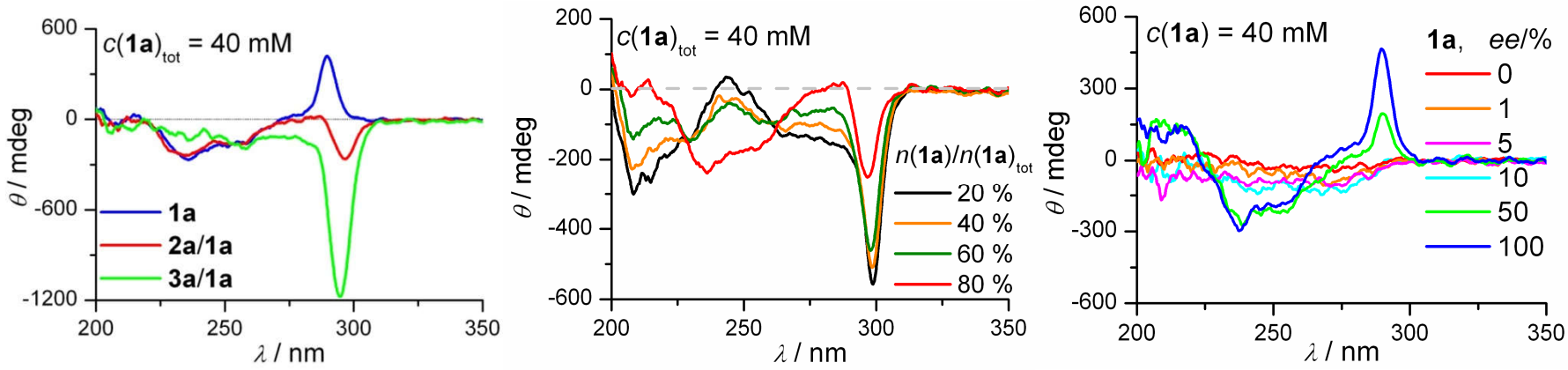

(a) (b) (c)

Figure S 34.CD spectra in acetonitrile of (a) **1a** and 10 mol% of **2a**/**1a** and **3a**/**1a** mixtures, showing chiral inversion independent of counter ion (nitrate or tetrafluoroborate), underlying the "Sergeant and Soldiers Principle". The **3a**/**1a** mixture was obtained by adding $Zn(BF_4)_2$ solution to the ligand solution; (b) different **1a**/**2a** mixtures. Note that 10 mol% of **2a**/**1a** mixture is equivalent to 80 % of complexed ligand in the mixture (red lines in (a) and (b)); (c) **1a** at variable optical purity.

UV Measurements

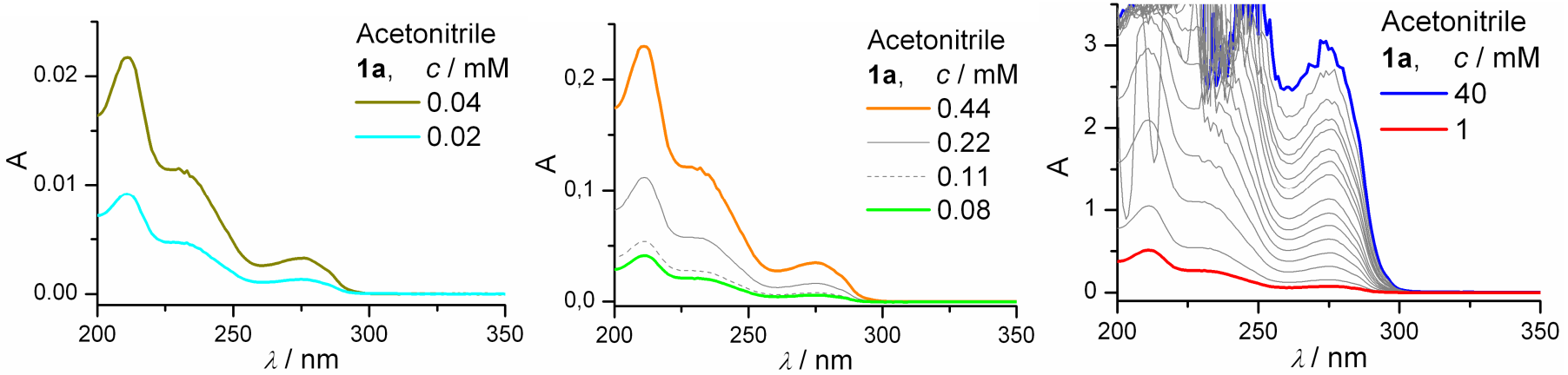

Figure S 35. UV spectra of **1a** at different concentrations in acetonitrile. The spectra are corrected for 0.1 mm path length.

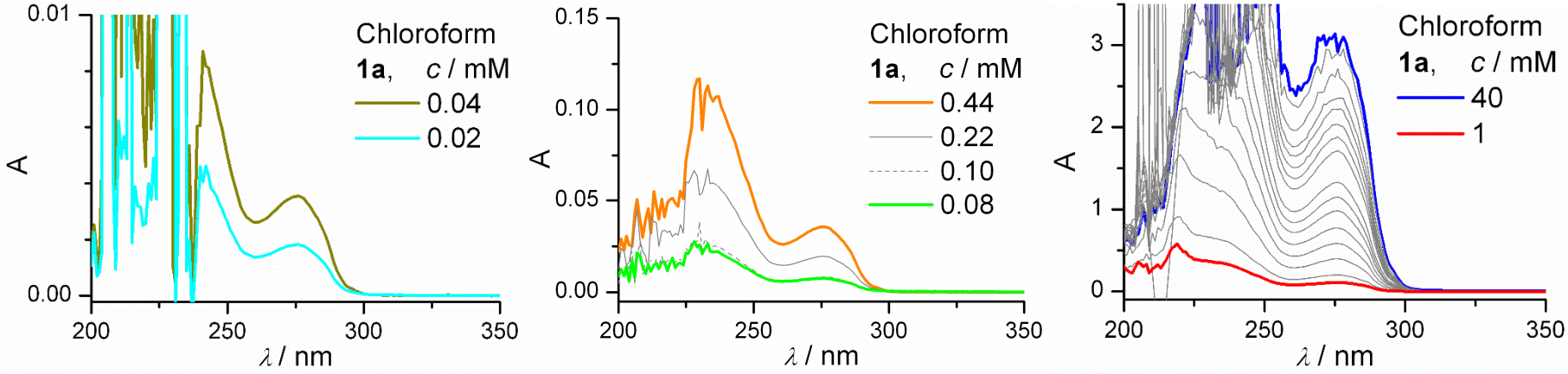

Figure S 36. UV spectra of **1a** at different concentrations in chloroform. The spectra are corrected for 0.1 mm path length.

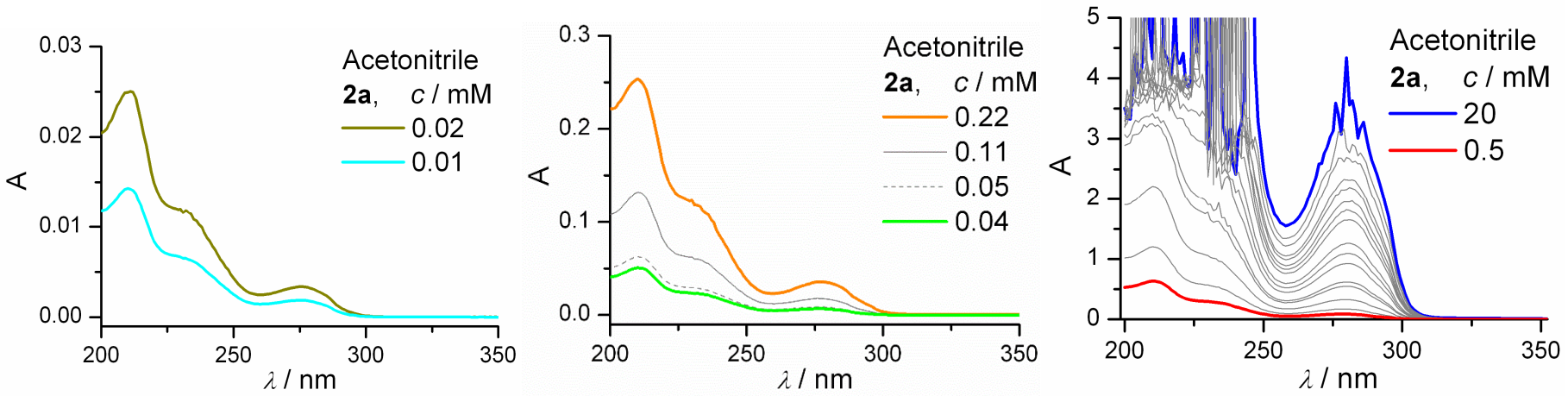

Figure S 37. UV spectra of **2a** at different concentrations in acetonitrile. The spectra are corrected for 0.1 mm path length.

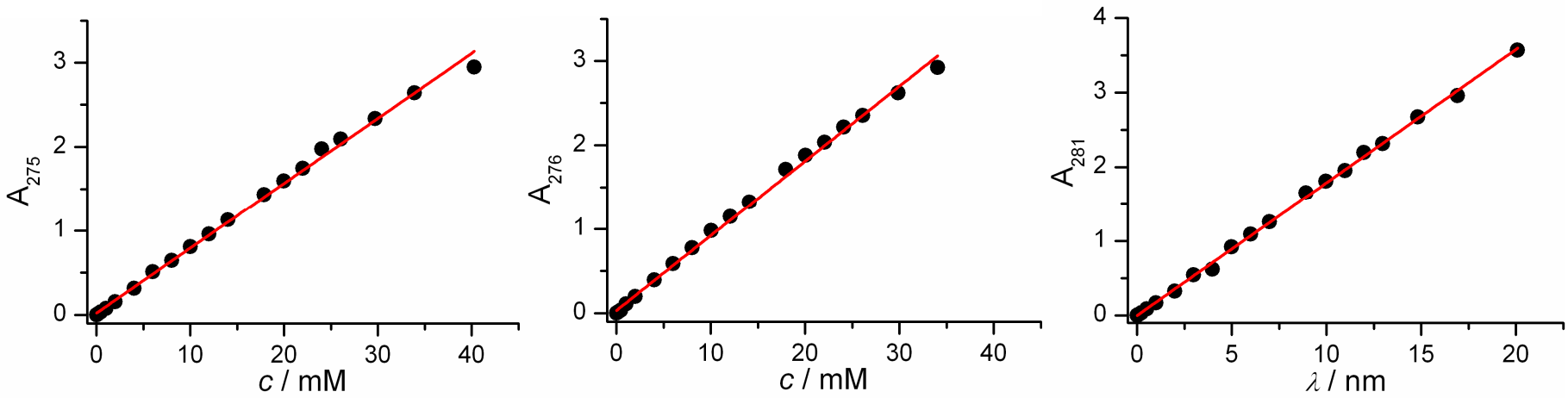

(a) (b) (c)

Figure S 38. Concentration vs. absorbance plot of (a) **1a** in acetonitrile; (b) **1a** in chloroform; (c) **2a** in acetonitrile, showing slight deviations from linearity. The data is corrected for 0.1 mm path length.

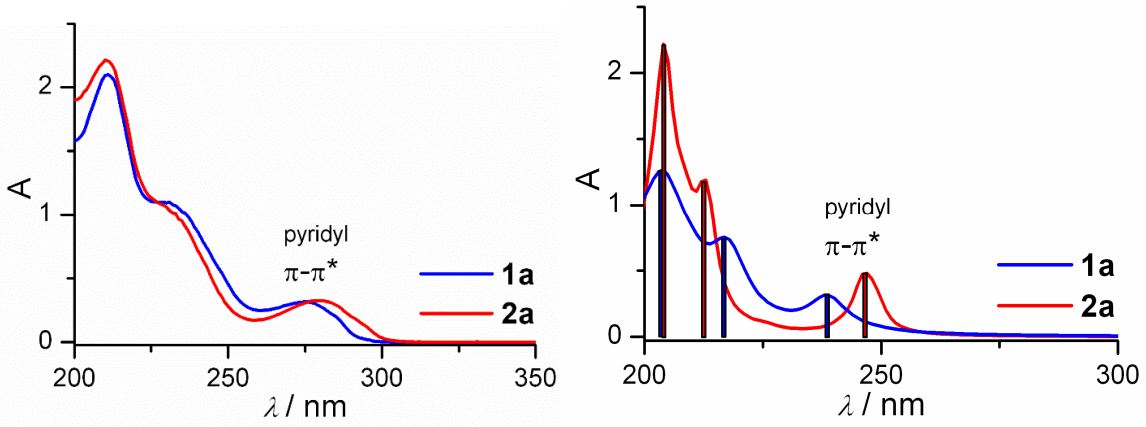

Figure S 39. Qualitative comparison of UV spectra of **1a** and **2a** in acetonitrile: (a) experimental (4 mM); (b) TD-DFT calculated.

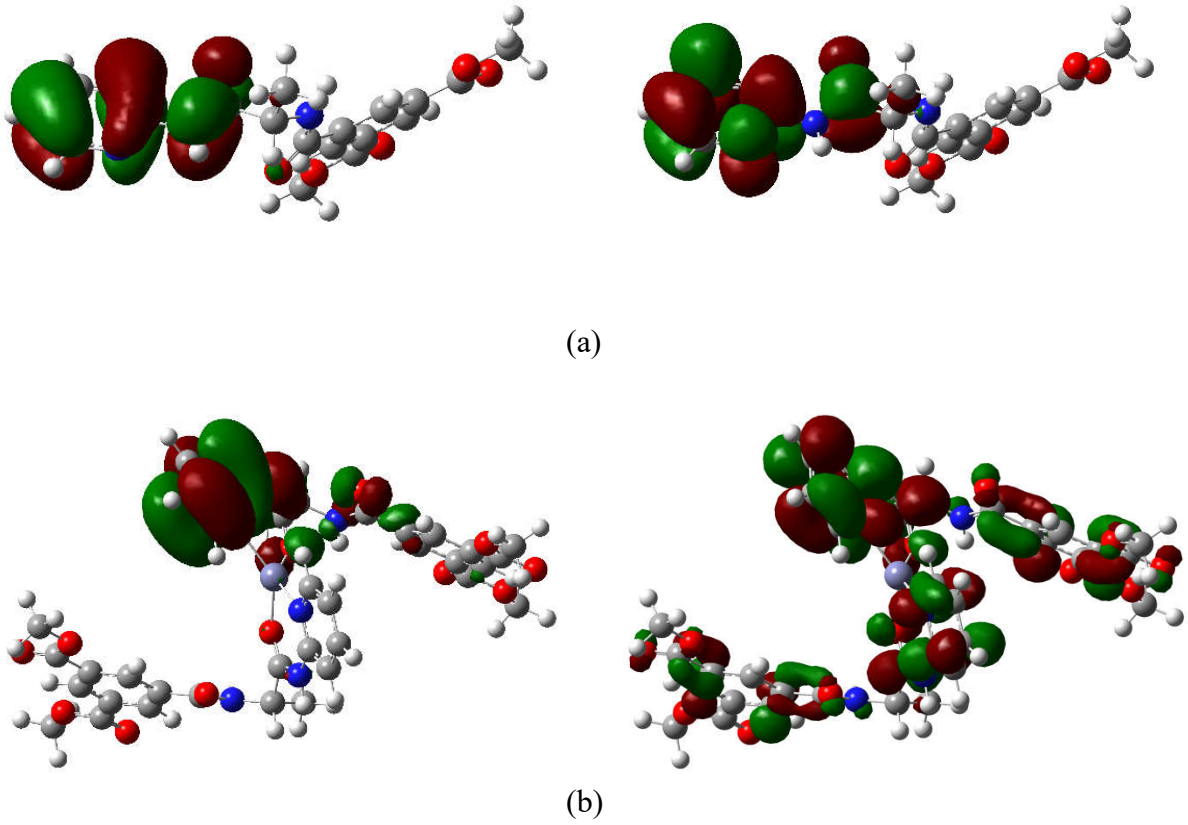

Figure S 40. Orbitals in pyridine π-π* electronic transitions for (a) **1a** and (b) **2a**.

IR Measurements

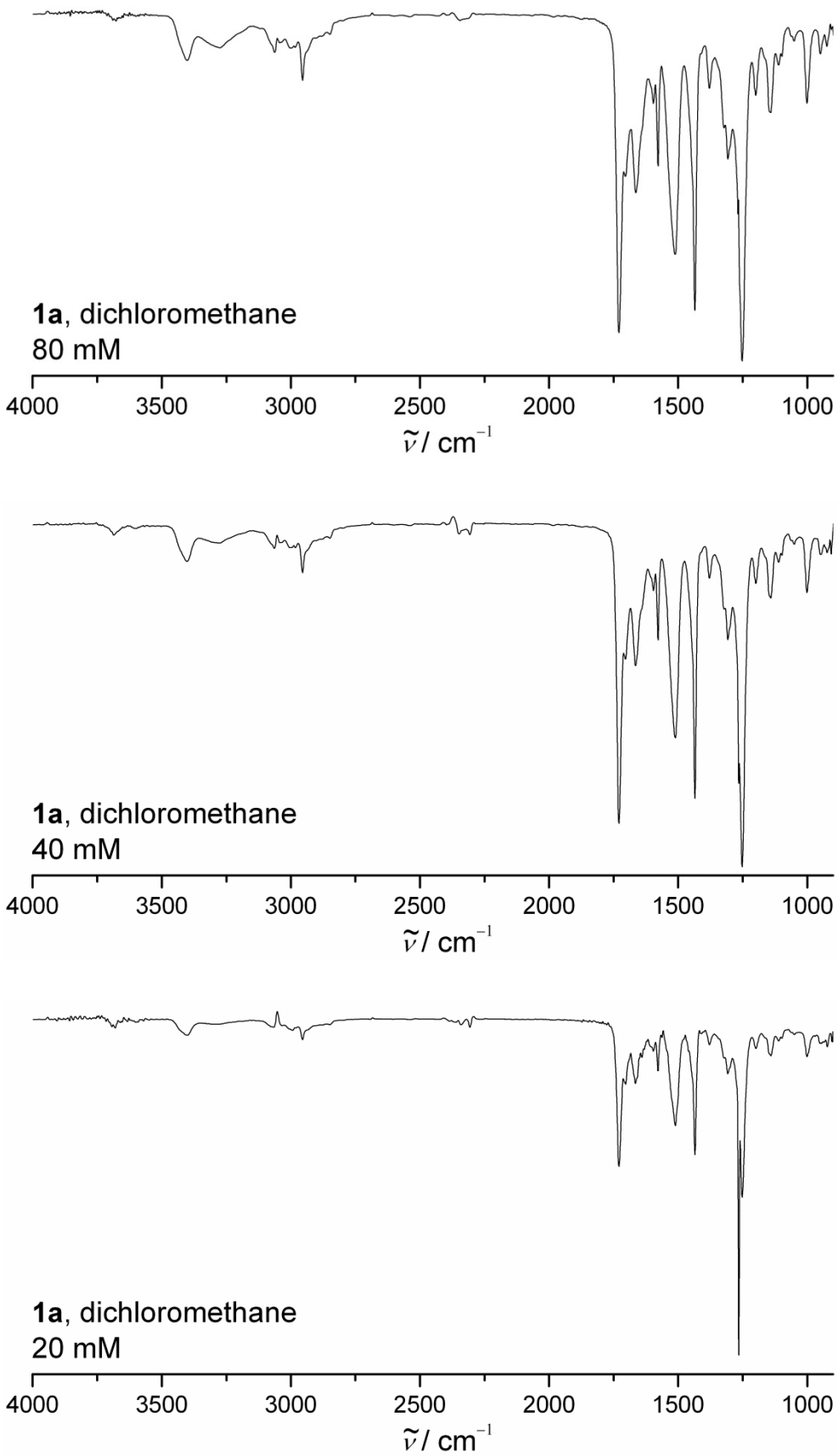

Figure S 41. FT-IR spectra of **1a** in dichloromethane at different concentrations.

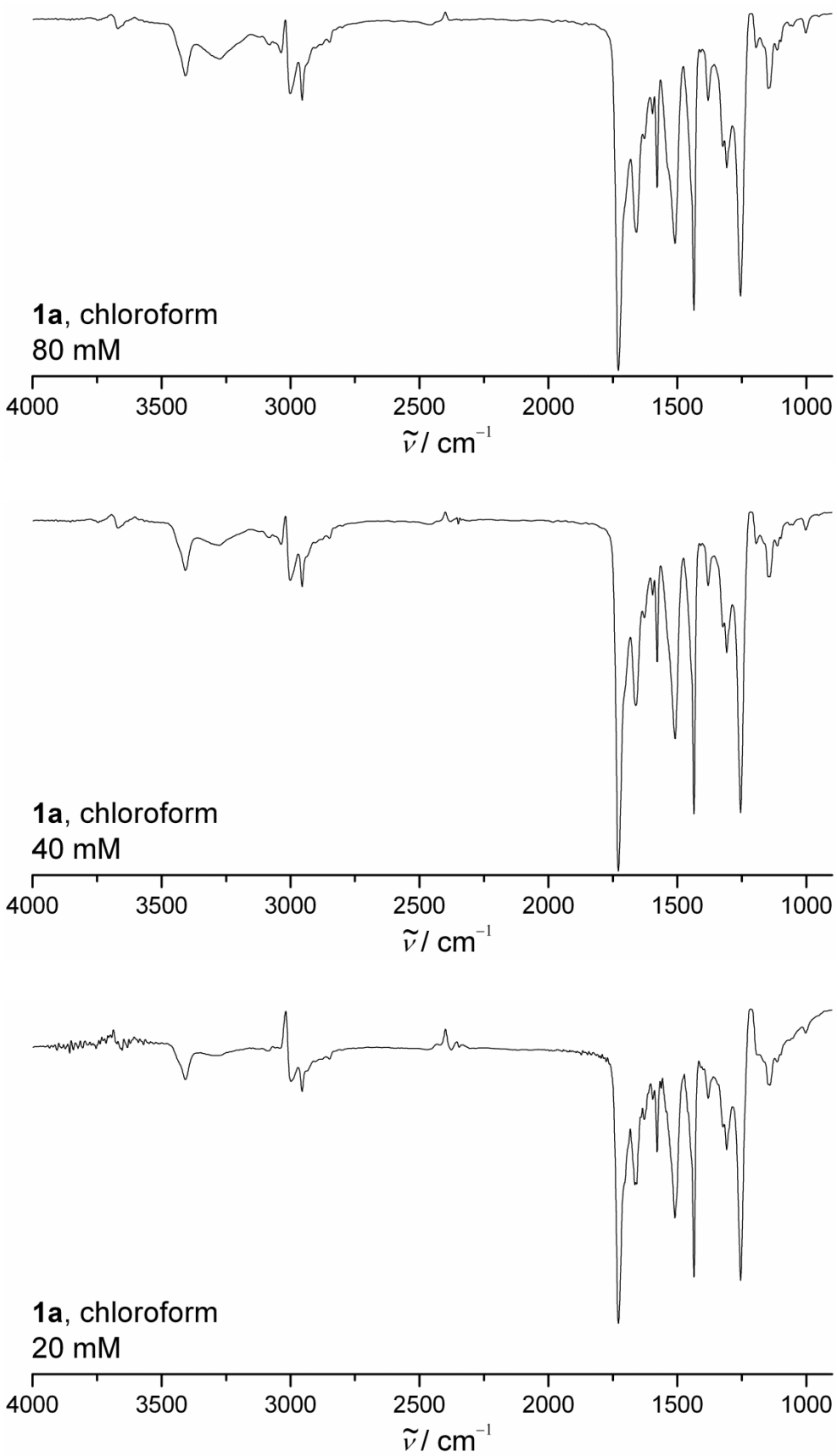

Figure S 42. FT-IR spectra of **1a** in chloroform at different concentrations.

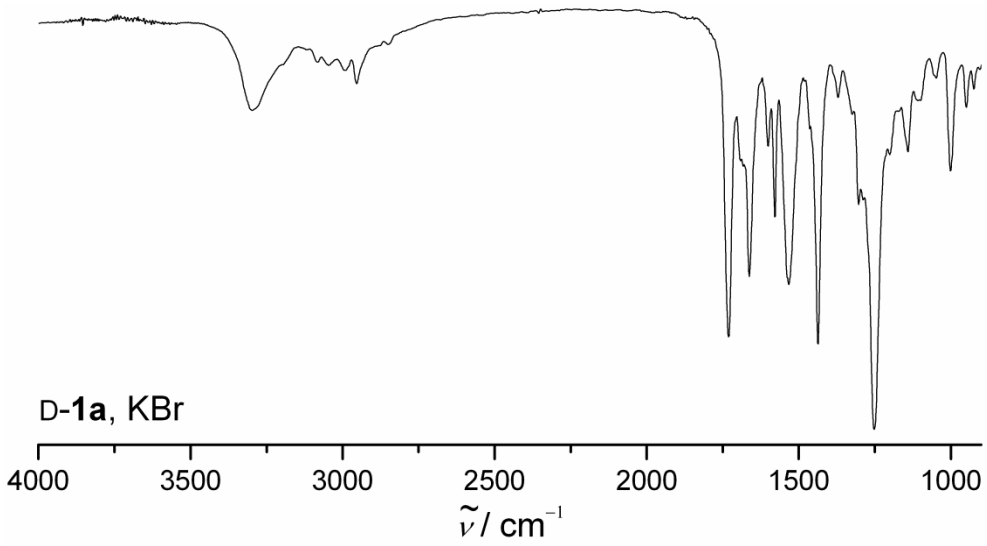

Figure S 43. FT-IR spectra of D-**1a** in the solid state (KBr).

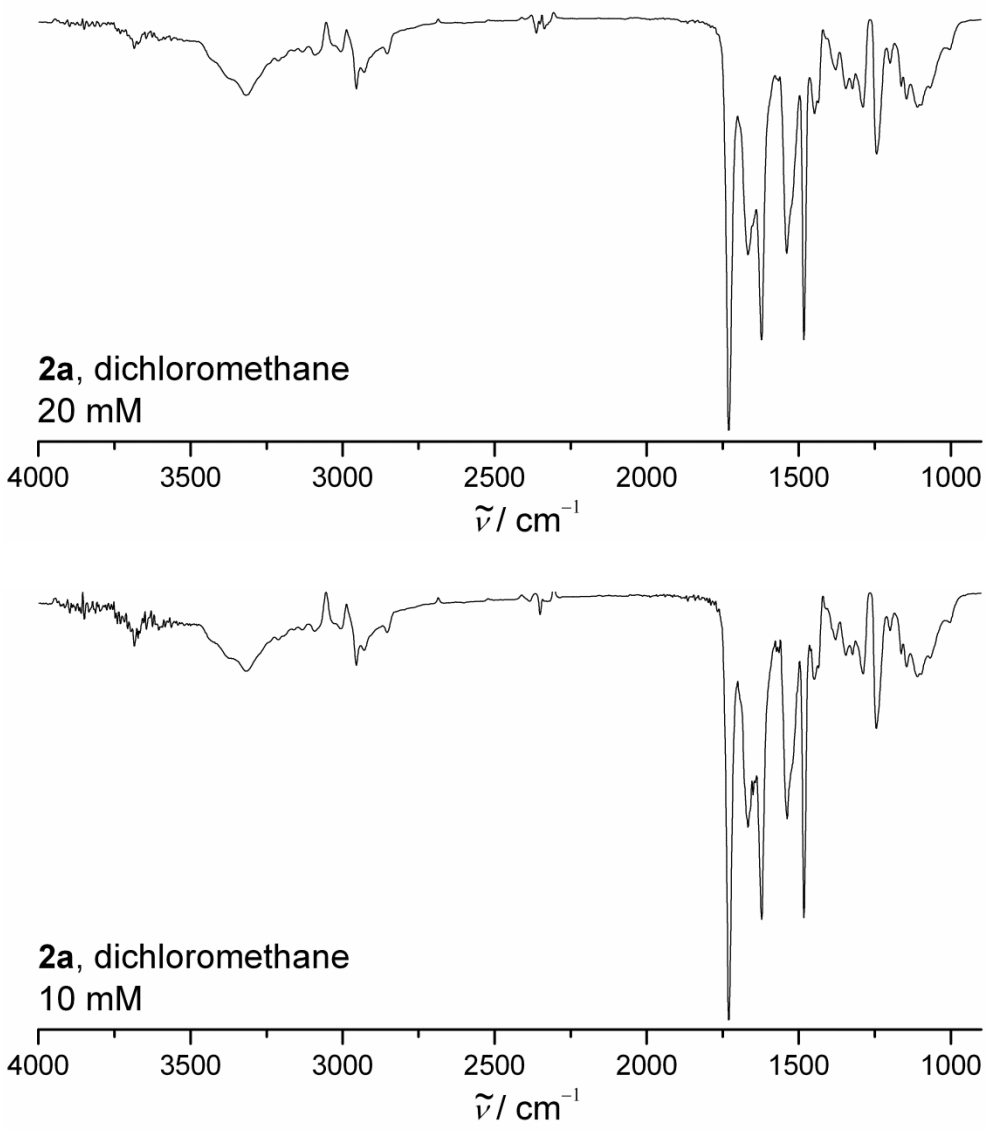

Figure S 44. FT-IR spectra of **2a** in dichloromethane at different concentrations.

Origin of Chiral Inversion

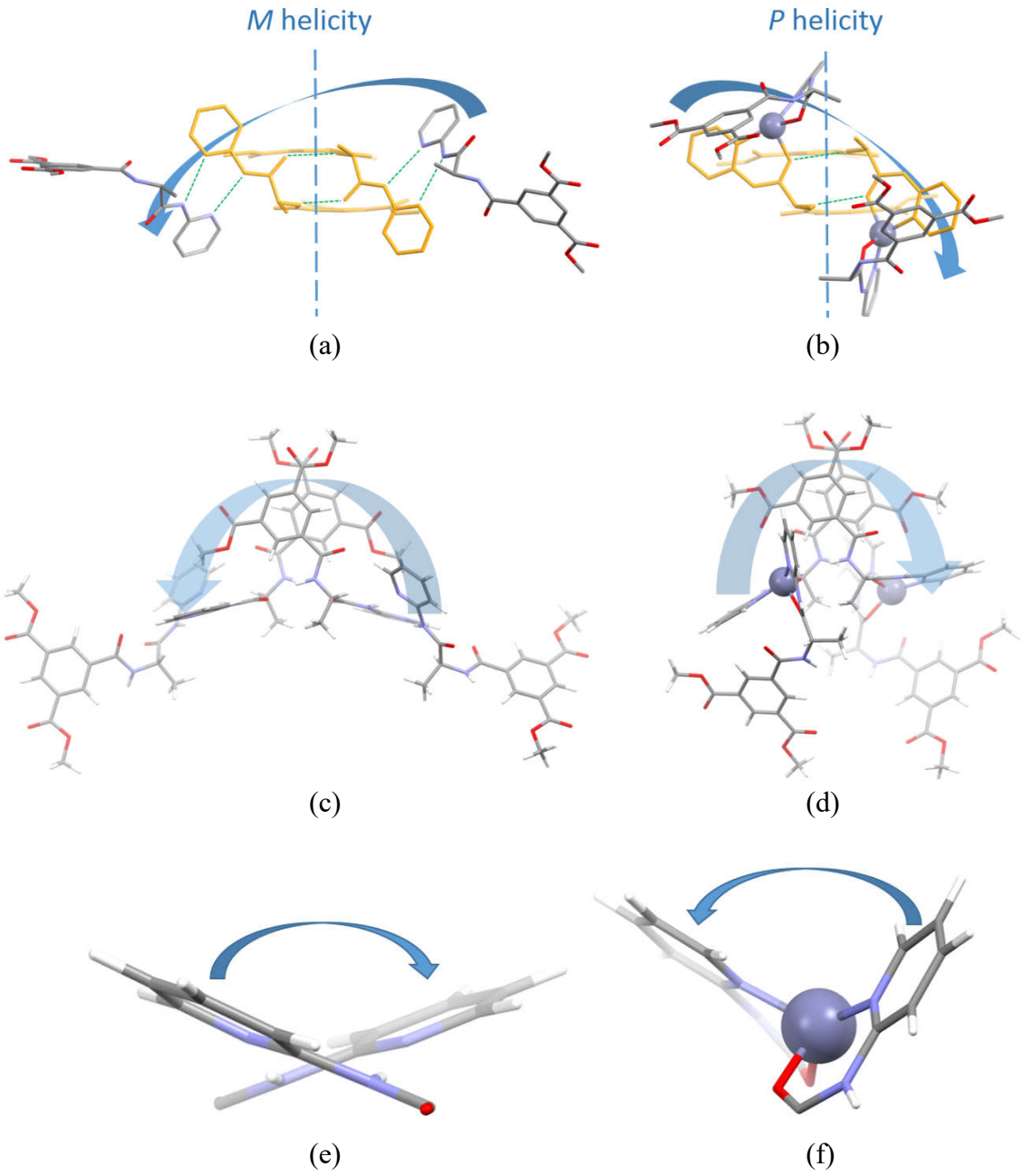

Figure S 45. DFT optimized structures of (a) **1a** (front view) and (b) **2a** (front view) half-turn helices in acetonitrile (the "half-turn" in **1a** is comprised of 4 ligand molecules as in the single crystal structure of D-**1a**, and the "half-turn" in **2a** is comprised of two zinc complex molecules *e.g.* 4 ligand molecules), showing opposite supramolecular chirality with respect to Herrick dimer (yellow coloured), in qualitative agreement with experimentally observed CD inversion. Top view: (c) **1a**, (d) **2a**. As a consequence of different supramolecular arrangement, the neighboring pyridyl moieties also adopt opposite conformations in (e) **1a** and (f) **2a**, which is most probably a direct cause for the CD signal inversion at pyridyl π-π* transition (≈ 300 nm).

References

S1 M. C. Burla, R. Caliandro, M. Camalli, B. Carrozzini, G. L. Cascarano, C. Giacovazzo, M. Mallamo, A. Mazzone, G. Polidori and R. Spagna, *J. Appl. Cryst.*, 2012, **45**, 351–356.

S2 G. M. Sheldrick, *Acta Cryst.*, 2008, **A64**, 112–122.

S3 P. van der Sluis and A. L. Spek, *Acta Cryst*., 1990, **A46**, 194–201.

S4 A. L. Spek, *Acta Cryst.*, 2009, **D65**, 148–155.

S5 W. L. Jorgensen, D. S. Maxwell, and J. Tirado-Rives, *J. Am. Chem. Soc*., 1996,**118**, 11225.

S6 U. C. Singh and P. A. Kollman, *J. Comput. Chem.*1984, **5**, 129–145.

S7 C. I. Bayly, P. Cieplak, W. Cornell, and P. A. Kollman, *J. Phys. Chem.* 1993, **97**, 10269–10280.

S8 C. Caleman, P. J. van Maaren, M. Hong, J. S. Hub, L. T. Costa, and D. van der Spoel, *J. Chem. Theor. Comput*.,2012, **8**, 61.

S9 U. Essmann, L. Perera, M. L. Berkowitz, T. Darden, H. Lee, and L. G. Pedersen, *J. Chem. Phys*.,1995, **103**, 8577.

S10 S. Nose, *Mol. Phys*. 1984, **52**, 255.

S11 M. Parrinello and A. J. Rahman, *Appl. Phys*. 1981, **52**, 7182.

S12 B. Hess, H. Bekker, H. J. C. Berendsen, and J. G. E. M. Fraaije, *J. Comp. Chem*. 1997, **18**, 1463.

S13 B. Hess, C. Kutzner, D. van der Spoel, and E. Lindahl, *J. Chem. Theory Comp*., 2008, **4**, 435.

S14 Y. Zhao and D. G. Truhlar, *Theor. Chem. Acc.*, 2008, **120**, 215–241.

S15 W. J. Hehre, K. Ditchfield, and J. A. Pople, *J. Chem. Phys.* 1972, **56**, 2257–2261.

S16 A. V. Marenich, C. J. Cramer, and D. G. Truhlar, *J. Phys. Chem. B*, 2009, **113**, 6378–6396.

S17 R. Bauernschmitt and R. Ahlrichs, *Chem. Phys. Lett.*, 1996, **256**, 454–64.

S18 J.-D. Chai and M. Head-Gordon, *Phys. Chem. Chem. Phys*., 2008, **10**, 6615–20.

S19 M. J. Frisch, G. W. Trucks, H. B. Schlegel, G. E. Scuseria, M. A. Robb, J. R. Cheeseman, G. Scalmani, V. Barone, B. Mennucci, G. A. Petersson, H. Nakatsuji, M. Caricato, X. Li, H. P. Hratchian, A. F. Izmaylov, J. Bloino, G. Zheng, J. L. Sonnenberg, M. Hada, M. Ehara, K. Toyota, R. Fukuda, J. Hasegawa, M. Ishida, T. Nakajima, Y. Honda, O. Kitao, H. Nakai, T. Vreven, J. A. Montgomery, Jr., J. E. Peralta, F. Ogliaro, M. Bearpark, J. J. Heyd, E. Brothers, K. N. Kudin, V. N. Staroverov, R. Kobayashi, J. Normand, K. Raghavachari, A. Rendell, J. C. Burant, S. S. Iyengar, J. Tomasi, M. Cossi, N. Rega, J. M. Millam, M. Klene, J. E. Knox, J. B. Cross, V. Bakken, C. Adamo, J. Jaramillo, R. Gomperts, R. E. Stratmann, O. Yazyev, A. J. Austin, R. Cammi, C. Pomelli, J. W. Ochterski, R. L. Martin, K. Morokuma, V. G. Zakrzewski, G. A. Voth, P. Salvador, J. J. Dannenberg, S. Dapprich, A. D. Daniels, Ö. Farkas, J. B. Foresman, J. V. Ortiz, J. Cioslowski, and D. J. Fox, (2009) Gaussian 09. Computer Program, Gaussian, Inc., Wallingford, CT, USA.

S20 F. E. Appoh, T. C. Sutherland, and H.-B. Kraatz, *J. Organomet. Chem.*, 2004, **689**, 4669.

S21 (a) W. H. Pirkle and T. C. Pochapsky, *J. Am. Chem. Soc.*, 1987, **109**, 5975–5982; (b) E. Murguly, R. McDonald, and N. R. Branda, *Org. Lett.*, 2000, **2**, 3269–3172; (c) I. Alkorta and J. Elguero, *J. Am. Chem. Soc.*, 2002, **124**, 1488–1493; (d) A. Tessa ten Cate, P. Y. W. Dankers, H. Kooijman, A. L. Spek, R. P. Sijbesma, and E. W. Meijer, *J. Am. Chem. Soc.*, 2003, **125**, 6860–6861.